UNIVERSITÀ DEGLI STUDI DI MILANO

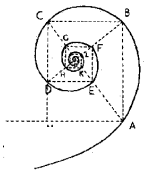

SCUOLA DI DOTTORATO IN MEDICINA MOLECOLARE

CICLO XXVIII

Anno Accademico 2014/2015

TESI DI DOTTORATO DI RICERCA

BIO/10

NON-CODING RNAs IN HIGH-GRADE SEROUS EPITHELIAL OVARIAN CANCER

Dottoranda: Paola TODESCHINI

Matricola N° R10252

TUTORE: Prof. Michele SAMAJA

CO-TUTORE: Dr.ssa Antonella Ravaggi

DIRETTORE DEL DOTTORATO: Ch. mo Prof. Mario CLERICI

Sommario

Introduzione: *Il carcinoma ovarico di istotipo sieroso ad alto grado (HGSOC) rappresenta il più letale tra i tumori ginecologici, principalmente poiché viene spesso diagnosticato in fase avanzata di malattia e poiché dopo un'iniziale risposta alla prima linea di trattamento, si assiste all'insorgenza di recidive di malattia resistenti alle terapie convenzionali. La mancanza di marcatori diagnostici e prognostici affidabili, oltre che di terapie efficaci, rappresenta il principale ostacolo nella gestione clinica delle pazienti affette da HGSOC. Di recente è stata individuata una nuova classe di RNA non codificanti (ncRNA), comprendente i microRNA (miRNA) e i long non-coding RNA (LncRNA), con funzione di regolazione dell'espressione genica e con un importante ruolo nella biologia tumorale. In particolare, i ncRNA appaiono coinvolti nella progressione tumorale e nello sviluppo di chemioresistenza; ciò suggerisce un loro possibile ruolo come potenziali biomarcatori diagnostici, prognostici e predittivi di risposta al trattamento. Le condizioni ipossiche all'interno del microambiente tumorale, favorendone la neovascolarizzazione, rappresentano un evento essenziale che contribuisce allo sviluppo di un fenotipo più aggressivo dell'HGSOC. Recentemente, è stato identificato un gruppo di miRNA, nominati miRNA regolati dall'ipossia (HRM), che rappresentano degli elementi chiave in risposta alle condizioni ipossiche, essendo coinvolti nella regolazione di meccanismi che conferiscono una maggiore aggressività tumorale. La complessità dei processi coinvolti nella risposta all'ipossia nell'HGSOC non è stata ancora del tutto compresa. In questo contesto, la scoperta di biomarcatori utili dal punto di vista clinico per la selezione di pazienti affette da tumori caratterizzati da una spiccata ipossia, potrebbe favorire l'applicazione di trattamenti personalizzati.*

Scopi dello studio: *Il mio progetto di dottorato è finalizzato allo studio di firme molecolari trascrizionali e post-trascrizionali caratterizzanti l'HGSOC, a livello sierico e tissutale. Nello specifico, la ricerca si è focalizzata sui seguenti punti: i) lo studio di miRNA circolanti, quali potenziali biomarcatori per la diagnosi precoce dell'HGSOC; ii) l'analisi dei profili di espressione di mRNA, miRNA e lncRNA dell'HGSOC e di tessuti sani di controllo; iii) la valutazione dell'espressione dei miRNA legati all'ipossia, nell'HGSOC e nei tessuti sani di controllo.*

Metodi: *A partire da due coorti indipendenti, sono stati raccolti 168 sieri di pazienti affette da HGSOC e 65 sieri appartenenti a donatori sani, che sono stati a loro volta stratificati in un training set, per l'individuazione di miRNA differenzialmente espressi tra le due popolazioni, e in un validation set, per la validazione dei dati. Prima dell'estrazione dell'RNA, ai campioni di siero sono stati aggiunti dieci oligonucleotidi sintetici ad RNA (RNA virali/C.Elegans) per consentire una normalizzazione accurata dei risultati. I profili di espressione dei miRNA sono stati ottenuti mediante tecnologia Agilent Microarray. Per la normalizzazione dei dati derivanti dall'analisi dei microarray è stato utilizzato un innovativo approccio statistico, basato sulla combinazione dei livelli degli oligo RNA sintetici e dei miRNA endogeni maggiormenti stabili all'interno del nostro sistema sperimentale. La validazione della firma molecolare nel training e nel validation set è stata ottenuta prima mediante PCR quantitativa (RT-qPCR) e successivamente confermata mediante una quantificazione assoluta, ottenuta con sistema droplet digital PCR (ddPCR).*
Inoltre, sono state raccolte 99 biopsie tumorali di HGSOC da pazienti a stadio III-IV di malattia, 76 delle quali appaiate ai campioni di siero. Essendo l'istogenesi di questa patologia ancora oggetto di dibattito, sono stati raccolti anche 30 campioni di epitelio ovarico sano e di epitelio di superficie tubarico, come controllo. I profili di espressione genica e dei miRNA sono stati ottenuti mediante tecnologia Agilent Microarray. I livelli di espressione dei miRNA, risultati differenzialmente espressi, sono stati associati alle variabili cliniche, quali la sopravvivenza globale (OS) e la sopravvivenza libera da progressione di malattia (PFS). Infine, un sottogruppo composto da 14 pazienti chemio-resistenti, 14 pazienti chemio-sensibili e 10 tessuti sani sono stati sequenziati allo scopo di individuare nuovi trascritti codificanti e non codificanti specifici dell'HGSOC.

Risultati: *Dall'analisi microarray 97 miRNA sono risultati significativamente differenzialmente espressi, tra i sieri di pazienti affette da HGSOC e i sieri di donatori sani (92 up-regolati e 5 down-regolati). Tra questi miRNA, i seguenti miR-1246, miR-595, miR-574-5p, miR-483-3p, miR-4290, miR-2278, miR-32, miR-4281 e miR-3148, che mostravano la più alta espressione media e il maggiore fold change misurati nel confronto tra i pazienti e i donatori sani, sono stati selezionati per ulteriori validazioni. In particolare, miR-1246, miR-595 e miR-2278 si sono confermati maggiormente espressi nel siero delle pazienti affette da HGSOC rispetto ai donatori sani, mediante PCR quantitativa (tutti i p-values<0.03), sia nel training che nel validation set. L'analisi della curva ROC (Receiver Operating Characteristic) ha mostrato miR-1246 come il miglior biomarcatore diagnostico, con una sensibilità dell' 87%, una specificità del 77% ed un'accuratezza dell' 84%. La quantificazione assoluta dei livelli circolanti del miR-1246, ottenuta mediante ddPCR, ha confermato il suo potenziale come biomarcatore diagnostico dell'HGSOC.*
L'analisi microarray dei profili tissutali dei miRNA ha rivelato un totale di 265 miRNA significativamente disregolati nei campioni di HGSOC rispetto ai tessuti sani (123 up-regolati e 142 down-regolati). Un gruppo

di 9 miRNA (miR-199b-5p, miR-423-5p miR-455-3p, miR-22-3p, miR-199a-3p, miR-15b-5p, miR-140-5p, miR-1246 e miR-320c) è emerso associato alla risposta al trattamento chemioterapico a base di platino e alla prognosi. In particolare, tra i campioni tumorali la up-regolazione del miR-1246 è risultata significativamente associata alla resistenza al platino e ad un breve OS e PFS (p-values<0.05). Le curve di sopravvivenza Kaplan Meier, basate sui livelli di espressione del miR-1246 misurati in RT-qPCR, hanno mostrato una significativa riduzione dell'OS e del PFS nei pazienti presentanti elevati livelli del miR-1246, rispetto ai soggetti con bassi livelli di espressione (p-value<0.001, HR=2.57; p-value=0.024, HR=1.68; rispettivamente). L'analisi multivariata ha confermato l'over-espressione del miR-1246 come fattore prognostico indipendente associato ad una riduzione dell' OS e del PFS. Inoltre, i livelli del miR-1246 hanno mostrato una down-regolazione nei campioni di HGSOC rispetto ai campioni di HOSE (p-value<0.0001), ma sono risultati invariati rispetto ai campioni di epitelio tubarico, sia nelle analisi ottenute mediante microarray, che mediante RT-qPCR. Questo risultato rispecchia il trend di espressione globale dei miRNA emerso dall'analisi delle componenti principali (PCA), sui dati di microarray.
Successivamente, ci siamo focalizzati sull'analisi di 16 miRNA appartenenti al gruppo dei miRNA regolati dall'ipossia, selezionati dopo un' approfondita analisi della letteratura che mostrava il loro coinvolgimento in altri tipi di tumori solidi. Tra questi, il miR-210 e il cluster miR-27a-3p/23a-3p/24-3p si sono confermati, mediante RT-qPCR, significativamente up-regolati nei campioni di HGSOC rispetto ai tessuti normali (tutti i p-values≤0.002). L' over-espressione del miR-23a-3p si è inoltre validata nel gruppo delle pazienti resistenti rispetto alle pazienti sensibili al trattamento chemioterapico a base di platino (p-value=0.03). Riguardo alla sopravvivenza, mediante analisi univariata, l'up-regolazione del miR-23a-3p è risultata associata ad una significativa riduzione del PFS (p-value=0.009, HR=1.8), ma non con una riduzione dell'OS. L'analisi multivariata ha inoltre confermato l'over-espressione del miR-23a-3p, come marcatore prognostico indipendente associato ad un breve PFS (p-value=0.01, HR=1.78).
Infine, le analisi preliminari riguardanti il sequenziamento del trascrittoma ci hanno permesso di identificare 1371 trascritti differenzialmente espressi tra campioni platino resistenti e platino sensibili. Tra loro, 125 trascritti mostrano un completo appaiamento con trascritti noti, 686 sono potenziali nuove isoforme o mostrano una generica sovrapposizione con trascritti noti. Le rimanenti 560 sequenze, se validate, possono rappresentare nuovi trascritti intergenici o mostranti un appaiamento a livello esonico con sequenze di riferimento.

***Conclusioni**: Questo studio mostra, per la prima volta, il miR-1246 come un potenziale biomarcatore sierico per la diagnosi dell'HGSOC, confermato da tre tecnologie (microarray, RT-qPCR and ddPCR) e validato in due coorti di pazienti indipendenti.*
L'analisi high-throughput ha individuato la maggior parte dei geni e dei miRNA disregolati nelle biopsie di HGSOC rispetto al tessuto sano di controllo. In particolare, i nostri risultati indicano un potenziale ruolo del miR-1246 come oncogene nella regolazione dei meccanismi responsabili della resistenza ai chemioterapici e come fattore prognostico di sopravvivenza delle pazienti affette da HGSOC.
Le analisi riguardanti i miRNA associati all'ipossia suggeriscono un importante ruolo dei miRNA nella risposta alle condizioni ipossiche, che si verificano all'interno delle masse di HGSOC. In particolare, l'over-espressione del miR-23a-3p nel gruppo delle pazienti resistenti al platino evidenzia l'importanza dell'ipossia nell'insorgenza dei meccanismi di chemio-resistenza. Inoltre, l'over-espressione del miR-23a-3p potrebbe rappresentare un marcatore prognostico indipendente nelle pazienti affette da questa neoplasia.
Infine, i risultati emersi dall'analisi preliminare dei dati riguardanti il sequenziamento del trascrittoma suggeriscono un marcato ruolo dei trascritti non-codificanti nei meccanismi di resistenza al platino nell'HGSOC. Gli eventuali trascritti validati verranno integrati con i profili di espressione dei geni e dei miRNA, precedentemente ottenuti, con l'obiettivo di identificare circuiti tumorali associati con la risposta al trattamento ed alla prognosi, e per meglio comprendere i meccanismi molecolari che caratterizzano la progressione e l'adattamento dell'HGSOC al microambiente ipossico.

Abstract

Introduction: *High-grade serous ovarian carcinoma (HGSOC) is the most lethal gynecologic malignancy, mainly because the disease is frequently diagnosed at an advanced stage and is characterized by the early onset of chemoresistant recurrences. The lack of reliable diagnostic and prognostic markers, together with the lack of effective therapies, are the major obstacles to the clinical management of patients with HGSOC. A new class of non-coding RNAs (ncRNAs), such as microRNA (miRNAs) and long non-coding RNAs (LncRNAs), with a function of gene expression regulation, have been discovered to play an important role in human cancers. Increasing evidences suggest that ncRNAs are involved in cancer progression and development of chemoresistance, and support their role as potential diagnostic, predictive and prognostic biomarkers. The hypoxic condition within the tumor microenvironment, improving the tumor neovascularization, represents an essential event contributing to the development of a more aggressive HGSOC phenotype. Recently, a group of miRNAs, termed hypoxia regulated-miRNAs (HRMs), have been identified as key elements in response to hypoxia, regulating important mechanisms involved in tumor progression. The complexity of hypoxia molecular mechanisms has not been fully elucidated yet in HGSOC, therefore there is an urgent need to discover novel biomarkers clinically useful to select patients with hypoxic tumor, that may benefit of tailored treatments.*

Aims of the study: *My PhD project aims at elucidating transcriptional and post-transcriptional signatures characterizing HGSOC, both at the serum and tissue levels. In detail, the research effort includes: i) the investigation of circulating miRNAs as novel potential biomarkers for HGSOC detection; ii) the analysis of mRNA, miRNA and lncRNA expression profiles of HGSOC and normal tissues; iii) the evaluation of hypoxia-regulated miRNA expression in HGSOC and normal tissues.*

Methods: *Sera from 168 HGSOC stage III-IV patients and 65 healthy donors were gathered together from two independent collections and stratified into a training set, for miRNA marker identification, and a validation set, for data validation. Nine synthetic viral/C.Elegans spike-in oligos were added to serum samples before RNA extraction, to allow accurate normalization. miRNA expression profiles were obtained using Agilent Microarray Technologies®. An innovative statistical approach for microarray data normalization, based on the contribute of spike-in oligos and the most invariant miRNAs, was developed to identify, in the training set, differentially expressed miRNAs. Signature validation in both the training and validation sets was performed by Real Time quantitative PCR (RT-qPCR) and confirmed by droplet digital PCR (ddPCR).*
A total of 99 tumor biopsies were collected from HGSOC stage III-IV patients, partially matched with the serum sample cohort (n=76). Thirty normal tissues were obtained from normal ovary (HOSE) and luminal fallopian tube surface epithelia, both representing the normal counterpart for HGSOC, whose histogenesis is still a matter of debate. Gene and miRNA expression profiles were obtained using Agilent Microarray Technologies®. miRNA expression levels were correlated with patient outcomes, as overall survival (OS) and progression-free survival (PFS). Additionally, a subgroup of 14 chemo-resistant and 14 chemo-sensitive HGSOC patients, together with 10 normal tissues were deep sequenced for the discovery of novel HGSOC specific coding and non-coding transcripts.

Results: *A panel of 97 miRNAs emerged significantly differentially expressed (92 up-regulated and five down-regulated) between sera of HGSOC patients and healthy donors by microarray analysis. Among them, the following miRNAs, i.e., miR-1246, miR-595, miR-574-5p, miR-483-3p, miR-4290, miR-2278, miR-32, miR-4281, and miR-3148, exhibiting both the highest average expression and log fold change measured in patients compared to healthy donors, were selected for further validation. miR-1246, miR-595 and miR-2278 were confirmed as significantly over-expressed in serum of HGSOC patients compared to controls by RT-qPCR (all p-values<0.03), in both the training and validation sets. Receiver Operating Characteristic (ROC) curve analysis revealed miR-1246 as the best diagnostic biomarker, with a sensitivity of 87%, a specificity of 77% and an accuracy of 84%. The absolute quantification of circulating miR-1246 by ddPCR confirmed its potential as diagnostic biomarker in HGSOC.*
Microarray analysis of tissue miRNA profiling revealed a total of 265 miRNAs significantly dysregulated (123 up-regulated and 142 down-regulated) in HGSOC compared to normal tissues. A group of nine miRNAs (i.e., miR-199b-5p, miR-423-5p miR-455-3p, miR-22-3p, miR-199a-3p, miR-15b-5p, miR-140-5p, miR-1246, and miR-320c) were associated with platinum response and prognosis. In particular, among tumor samples, miR-1246 up-regulation was consistently associated with platinum-resistance, poor OS and poor PFS (p-values<0.05). Kaplan-Meier survival curves, according to miR-1246 expression levels obtained by RT-qPCR, showed that OS and PFS decreased in patients with high miR-1246 expression compared to those with low miR-1246 expression (p-value<0.001, HR=2.57; p-value=0.024, HR=1.68; respectively). In addition, multivariate analysis revealed miR-1246 over-expression as an independent prognostic factor for poor OS and PFS (p-value=0.002, HR=2.31; p-value<0.05, HR=1.59; respectively).

Interestingly, compared to normal tissues, both with microarray and RT-qPCR techniques, miR-1246 showed a down-regulation compared to HOSEs (p-value<0.0001), but we did not detect a significantly differential expression compared to fallopian tubes. This result mirrors the global miRNA expression trend revealed by principal component analysis (PCA) on microarray data.
Subsequently, we focused our analysis on a group of 16 miRNAs belonging to the group of hypoxia-regulated miRNAs (HRMs) emerged from literature as relevant in other solid tumors. Among them, we confirmed miR-210 and miR-27a-3p/23a-3p/24-3p cluster as significantly up-regulated in HGSOC vs normal tissues by RT-qPCR (all p-values≤0.002). More interestingly, we validated the significant over-expression of miR-23a-3p in the group of patients resistant to platinum-based chemotherapy compared to platinum-sensitive patients (p-value=0.03). In addition, in univariate survival analysis miR-23a-3p over-expression showed a significant correlation with decreased progression-free survival (p-value=0.009, HR=1.8), but not with overall survival variable. Importantly, miR-23a-3p over-expression has emerged as an independent prognostic marker for shortened progression-free survival in multivariate Cox regression analysis (p-value=0.01, HR=1.78).
Finally, the preliminary analysis of the transcriptome sequencing allowed us to identify 1371 transcripts differentially expressed between platinum-resistant and platinum-sensitive samples. Among them, 125 transcripts showed a complete match of intron chain with known transcripts, 686 were potentially novel isoforms or showed a generic overlap with known transcripts. The remaining 560 sequences, if validated, could be novel intergenic transcripts or transcripts with an exonic overlap with reference ones.

***Conclusions**: This study demonstrates, for the first time, miR-1246 as a potential diagnostic serum biomarker in HGSOC, as assessed by three independent technologies (microarray, RT-qPCR and ddPCR) and validated in two independent cohorts of patients.*
Moreover, high-throughput analysis reveals most of the gene and miRNA dysregulated in HGSOC biopsies compared to the normal counterpart. In particular, our findings indicate, for the first time, that miR-1246 over-expression correlates with a platinum-resistant HGSOC phenotype and may constitute a novel prognostic factor for HGSOC patients.
Furthermore, our results regarding HRMs suggest an important role of miRNAs in response to hypoxic conditions within HGSOC. Particularly, the miR-23a-3p over-expression in the group of platinum-resistance patients may contribute to explain the importance of hypoxia in HGSOC mechanism of drug resistance and could represent an independent prognostic marker for HGSOC patients.
Lastly, preliminary data emerged from transcriptome analyses, suggesting a prominent non-coding role in HGSOC platinum resistance, will be integrated with gene and miRNA expression profiles previously obtained, with the aim to identify tumor circuits associated with response to treatment and prognosis, as well as to better elucidate the molecular mechanisms characterizing HGSOC progression and adaptation to hypoxic tumor microenvironment.

TABLE OF CONTENTS

1. INTRODUCTION

1.1 High-Grade Serous Epithelial Ovarian Cancer

1.1.1 Background

Ovarian cancer is the fifth leading cause of cancer death among women worldwide and the most lethal gynaecological malignancy. In the United States there are around 22,000 new cases of ovarian cancer diagnosed each year and more than 14,000 cancer-related deaths [Siegel RL et al. 2016]. The majority of ovarian cancers are of epithelial origin, whereas fewer ovarian cancers develop from other cell types, such as sex-cord stromal, germ cell, or mixed cell-type tumors [Kalir T et al. 2013]. Currently, based on histopathology, immunohistochemistry and molecular genetic alterations, epithelial ovarian cancers (EOCs) are classified into five main subtypes: high-grade serous (70%), endometrioid (10%), clear cell (10%), mucinous (3%) and low-grade serous (<5%) [Prat J 2012]. Although traditionally referred to as a single entity, these EOC histotypes are essentially distinct diseases, as indicated by their differences in epidemiological and genetic risk factors, precursor lesions, patterns of spread, molecular events during oncogenesis, response to chemotherapy and prognosis.

1.1.2 Clinicopathological features

The most common histological EOC, the high-grade serous ovarian carcinoma (HGSOC), is generally diagnosed late (stage III-IV), when multiple synchronous tumor lesions are localized to the ovary, as well as in other anatomical sites within the peritoneum cavity. HGSOC develops rapidly, and is highly aggressive. The five-year survival rate for stage III-IV HGSOC is less than 30%, as patients, despite an aggressive surgery and initial response to platinum agents, become progressively resistant and die from incurable disease. This neoplasm accounts for 90% of the deaths from ovarian cancer [Kurman RJ et al. 2016].

1.1.3 Morphological and immunohistochemical features

Histologically, HGSOC is characterized by a heterogeneous architecture, composed by a solid mass of cells, including nested, papillary (micropapillary or macropapillary), glandular (slit-like or round spaces) and cribriform cells. Necrosis and multinucleate cells are often observed. Commonly psammoma bodies are present [Ramalingam P 2016]. It also exhibits moderate to marked nuclear atypia and a mitotic activity greater than 12/10 high-power microscopic fields (HPFs) [Malpica A et al. 2004]. Most HGSOCs show an intense immunoreactivity for p53, MIB1, WT1, bcl-2, c-kit, Her-2 neu, estrogen receptor (ER), HLA-G and p16 [O'Neill CJ et al. 2005]. In particular, p53 immunohistochemistry expression can exhibit two different patterns: the usual and the most commonly observed is characterized by strong diffuse nuclear staining in approximately 60% of cells or greater. This pattern correlates with a missense mutation. The other pattern is the complete absence of staining, which correlates with a nonsense mutation, resulting in a truncated

protein that is not detected by the p53 antibody [Yemelyanova A et al. 2011]. HGSOC also shows a high proliferation index, as indicated by an increased nuclear expression of Ki-67 [Prat J 2012]

1.1.4 Molecular features

Currently, our understanding of ovarian carcinogenesis and its role in tumor classification is mainly based on morphological features, but the importance of molecular classification is becoming increasingly evident. In recent years, the advent of next-generation sequencing and genome-wide analysis has greatly facilitated attempts to better characterize HGSOC molecular genetic profile and to discover novel HGSOC-associated genes. Recent studies have shown that HGSOCs are characterized by high genomic structural variations. They harbor frequent DNA amplifications and deletions, including heterozygous and homozygous loss and gene breakage [Kuo KT et al. 2009; Cancer Genome Atlas Research Network 2011], that make this cancer an extreme example of a chromosomally unstable (C-class) malignancy [Ciriello G et al. 2013]. In HGSOC, with the exception of TP53, which is inactivated in more than 95% of cases, somatic point mutations in other driver genes occur very infrequently. Importantly, there is a frequent inactivation (by germline, somatic and epigenetic mutations) of the BRCA1/2 genes involved in the DNA damage repair pathway. BRCA1 and BRCA2 are fundamental components of the homologous recombination DNA repair machinery, that is required to resolve DNA double-strand breaks (DSB) [Walsh T et al. 2010] . Initially, BRCA1 and BRCA2 gene mutations were observed in hereditary forms of HGSOC disease, that represent approximately 10%-15%, then sporadic forms (90%) were identified. Women with germline mutations in BRCA1 or BRCA2 have an increased risk (30%-70%) of developing HGSOC ovarian cancer by the age of 70. The sporadic forms of HGSOC, that harbor somatic mutation in BRCA1/2 suppressor genes, are defined BRCAness, to describe their genetic features and molecular behavior similar to HGSOC hereditary forms carrying germline mutations [Rigakos G and Razis E 2012]. As reported by Venkitaraman et al, the early loss of p53 function observed in sporadic form of cancers could create a permissive environment for the loss of BRCA1 or BRCA2 function [Venkitaraman AR 2002]. These studies suggest that loss of TP53 and BRCA inactivation are crucial initial steps of HGSOC carcinogenesis, followed by chromosomal instability, DNA copy number change, and segregation into molecular subtypes, as reported in the model schematically represented in Figure 1.1 [Bowtell DD 2010]. Among homozygous deletions, loci containing Rb1, CDKN2A/B, CSMD1, DOCK4, PTEN, and NF1 are most common [Vang R et al. 2009]. Additionally, HGSOC is characterized by high level of DNA copy number gains or losses, which include CCNE1 (cyclin E1), NOTCH3, AKT2, RSF1, and PIK3CA [Nakayama K et al. 2007]. In 2011, the Cancer Genome Atlas (TCGA) consortium performed a large-scale, multiplatform genomic profiling study to comprehensively characterize genomic and epigenetic abnormalities of HGSOC [Cancer Genome Atlas Research Network 2011]. A total of 489 clinically-annotated, stage II-IV, HGSOC tumor samples were analyzed for mRNA and microRNA expression, DNA copy number and DNA promoter methylation. Whole-exome DNA

sequencing was performed on 316 of these tumor samples. Missense or nonsense mutations in TP53 have been reported in more than 96% of HGSOC cases analyzed. BRCA1 and BRCA2 were found mutated in 22% of tumors, harboring a combination of germline and somatic mutations. Important focal DNA copy number alterations and promoter methylations were also detected in a total of 168 genes. The known tumor suppressor genes PTEN, RB1, and NF1 were in regions of homozygous deletions and were among the significantly mutated genes. Amplification of CCNE1 was another frequent finding. NOTCH3 and FOXM1 signaling were also identified to be involved in HGSOC development [Cancer Genome Atlas Research Network 2011].

On the basis of gene expression cluster analysis of TCGA dataset, four robust transcriptional subtypes of HGSOC have been delineated and validated by gene expression profiling: *Immunoreactive, Differentiated, Proliferative and Mesenchymal* [Cancer Genome Atlas Research Network 2011; Tothill RW et al. 2008; Konecny GE et al. 2014]. These molecular subtypes were associated with distinct clinical outcomes and microenvironmental features. Surprisingly, however, not statistically significant difference in survival times among TCGA subtypes, in the 489 HGSOC patients analyzed, was observed. These molecular subtypes have not yet been integrated into the clinical setting.

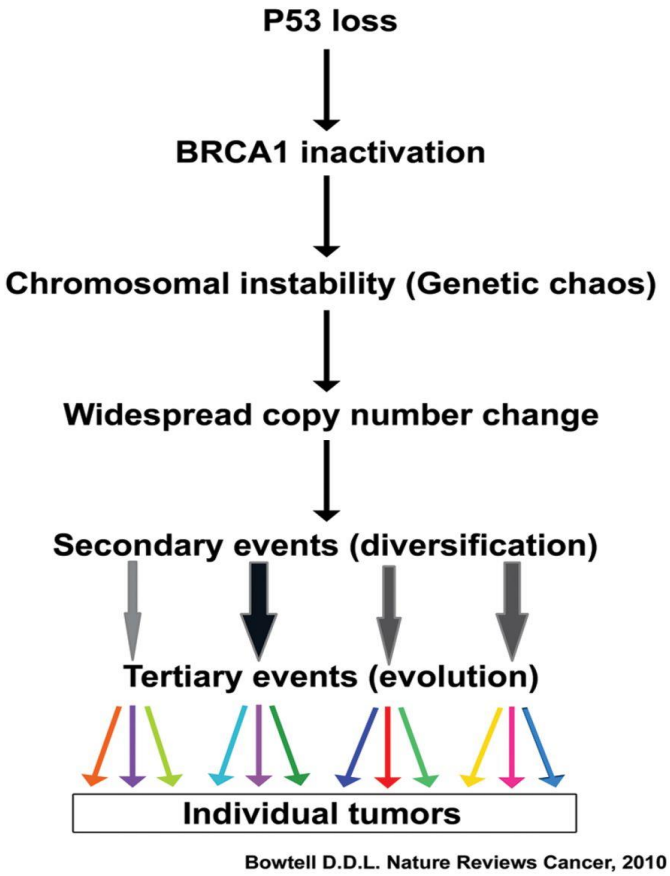

Figure 1.1: Schematic model of genetic events involved in the initiation and progression of high-grade serous ovarian cancer.

1.1.5 Histogenesis

Although HGSOC has been hypothesized to arise from the ovarian surface epithelium (OSE) or cortical inclusion cysts, multiple studies in the past three decades failed to identify a reliable precursor lesion of this disease. In the last decade, a growing body of evidence suggests that the majority of ovarian HGSOCs could develop from the epithelium of the fimbrial end of the fallopian tube. The initial evidence implicating the fimbrial epithelium has been described in women who had BRCA germline mutations and underwent prophylactic bilateral salpingo-oophorectomy. Pathologists, using the Sectioning and Extensively Examining the Fimbria (SEE-FIM) protocol, a new method of fallopian tube sampling, identified foci of small in situ serous tubal intraepithelial carcinoma (STIC) [Piek JM et al. 2001; Medeiros F et al. 2006; Crum CP et al. 2007]. Surprisingly, similar lesions were not detected in the ovaries of the same women. Even more, epidemiological studies showed that women who underwent prophylactic salpingectomy displayed a significantly decreased risk of HGSOC, compared with women that conserved fallopian tubes, further supporting the tubal origin of HGSOC [Ohman AW et al. 2014; Cherry C et al. 2013]. Additionally, another important evidence supporting the proposal that STIC could be the most likely HGSOC precursor was the identification of identical TP53 mutations, indicating a clonal relationship between the two malignancies [Kuhn E et al. 2012]. Further studies revealed the presence of STIC within the fallopian tubes, systematically examined, not only in those patients carrying BRCA1/2 germline mutation, but also in 50% to 60% of patients with sporadic HGSOC [Przybycin CG et al. 2010; Kindelberger DW et al. 2007]. In the percentage of women in which a STIC lesion was not identified, it has been hypothesized that a possible mechanism of HGSOC origin could be the implantation of the malignant cells from fimbrial tubal epithelium into the ovary (endosalpingiosis) or mesothelial surface invaginations (inclusion cysts). Then, they develop into a tumor mass that gives the impression that the tumor originated in the ovary (Figure 1.2) [Kurman RJ and Shih IeM 2010].

On the other hand, in 2013, a group of researchers identified in a mouse model the presence of a stem cell niche of the ovarian surface epithelium (OSE). Those cells were localized in a transitional/junction area between OSE, mesothelium and tubal (oviductal) epithelium, at the hilum region of the mouse ovary. Those stem cell niches confined in that specific area may explained the susceptibility of transitional zones to malignant transformation and have important implications in HGSOC pathogenesis [Flesken-Nikitin A et al. 2013]. More recently, Kim et al have demonstrated, in mutant mice harboring TP53 mutation and underwent fallopian tube removal, that HGSOC developed from surface ovarian epithelium, leading to widespread metastases into the peritoneal cavity. They concluded that, despite ovarian epithelium cells intrinsically have less tumorigenic potential compared to fimbrial tubal epithelium cells, they can be an independent source of HGSOC [Kim J et al. 2015]. This evidence could clarify the origin of a subset of HGSOCs with no apparent STIC precursor lesions or involvement of fallopian tube. Therefore, at present, the

reliable site of origin of HGSOC is still debated. More experimental evidences are necessary to better elucidate the relative contribution of ovarian and fallopian sites to the genesis of HGSOC.

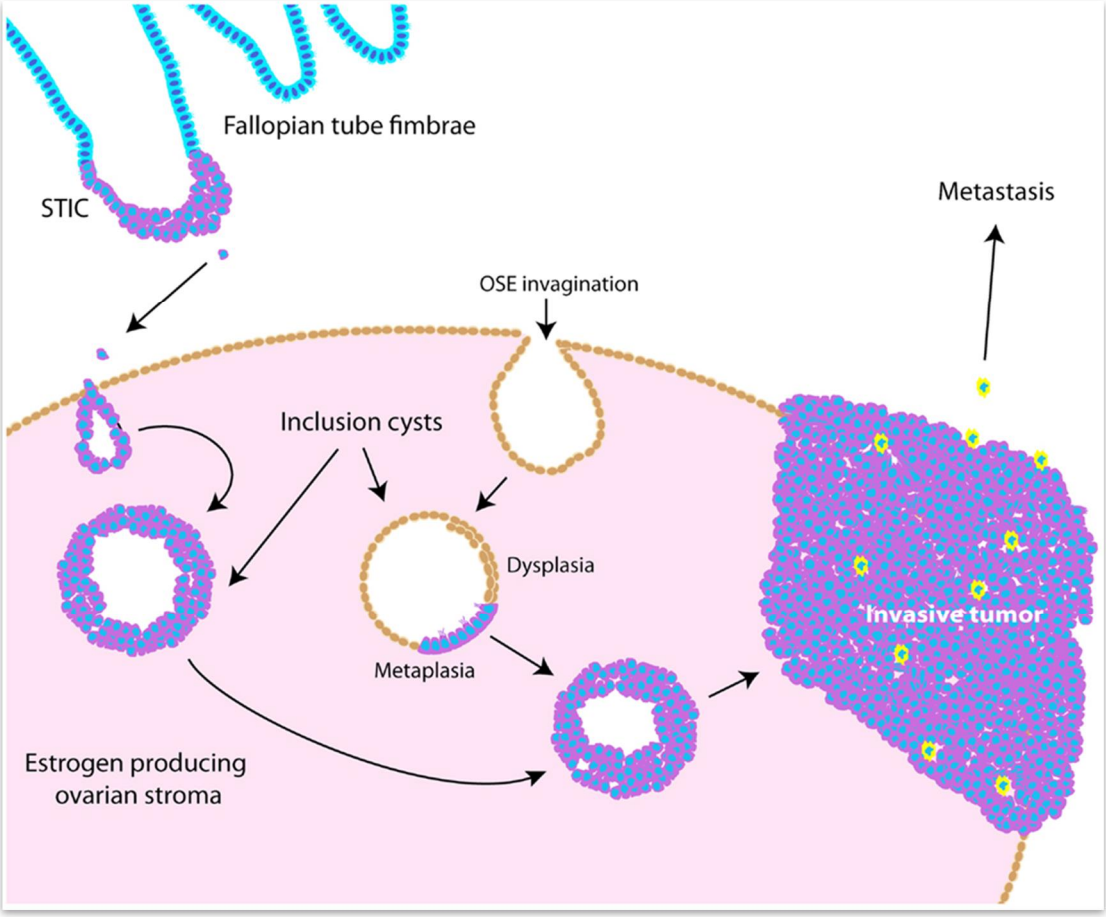

Figure 1.2: Fallopian tube and ovarian surface epithelial hypotheses on origin of HGSOC.

1.1.6 Diagnosis and screening

Approximately 70% of HGSOC are diagnosed at advanced-stage, when the neoplasm has extensively spread throughout the peritoneal space, generating multiple metastasis by dissemination into the peritoneum (stage III) and to distant organs (stage IV). The often asymptomatic nature of HGSOC primary lesions and the dramatically rapid spread of this malignancy out of the pelvis make early-stage detection a highly rare event. At the moment, serum CA-125, in combination with ultrasound, is the most common used biomarker for HGSOC diagnosis. Since CA-125 is associated with a high false-positive rate among benign gynaecologic conditions, such as endometriosis, that mainly affects pre-menopausal women, its use is mainly reserved for EOC diagnosis in post-menopausal cases. However, in the current clinical setting, CA-125 is used as a serum biomarker in the differential diagnosis between EOC and benign pelvic masses also in pre-menopause women, despite its relatively low specificity. Furthermore, CA-125 shows low sensitivity in identifying patients with early-stage EOC disease, being increased in only

50% of patients with stage I [Bandiera E et al. 2011]. In the last years, several investigations reported human epididymis protein 4 (HE4) as one of the most promising diagnostic serum marker for EOC, especially in combination with CA-125 [Drapkin R et al. 2005]. Based on these encouraging results, Moore et al. have developed the Risk of Ovarian Malignancy Algorithm (ROMA), a scoring system based on the dual marker combination of HE4 and CA-125, together with menopausal status, which showed an effective performance for the detection of EOC [Moore RG et al. 2009]. Accordingly, nowadays, ROMA is becoming more and more widespread in clinical practice for discrimination of benign masses from EOC.

Over the past two decades, clinical screening trials, aimed at improving early-stage detection strategies of HGSOC, have failed to provide survival benefit. For instance, recent data from the Prostate, Lung, Colorectal and Ovarian (PLCO) trial, a large multicenter prospective study, demonstrated that, despite intensive annual screening for nearly 35,000 women with CA-125 and transvaginal ultrasound, 70% of the women presented with advanced stage disease, which was no different from unscreened populations [Buys SS et al. 2011]. Another recently published UK collaborative trial of ovarian cancer (UKCTOCS), analyzed more than 200,000 postmenopausal women for the predictive role of CA-125 alone or in combination with ultrasound scan. Results showed a modest reduction in mortality, by an estimated 20% after up of 14 years, with almost 50% of ovarian cancer detected by multimodal screening or ultrasound alone [Jacobs IJ et al. 2016]. Although additional analysis are expected to clarify better some points of the study, the modest reduction in mortality mirrors the limited sensitivity and specificity of currently known predictors of disease, like pelvic examination, CA-125 levels and transvaginal ultrasound, which finally impact on the ability to improve early disease detection. On the basis of current results, that have not shown any decrease in morbidity and mortality, widespread screening, using the aforementioned diagnostic methods, is not yet justified. To make a substantial impact on reducing the rate of mortality, the goal in screening should be the early detection of low-volume advanced stage, rather than early stage detection, with the use of highly sensitive and specific biomarkers expressed early in ovarian carcinogenesis [Menon U et al. 2009]. However, at present, the most effective strategy to reduce the mortality in HGSOC patients is the complete surgical removal of the ovaries and fallopian tubes in women who carry germline BRCA1/ BRCA2 mutations or with a strong family history of breast and/or ovarian cancer, as demonstrated by meta-analysis studies [Domchek SM et al. 2010; Rebbeck TR et al. 2009]. Moreover, as most hereditary HGSOC are thought to derive from fallopian tubes, based on the current understanding of HGSOC carcinogenesis, only salpingectomy is recommended in young BRCA1/BRCA2-mutant carriers to avoid the effects of early menopause [Kwon JS et al. 2013]. In this scenario, the advances in genome wide analyses could improve the discovery of new genetic abnormalities associated with HGSOC onset and then promote the identification of women with an increased genetic risk of developing HGSOC.

1.1.7 Standard management

Considering that most HGSOCs are widespread throughout the abdomen at presentation, their frontline treatment consists of surgical tumor debulking, which typically includes a combination of peritoneal washing, hysterectomy, bilateral salpingo-oophorectomy, omentectectomy, lymph nodal and peritoneal biopsies, removing as much of tumor as possible. The main goals of HGSOC surgery are first *to stage* the tumor, defining how far it has spread from the ovaries, and secondly to perform an *optimal-debulking* achieving minimal residual tumor (RT< 1 cm). After surgery, the chemotherapy with a combination of platinum compounds and taxanes represent the gold standard first-line treatment for patients with HGSOC [McGuire WP et al. 1996; Piccart MJ et al. 2000]. Neoadjuvant chemotherapy with interval debulking surgery is another option for patients that present unresectable disease or medical comorbidities, and for whom primary surgery is not considered feasible. However, there are no strong evidences supporting that neoadjuvant chemotherapy before debulking surgery is a superior strategy in term of overall survival (OS) and progression-free survival (PFS) [Gultekin M et al. 2008]. Despite radical surgery and initial high response to first-line chemotherapy, patients frequently experience relapse, with disease that acquires increasing resistance to platinum agent at each recurrence. Recurrent ovarian cancer is classified as platinum resistant, defined as relapsing within 6 months, or platinum sensitive, defined as relapsing more than 6 months after completing initial platinum-based chemotherapy [Chien J et al. 2013]. Patients with platinum resistant disease are typically treated with other agents, such as pegylated liposomal doxorubicin (PLD), topotecan, gemcitabine, weekly paclitaxel, trabectidin or can be enrolled in clinical trials. Platinum-based therapy was introduced in clinical practice in the late 1970s, and subsequently, it was combined with taxanes. Over the past 40 years, only little improvements has been achieved in developing novel high-efficient compounds, with acceptable side effects. Thus, novel therapies are urgently required to improve outcomes of patients with HGSOC. Among the most promising targets identified in ovarian cancer, a leading role belongs to angiogenesis molecules. In recent years, several phase II studies have demonstrated the acceptable toxicity profile and therapeutic activity of Bevacizumab (BV), a monoclonal recombinant antibody that binds VEGF-A, in the treatment of relapsed ovarian cancer [Ellis LM and Hicklin DJ 2008; Raspollini MR et al. 2005]. In 2011, two phase III trials, GOG-02188 and International Collaboration on Ovarian Neoplasms (ICON) 7, reported that the addition of bevacizumab to the combination of carboplatin and paclitaxel, followed by maintenance therapy significantly improved progression-free survival (PFS) (GOG-0218, HR: 0.72, p-value<0.001; ICON7, HR: 0.81, p-value<0.004) [Burger RA et al. 2011; Perren TJ et al. 2011]. These results led the European Medicines Agency (EMA) to the approval of Bevacizumab in combination with carboplatin and paclitaxel as first-line treatment in EOC.

1.1.8 Novel treatment strategies

Currently, novel agents are under investigation in HGSOC medical treatment. In particular, recent genome-wide studies have partially elucidated the mechanisms underlying chemoresistance, and the novel genetic mutations identified can be used as molecular targets for new selective pharmacological agents [Cancer Genome Atlas Research Network 2011; George J et al. 2013; Patch AM et al. 2015]. Different chemotherapeutic agents, such as platinum compounds, liposomal doxorubicin and trabectedin, are observed to have higher response rates in patients with BRCA mutation or with BRCAness phenotype [Yang D et al. 2011]. In this setting, also PARP inhibitors have been studied. PARPs, poly (ADP-ribose) polymerases (PARP), are a family of multifunctional enzymes that play an important role in the repair of DNA single-strand breaks. PARP inhibitors block the enzymatic activity of PARP by attaching to the enzyme's active center and competing with its natural substrate [Rouleau M et al. 2010; Do K and Cehn AP 2012]. The inhibition of PARPs causes the accumulation of DNA single-strand breaks, leading to DNA double-strand breaks. Normal cells are able to repair this damage by homologous recombination but, in BRCA1/2 mutation carriers, these lesions are not repaired, resulting in cell cycle arrest and cell death. The first-in-human clinical trial of the PARP inhibitor Olaparib has been conducted in patients with BRCA1/2-mutated advanced ovarian, breast and prostate cancers. The results from this phase I trial showed that the clinical benefits of Olaparib for BRCA-associated HGSOC was significantly greater in platinum-sensitive disease compared to platinum-resistance and refractory disease [Fong PC et al. 2009]. Olaparib demonstrated a very acceptable side effect profile when compared with conventional chemotherapies. A durable antitumor activity was found in cancer associated with the BRCA1 or BRCA2 mutation. These data indicate that using PARP inhibition to target a specific DNA-repair pathway has the necessary selectivity profile and a wide therapeutic window for BRCA-deficient cells, supporting the clinical relevance of the hypothesis that BRCA mutation-associated cancers are susceptible to a synthetic lethal therapeutic approach [Ashworth A 2008; Kaelin WG 2005]. In the ICEBERG2 study, Audeh et al. provided positive proof of concept of the efficacy and tolerability of genetically targeted treatment with Olaparib in BRCA-mutated advanced ovarian cancer [Audeh MW et al. 2010]. In 2014, EMA approved Olaparib as monotherapy and, currently, it is the best-studied oral PARP inhibitor for maintenance treatment of platinum-sensitive recurrent BRCA-mutated (germ line and/or somatic) HGSOC with clinical response to platinum-based chemotherapy.

1.1.9 Prognostic and predictive factors

Taking in consideration that the majority of patients with HGSOC presents with stage III-IV, it is well recognized that the amount of residual tumor after surgical staging and debulking is the most important prognostic factor. From a clinical perspective, advanced stage means more extensive disease that is less likely to be optimally debulked, compared to a tumor that is confined to the pelvis [Cho KR and Shih IeM 2009; Bristow RE et al. 2002]. In addition, it is important to consider

that the smaller is the residual tumor after surgery, the more effective chemotherapy is likely to be. Patients in whom all macroscopic disease can be completely resected (RT=0) have a significantly better prognosis [Eisenkop SM et al. 2006]. There is some prognostic stratification based on size of residual disease (i.e. RT<1 cm, 1-2 cm, >2 cm) in patients with macroscopic residual disease, but it is relatively minor [Hoskins WJ et al. 1994]. It is not clear at this time whether resectability reflects an intrinsically more favorable disease type, or whether increased surgical effort leads to better outcomes independently of intrinsic tumor characteristics. Actually, it has been showed that tumor molecular traits, as preoperative CA-125 and TP53 mutation, could influence the cytoreductibility of the tumor. In particular, Eltabbakh et al demonstrated that women affected by HGSOC, characterized by strong TP53 mutation, are significantly less likely to achieve complete debulking, than patients harboring tumors with moderate expression of p53 [Eltabbakh GH et al. 2004]. This evidence support the idea that genomic instability and specific genetic aberrations can lead to a more aggressive tumor phenotype, physically more invasive and less resectable. In the last years, an increasing number of studies have been focused on the identification of gene signatures able to explain and predict the response to therapy in HGSOC [Lloyd KL et al. 2015], but with unsatisfactory results. Nowadays, molecular markers of prognosis and response to therapy in HGSOC are relatively few and none has entered into routine clinical practice. Whereas, gene expression based tools, as MammaPrint and Oncotype DX, used to predict metastases and recurrence are already available for other disease, like breast and prostate cancer, respectively [Slodkowska EA and Ross JS 2009; Oncotype DX®]. More recently, studies with paired EOC tumor samples, collected at primary surgery and at following disease relapse, have provided some of the first insights into clonal variations and mechanisms of resistance. [Cooke SL et al. 2010; Stronach EA et al. 2011]**.** Interestingly, Marchini et al, analyzing matched tumor samples collected at first and second surgery, observed a low level (2%) of concordance between matched samples in terms of mutations in genes involved in key processes of tumor growth and drug resistance [Beltrame L et al. 2015]. Moreover, Patch et al, using whole-genome sequencing of tumor and germline DNA samples from 92 primary tumors and matched acquired resistant disease, observed several molecular events associated with platinum-resistance, including reversions of germline BRCA1 or BRCA2 alleles and recurrent promoter fusion associated with overexpression of the drug efflux pump MDR1 [Patch AM et al. 2015]. These results strongly support the necessity to analyze, at the molecular level, biopsies collected during HGSOC disease progression, to identify genomic features involved in drug resistance and to discover new molecular targets for the management of relapsed HGSOC patients.

1.1.10 Tumor microenvironment: Hypoxia

Hypoxia is a common feature of tumor microenvironment, albeit with variable incidence and severity in different tumor types and within a single tumor. The development of rapidly expanding tumor masses, as HGSOCs, require the presence of a vascular network supplying oxygen and nutrients essential for their growth, although, when tumor cell proliferation exceed angiogenesis, the highly abnormal microvasculature fails to cover the oxygen requirement. As a consequence, tumor cells are exposed to an environment chronically deficient in O_2 [Terraneo L et al. 2010]. Cellular adaptive responses to low oxygen microenvironment are mainly orchestrated by the activation of transcription factors called hypoxia-inducible factors (HIFs). Structurally, HIFs are heterodimeric proteins comprising an oxygen-regulated HIF-1α or HIF-2α subunit and a constitutively expressed HIF-1β subunit. While HIF1β is constitutively expressed, HIF-α levels are tightly regulated in response to changes in oxygen tension. In normoxia, HIF-α subunits are undetectable due to rapid hydroxylation by the von Hippel Lindau protein (pVHL) and to immediate degradation by the ubiquitin-proteasome system. Under hypoxic conditions, however, HIF-α proteins are stabilized from degradation for heterodimerization with HIF-1β. Once formed, this heterodimer binds to hypoxia response elements (HREs), in the promoter regions of specific hypoxia-sensitive genes, and thereby induce downstream transcription [Hashimoto T and Shibasaki F 2015]. The persistent exposure of tumor cell to hypoxia, or low oxygen tension, induces pro-survival changes in gene expression and in particular the activation of the angiogenic process, termed “angiogenic switch”. Angiogenesis, which is the process of developing new microvessels from pre-existing ones, is tightly regulated by a balance of pro-angiogenic mediators, like vascular endothelial growth factor (VEGF)-A and anti-angiogenic mediators, like angiopoietins (Ang1 and 2). HGSOCs express high levels of pro-angiogenic factors that contribute to the progression and aggressiveness of the disease [Gómez-Raposo C et al. 2009]. For this reason, important effort has gone into discovering novel anti-angiogenic agents in HGSOC, as Bevacizumab. As aforementioned, this immunoglobulin G1 monoclonal antibody targeting VEGF-A has been approved in clinical practice, in addition to platinum and taxane combination, in the first-line setting and in maintenance therapy, in patients with advanced stage ovarian cancer. However, despite the presumed stability of the tumor endothelium, resistance to anti-VEGF agents has rapidly emerged in those patients. It has been hypothesize that the VEGF blockage could intensify the oxygen deprivation, leading to an increased hypoxic state in the tumor microenvironment. In support to this hypothesis, *in-vivo* studies have showed that the cleavage of blood vessels could further stimulate tumor cells to acquire invasive and metastatic features, showing an extremely capability of tumor cells to adapt and survive in hypoxic conditions [Paolicchi E et al. 2016; Choi HJ et al. 2015; Sennino B and McDonald DM 2012]. This tumor cell adaption to hypoxia, supported by a high genomic instability, is one of the main problem in fighting cancer. Indeed, hypoxia plays an active role in tumor progression, and confers increased resistance to standard chemo- and radio-therapies in cancer cells [Cavazos DA and Brenner AJ 2015].

1.2 Non-coding RNAs

1.2.1 Background

The completion of the Human Genome project revealed that the protein coding genes (around 20000) cover less than 2% of the entire genome [ENCODE Project Consortium 2007]. This suggested that the majority of the genome, of mammals and other complex organisms, that was commonly defined 'junk DNA', due to its overwhelming burden of transposons, pseudogenes, and simple sequence repeats [de Koning AP et al. 2011], is transcribed into non-coding RNAs (ncRNAs), many of which are alternatively spliced and/or processed into smaller products. As represented in Figure 1.3, at present, ncRNAs are mainly categorized as "housekeeping", a group of ncRNAs constitutively expressed, and regulatory ncRNAs. The first class includes ribosomal RNA (rRNA), transfer RNA (tRNA), splicing RNA (sRNA), nucleolar RNA (snoRNA) and small nuclear RNA (snRNA). Whereas, the regulatory ncRNA class includes different molecules that have crucial roles in the control, at various levels, of gene expression in physiology and development, including chromatin architecture/epigenetic memory, transcription, RNA splicing, editing, translation and turnover. Currently, regulatory ncRNAs include small ncRNAs (less than 200 nucleotides), comprising small interfering RNA (siRNA), piwi-interacting RNA (piwiRNA), and microRNA (miRNA) [Kim VN et al. 2009]. In addition, more recently, another subtype of regulatory ncRNA, endogenous cellular RNAs of more than 200 nucleotides in length, termed long ncRNAs, has been included. Long ncRNAs can act in different ways in the cell; for instance, they regulate gene expression and influence protein localization [Kung JT et al. 2013; Gutschner T and Diederichs S 2012].

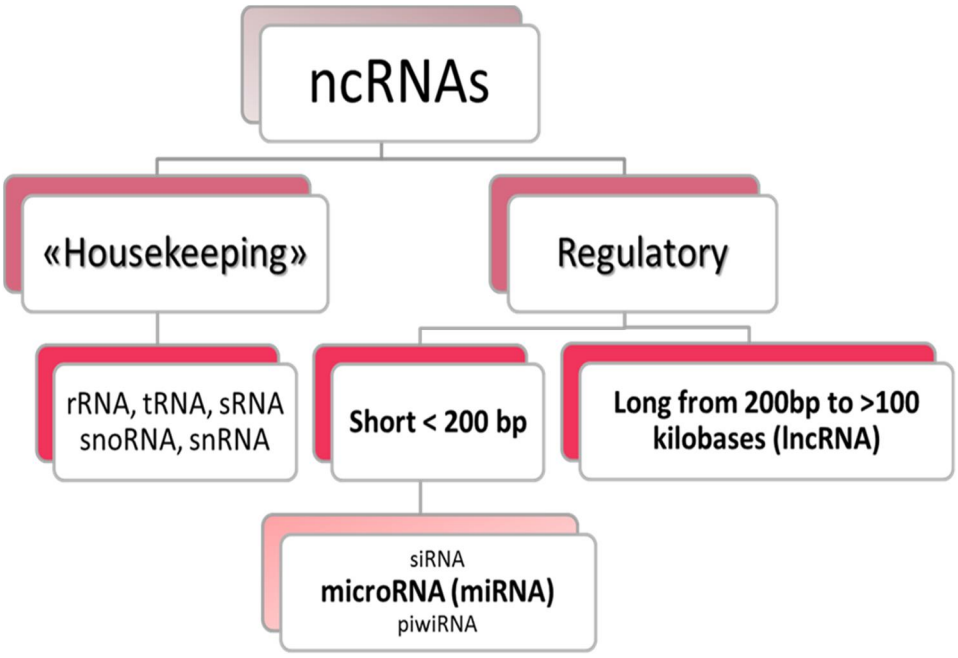

Figure 1.3: Non-coding RNAs in mammalian cells.

1.2.2 microRNAs

microRNAs (miRNAs or miRs) are endogenous, small non-coding single-stranded RNAs of ~22 nucleotides in length, highly conserved in a wide range of species, which function at post-transcriptional level as negative regulators of gene expression. miRNAs were first described in 1993, when a small RNA, *lin-4*, was discovered to negatively regulate LIN-14 levels, a protein involved in the developmental timing of the nematode *C.Elegans* [Lee RC et al. 1993]. However, the term 'microRNA' was only coined in 2001, when tens of small RNAs with regulatory potential were discovered in *C.Elegans* [Lee RC and Ambros V 2001]. Since then, hundreds of similar small RNAs and number of different mechanisms for translational control by small RNAs in *C.Elegans, Drosophila* and mammals have been discovered. miRNAs play critical regulatory roles in the coordination of a wide variety of critical cellular processes like proliferation, differentiation, cell cycle regulation, apoptosis, stem cell maintenance, hypoxia and metabolism. miRNA expression is highly cell type and tissue specific, and it is present at different developmental stages, suggesting their important regulatory functions. Additionally, miRNAs are involved in pathological conditions like cardiovascular disease, obesity and cancer [Dalmay T and Edwards DR 2006; Hwang HW and Mendell JT 2006].

To date, approximately 2,000 human hairpin precursor miRNAs, expressing 2,588 mature miRNA sequences have been annotated in the miRNA registry (http://www.mirbase.org/, miRBase release 21, updated 2014), targeting and regulating the majority of coding genes [Kozomara A and Griffiths-Jones S 2014]. Typically, both the gene locus and precursor miRNA (pre-miRNA) of a miRNA is referred as "mir", while the mature miRNA product is designated "miR". Each miRNA is preceded by three letters specific for each species, for humans (Homo sapiens) those letters are "hsa" (e.g. hsa-miR-200). miRNAs have been numbered in order of discovery. Multiple miRNAs can be evolutionary related, with a nearly identical sequence, thus a letter after the number is used to differentiate among multiple members of the same family (e.g. hsa-miR-200a and hsa-miR-200b). If different genomic loci produce identical miRNAs, additional number is given after the full name (e.g. hsa-miR-200-1 and hsa-miR-200-2). Two miRNAs, originating from opposing sides of the same double-stranded RNA, are named with a tag indicating from which mature sequence comes from (e.g hsa-miR-200a-3p from the 3' arm and hsa-miR-200a-5p from the 5' arm) (http://www.mirbase.org/).

1.2.3 miRNA biogenesis and mechanisms of action

miRNA biogenesis in human cells is a complex process comprising multiple steps, as illustrated in Figure 1.4. miRNAs can be organized as individual genes in intergenic regions or in genic regions (usually in introns or in non-coding exons), or localized as clusters representing miRNA families, which are commonly related in sequence and function. miRNAs are mainly transcribed by RNA polymerase II (rarely by RNA polymerase III) into long primary miRNA transcripts, either alone or in clusters, and folded into typical hairpin structurers of variable size, having a 5' cap and a 3' poly-A-

tail, known as primary miRNAs (pri-miRNAs). Subsequently, these pri-miRNAs are recognized and cleaved in the nucleus by the Microprocessor complex, containing RNase III enzyme Drosha ant its cofactor RNA binding protein, DiGeorge Syndrome Critical Region 8 (DGCR8), resulting in individual stemloop hairpin precursor miRNAs (pre-miRNAs) [Lee Y et al. 2004]. Then, pre-miRNAs are actively and rapidly exported from the nucleus to the cytoplasm by Exportin 5, a Rna-GTP dependent nuclear export receptor. In the cytoplasm, pre-miRNAs are further processed by another RNase III enzyme, called Dicer, and its RNA binding co-factor TRBP (the human immunodeficiency virus transactivating response RNA-binding protein), into a transient 19–24 nucleotide imperfect miRNA/miRNA* duplexes [Bohnsack MT et al. 2004]. Only one strand of the miRNA duplex (mature miRNA) is incorporated into a large protein complex, called RNA-induced silencing complex (RISC), containing Argonaute proteins (AGO1-AGO4). Each of the four AGO proteins possesses repressive capabilities, but only AGO2 has the potential to cleave target sequences due to its RNaseH-like domain [Peters L and Meister G 2007]. The mature miRNA leads RISC to cleave mRNA, to induce translational repression or to enhance mRNA degradation, depending on the degree of complementarity between the miRNA and its target [Hutvanger G and Zamore PD 2002]. The last two processes are more commonly associated with mismatched miRNA/target sequences that are the most likely scenario in mammals. Although the most frequent site of interaction is the 3' untranslated region (UTR) of the target mRNA, several miRNAs have been described to bind to the open reading frame (ORF) sequences, as well as to the 5'UTR [Lytle JR et al. 2007]. This final interaction has been associated with activation, rather than repression. miRNAs can also bind directly to proteins, in particular RNA-binding proteins, in a sequence-dependent manner and prevent these proteins from binding to their RNA targets. These decoy activities of miRNAs are RISC-independent [Eiring AM et al. 2010]. miRNAs can also regulate gene transcription by binding directly or by modulating methylation patterns at the target gene promoter level [Gonzalez S et al. 2008; Kim DH et al. 2008].

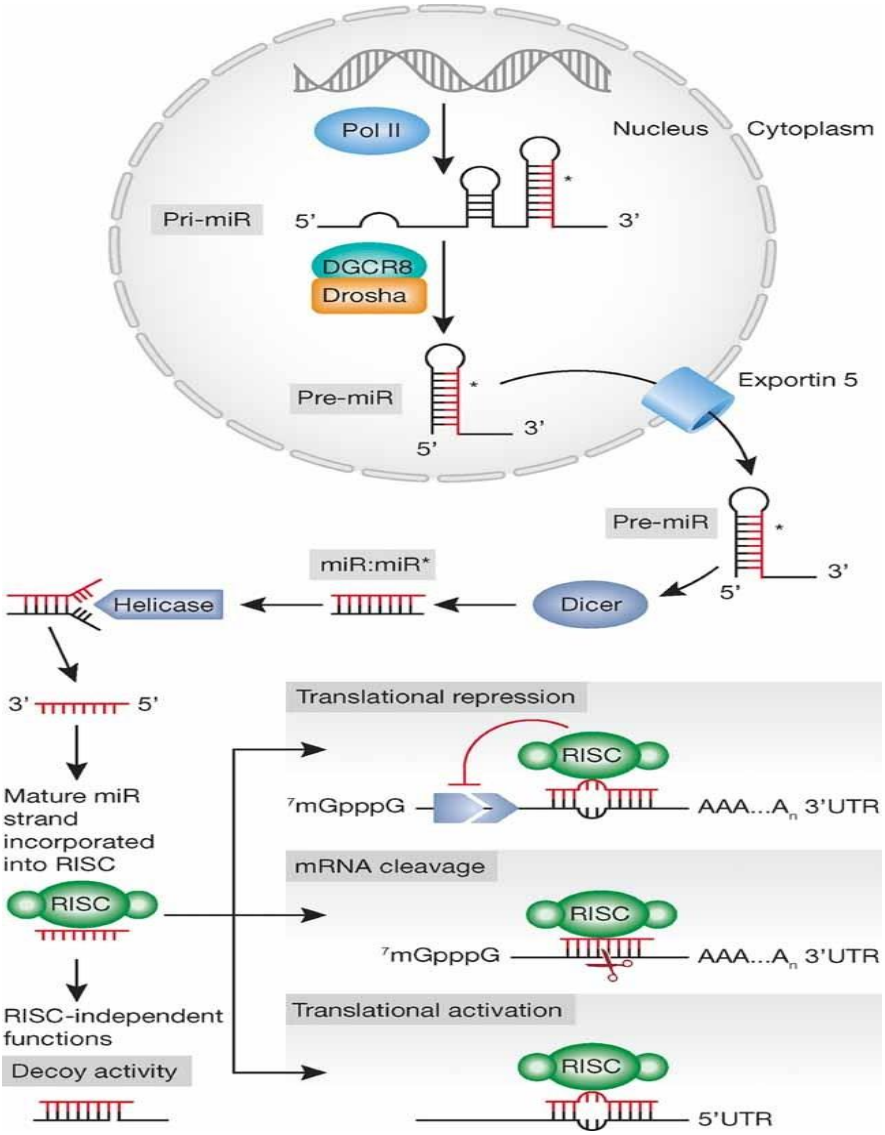

Figure 1.4: microRNA biogenesis and effector pathways.

1.2.4 miRNA involvement in human cancer

Cancer development and progression, associated with an abnormal alteration in several biologic mechanisms, such as, in particular, proliferation and apoptosis, not only lead to a misregulation of a plethora of protein-coding genes, but also to a global change in miRNA expression profile. The first evidence of miRNA involvement in human cancer disease has emerged from chronic lymphocitic leukemia studies. Croce et al identified the tumor suppressor miR-15/miR-16-1 cluster, located in a critical region of CLL frequently deleted [Cimmino A et al. 2005]. A couple of years later, all the known miRNA genes were mapped and many of them were found in genomic regions involved in cancer. In particular, miRNA genes were frequently located in regions showing chromosomal alterations, such as amplification or loss of heterozygosity and mutations, or in

fragile sites and common breakpoint areas near oncogenes or tumor suppressors genes [Calin GA et al. 2004]. In addition to structural genetic alterations, other mechanisms may affect miRNA dysregulation in cancer, as histone deacetylase inhibition and promoter hypermethylation. For instance, many genomic sequences of miRNA genes were found associated with CpG islands [Weber B et al. 2007]. Moreover, mutations in miRNA target site or in miRNA mature sequences can occur, inducing imperfect target recognition and inhibition of downstream protein complex processes. Deregulation in miRNA expression can be also affected by alteration in the miRNA biogenesis machinery. For instance, studies have reported a significant association between loss of Dicer and/or Drosha and outcome of patients, in several types of tumor, as lung cancer and ovarian carcinoma. Furthermore, miRNA expression profiles can be influenced by changes in the tumor microenvironment, such as tumor hypoxia [Kulshreshtha R et al. Mar 2007; Kulshreshtha R et al. Jun 2007; Giannakakis A et al. 2008; Kulshreshtha R et al. 2008; Crosby ME et al. 2009;]. On the regulation of gene expression, miRNAs may act as oncogenes or tumor suppressors, depending on whether they target tumor suppressor genes or oncogenes, respectively. Interestingly, the activity of miRNAs is high-context dependent. Indeed, the same miRNA can act as an oncogene in one type of cells and as a tumor suppressor in another, suggesting important regulatory functions [Croce CM 2009]. Accordingly, oncogene miRNAs are often overexpressed in some cancer types, whereas, in other cancers, when they act as tumor suppressor, they are commonly down-regulated. For example, miR-221/222 cluster, generally, is up-regulated and acts as oncogene targeting some important tumor suppressor genes (PTEN, p27 and p57), increasing proliferation of cancer cells in breast, lung and liver cancer. Conversely, the same cluster is down-regulated in erythroblastic leukemias, where it targets c-KIT oncogene [Garofalo M et al. 2012]. In the last years, the advent of high-throughput profiling techniques, as miRNA microarrays and RNA-Seq (RNA Sequencing), improved the miRNA expression analysis [Creighton CJ et al. 2009; Farazi TA et al. 2011]. In particular, It has been revealed a role of miRNAs in tumor progression, through targeting mRNAs involved in cell survival, proliferation, differentiation, angiogenesis and apoptosis, but specific miRNA pattern profiles have been discovered in different cancer types. Moreover, miRNA expression profiles have been correlated with clinical and biological features of tumors, including histological type, differentiation, aggressive behavior, prognosis and response to therapy. miRNA profiles can distinguish not only between normal and cancerous tissue and identify tissues of origin, but they can also discriminate different subtypes of a particular cancer or even specific oncogenic abnormalities: miRNAs, for example, are differentially expressed between basal and luminal breast cancer subtypes [Sempere LF et al. 2007] and can specifically classify estrogen receptor, progesterone receptor and HER2/neu receptor status [Iorio MV et al. 2005]. Even more importantly, several groups in recent years have reported how miRNA profiling can predict disease outcome or response to therapy [Li X et al. 2010; Caramuta S et al. 2010], for example miR-155 overexpression and let-7a downregulation, which are able to predict poor disease outcome in lung cancers [Yanaihara N et al. 2006]. The evaluation of miRNA expression predicting the response to

specific drugs is another important goal, since it might help for a more accurate selection of patients potentially responsive to a specific therapy. For example, high miR-21 expression levels were detected to be associated with worse survival and poor response to adjuvant chemotherapy, both in colon adenocarcinomas [Schetter AJ et al. 2008] and in pancreatic cancer patients treated with gemcitabine [Giovannetti E et al. 2010]. In summary, the potential of miRNA signatures to distinguish between tumor and normal tissues, to discriminate between different subgroups of tumors and to predict outcome and response to therapy has focused scientists' attention on these small molecules as potential clinical biomarkers, either diagnostic, predictive or prognostic.

1.2.5 miRNAs in ovarian cancer tissues

In the last years, several studies have demonstrated that several miRNAs are considerably dysregulated in advanced stage or high-grade ovarian cancers (OCs), suggesting their important roles in malignant transformation and tumor progression. Zhang et al reported that OC is characterized by massive miRNA deregulation, mainly due to genetic and epigenetic mechanisms [Zhang L et al. 2008]. Deletion occurs in up to 15% of genomic loci harboring miRNAs and epigenetic silencing is involved in 30% of down-regulated miRNAs, while mutations in cancer-associated miRNAs are rare in OC [Katz B et al. 2015]. Actually, despite multiple studies showed altered miRNA expression pattern in OC tumor cells compared to normal tissues, there is only a little overlap between the results of these studies. These inconsistent data may be explained by some different aspects: the source of the samples used (flash frozen tissues, formalin fixed paraffin embedded tumors, cell line cultures), the inclusion criteria (histotype, stage, grade), the source of the normal tissues (ovarian surface epithelium brushing, ovarian biopsies, cell line cultures), the size of the study cohort and technical variables (sample management, RNA extraction protocol and platforms used for miRNA analyses). In 2007, Iorio et al published the first report regarding miRNA expression in OC compared to normal ovarian tissue. They found a total of 29 miRNAs dysregulated between groups. In particular, four miRNAs (miR-141, miR-200a, miR-200b, and miR-200c) emerged up-regulated, while 25 were down-regulated, including miR-199, miR-140, miR-145, and miR125b1 in cancer samples [Iorio MV et al. 2007]. Later, in 2008, Zhang et al, comparing 18 EOC cell lines and four immortalized cell lines derived from OSE, found four miRNAs over-expressed in EOC cell lines and 31 miRNAs down-regulated, including the tumor suppressor miRNAs let-7d and miR-127 [Zhang L et al. 2008]. These studies showed that miRNA expression profiles could distinguish malignant from normal ovarian surface epithelium. Since then, several studies have investigated the differences between the miRNA profiles of ovarian surface epithelium and OC, and the potential role of miRNAs in OC diagnosis, prognosis and treatment. Two of the most frequently identified deregulated miRNAs in OC are the miR-200 and the let-7 families. The miR-200 family consists of five miRNAs (miR-200a, miR-200b, miR-200c, miR-141 and miR-429) arranged in two clusters in the human genome. miR-200a, miR-200b and miR-429 are located on chromosome 1, while miR-200c and miR-141 are on chromosome 12 [Park SM et

al. 2008]. In several studies, the expression of miR-200 family members has been associated with survival in EOC patients. In particular, Nam et al, using DNA microarray and northern blot analyses, identified 23 miRNAs differentially expressed between 20 serous OC tissues and eight normal ovarian tissues. They observed that high expression of miR-200a/b/c, miR-18, miR-93, miR-141, and miR-429 and low expression of let-7b and miR-199a significantly correlated with PFS and OS [Nam EJ et al. 2008]. Hu et al, in a study including 55 patients with stage III and IV of all histologic subtypes, showed a decreasing expression of miR-200a/b/c and miR-429 in patients with recurrence compared to recurrence free patients [Hu X et al. 2009]. Moreover, Marchini et al demonstrated that loss of miR-200c was associated with poor PFS and OS, in multivariate analysis of stage I EOC [Marchini S et al. 2011]. Currently, as emerged from the diverging results in above citied studies, the prognostic role of miR-200 family in EOC is not completely elucidated. The miR-200 family members have been shown to play a critical role in the suppression of epithelial to mesenchymal transition (EMT). Park et al observed a positive correlation in the expression of E-cadherin with the expression of miR-200c in ovarian cancer tissues. Actually, the over-expression of miR-200 a/b/c and/or miR-141 seems to down-regulate ZEB1 and ZEB2 levels, and leads to higher levels of E-cadherin and an epithelial phenotype [Park SM et al. 2008].

The let-7 (lethal-7) family includes 13 human homologs tumor suppressor miRNAs located on nine different chromosomes. These loci have been identified situated in cancer-associated regions or in fragile sites and are typically down-regulated in OC [Dahiya N et al. 2008]. Let-7 suppresses multiple ovarian cancer oncogenes, which include KRAS, HRAS, c-Myc and HMGA-2 [Johnson SM et al. 2005; Büssing I et al. 2008]. Low expression of the let-7 family has been identified as a potential marker for early diagnosis, and associated with a decreased overall survival in several studies of OC [Yang N et al. 2008; Nam EJ et al. 2008]

A number of studies attempted to identify specific miRNA expression profiles according to histological subtypes. Particularly, Iorio et al showed that miR-200a and miR-200c were over-expressed in three types of ovarian cancer: serous, clear cell, and endometrioid. Whereas, miR-200b and miR-141 were up-regulated in endometrioid and mucinous carcinoma [Iorio MV et al. 2007]. Calura et al performed a miRNA array analysis of 257 stage I EOC of different histotypes. They found high expression levels of miR-30a-3p and miR-30a-5p in clear cell carcinoma (CCC), whereas mucinous carcinoma (MC) expressed high levels of miR-192 and miR-194 [Calura E et al. 2013]. Moreover, Vilming Elgaaen et al identified 12 miRNAs differently expressed between CCC and HGSOC. In particular, miR-509-3-5p, miR-509-5p, miR-509-3p, miR-508-5p, and miR-510 were the most dysregulated miRNAs between histotypes [Vilming Elgaaen B et al. 2014]. Therefore, further investigations on the potential of these miRNAs to classify OC histological subtypes are needed.

The most important milestone of integrated genomic analysis in HGSOC has been recently provided by TCGA on a total of 489 HGSOC samples. Cluster analysis on miRNA expression data defined three subtypes of HGSOC. Notably, miRNA subtype 1 overlapped the mRNA *Proliferative*

subtype and miRNA subtype 2 overlapped the mRNA *Mesenchymal* subtype, both above mentioned [Cancer Genome Atlas Research Network 2011]. TCGA has offered the foundations for many other studies investigating HGSOC prognosis. In particular, Yang et al, using the TCGA database, identified a miRNA-regulatory network that defined a robust integrated mesenchymal subtype associated with poor overall survival in 459 cases of serous ovarian cancer and 560 cases of an independent data cohort. Moreover, these analyses highlighted the central role of a miRNA regulatory network, consisting of eight miRNAs (miR-25, miR-29c, miR101, miR-128, miR-141, miR-182, miR-200a and miR-506) and predicted to regulate the 89% of targets in the mesenchymal subtype of HGSOC [Yang D et al. 2013]. Creighton et al, referring to the catalog of TCGA, developed an integrated analysis to improve the in silico miRNA-gene targeting predictions and to demonstrate the rich resource of TCGA in identifying miRNA candidates for functional targeting in cancer [Creighton CJ et al. 2012].

As aforementioned, it has been shown that miRNAs could play a crucial role in response to chemotherapy treatment in OC. A total of 27 miRNAs have been associated with responsiveness to chemotherapy [Hong L et al. 2013]. Yang et al. found that miR-214, which targets PTEN, is frequently expressed in ovarian cancer tissues and that let-7i, which enhances resensitization to platinum resistance, is expressed less in the same tissues [Yang N et al. 2008]. Aqeilan et al. found that miR-15 and miR-16 cause cellular resistance to many drugs, through targeting the BCL2 gene [Aqeilan RI et al. 2010]. Leskelä et al showed that the miR-200 family (miR-141, miR-200a, miR-200b, miR-200c, and miR-42) is implicated in the response to paclitaxel treatment and progression-free survival, via tubulin III regulation. In particular, miR-200c is significantly associated with recurrence of ovarian cancer and miR-429 is associated with progression-free and overall survival rates [Leskelä S et al. 2011]. In a study conducted on a total of 198 serous ovarian cancer samples, Vecchione et al identified miR-217, miR-484 and miR-618 able to predict the chemoresistance of these tumors. They also demonstrated that miR-484 was able to improve chemosensitivity through the regulation of angiogenesis, by targeting VEGFR2 [Vecchione A et al. 2013]. Additionally, a recent study has shown that let-7g selectively affects the sensitivity of a drug resistant ovarian cancer cell to taxanes by targeting IMP-1, an RNA binding protein which stabilizes MDR-1 (multidrug resistance-1), a membrane protein that pumps drugs into the extracellular space. Accordingly, the expression of let-7g resulted in a decrease in MDR-1 protein levels and sensitized the cells to taxane treatment [Boyerinas B et al. 2012]

A novel potential treatment option for ovarian cancer includes supplementation of miRNAs that are down-regulated in cancer tissue for recovery of function and inhibition of the function of up-regulated miRNAs by administration of complementary nucleic acids. Garzon et al showed that the effect of up-regulated oncomiR could be suppressed using an antagomir, an oligonucleotide complementary to the miRNA administered as an antisense oligonucleotide [Garzon R et al. 2010]. Dai et al established a therapy for ovarian cancer based on targeted delivery of miR-29a to cancer tissues for the purpose of reexpressing PTEN, a tumor suppressor. The potential antitumor effect

of a miR-29a-transfected chimera was apparently based on expression of downstream molecules and apoptosis of ovarian cancer cells [Dai F et al. 2012]. Cittelly et al found that recovery of the level of miR-200c by transfection, which is known to increase sensitivity to platinum-based anticancer drugs, suppressed carcinogenesis and decreased the number of cancer cells. The recovery of miR-200c immediately before highly cytotoxic chemotherapy improves the treatment response or reduces the effective dose of the anticancer drugs [Cittelly DM et al. 2012]. These functional studies suggest that the modulation of miRNA misexpression is an attractive target for cancer therapeutics. However, before proceeding with clinical trials, additional analyses and validations of the administration of complementary nucleic acids, as miRNA mimics and antisense mRNAs, both *in-vitro* and *in-vivo*, are necessary to better verify their efficacy.

1.2.6 Circulating miRNAs in cancer

In the last years, several investigations have discovered that miRNAs can move from tumor tissue to blood circulation. Circulating miRNAs are extremely stable and can withstand multiple freeze-thaw cycles, long period of storage, temperature and pH changes and show resistance to blood RNase activity [Chen X et al. 2008]. Indeed, serum and other body fluids are known to contain ribonucleases, but the majority of miRNAs are packaged with ribonucleoproteins, as Argonaute2 proteins, protecting them against enzyme digestion. Furthermore, several studies have identified miRNAs complexed with lipoproteins and two types of cell-derived lipid vesicles: exosomes and microvesicles. Lipoproteins are complexes that consist of a lipid core surrounded by a shell of apolipoproteins that allow the lipids to travel in the bloodstream. Exosomes are small (30-100 nm) lipoprotein vesicles, that are released into the extracellular environment when endosomally-derived multivesicular bodies fuse with the plasma membrane. Microvesicles are larger than exosomes (100nm-1μm) and are released from the plasma membrane of stimulated cells [Etheridge A et al. 2011]. Lawrie et al detected, for the first time, the presence of serum miRNAs in cancer patients. They found that miR-155, miR-210, and miR-21 were higher in serum from patients with diffuse large B-cell lymphoma, and high level of miR-21 expression was associated with patients' relapse free survival [Lawrie CH et al. 2008]. Subsequently, serum miRNAs were tested as biomarkers for disease monitoring in prostate cancer, and for the early detection both in the lung and colorectal carcinomas. Moreover, similar studies have been performed in many types of cancer including gastric, breast and ovarian cancer [Zhu C et al. 2014; Shimomura A et al. 2016; Nowak M et al. 2015]. Currently, miR-test, based on a serum signature of 13 miRNAs, represents one of the most promising tool for lung cancer screening in high-risk individuals [Montani F et al. 2015]

1.2.7 Circulating miRNAs in ovarian cancer

Given the stability of miRNAs in the peripheral blood and tumor-specific miRNA profiling, circulatory miRNAs may be superior potential biomarkers for ovarian cancer diagnosis and prognosis than tissue miRNAs. In recent years, several circulating miRNAs have been identified as

biomarkers with implications in ovarian cancer early detection, association with clinicopathological features and prognosis. The differentially expressed miRNAs of each study are summarized in Table 1.1. The first study in OC was performed by Taylor et al in 2008, investigating exosomes from the peripheral blood circulation of ovarian cancer patients. They found that the eight miRNAs over-expressed in serous ovarian cancer tissue (miR-21, miR-141, miR-200a, miR-200b, miR-200c, miR-203, miR-205 and miR-214) were also elevated in serum-derived exosomes. These circulating miRNA levels were also significantly higher compared with those detected in patients with benign disease [Taylor DD and Gercel-Taylor C 2008]. In another study, Resnick et al empirically selected 21 miRNAs from the OC tissue profile. They identified five miRNA significantly over-expressed (miR-21, miR-29a, miR-92, miR-93 and miR-126) and three under-expressed (miR-127, miR-155 and miR-99b) in the serum of OC patients compared with controls [Resnick KE et al. 2009]. Kan et al confirmed the overexpression of miR-200a, miR-200b and miR-200c in serum of serous OC patients, compared to controls. Moreover, a multivariate model combining miR-200b and miR-200c was able to discriminate patients with HGSOC from age-matched healthy donors [Kan CW et al. 2012] Another study on serous OC was conducted by Chung et al using microarray and RT-qPCR. They detected four serum miRNAs (miR-132, miR-26a, let-7b, miR-145) significantly down-regulated in OC patients compared to controls, making these miRNAs potential candidates for novel diagnostic biomarkers [Chung YW et al. 2013]. Zheng et al performed a study on a large cohort of plasma samples of 360 OC patients and 200 healthy controls, grouped into screening, training and validation sets. Using TaqMan low-density array, they identified higher miR-205 and lower let-7f expression in plasma samples from tumor patients compared to controls. Moreover, the two miRNA combination provided a higher diagnostic accuracy for OC, especially in patients with stage I disease [Zheng H et al. 2013]. For the first time, Shapira et al conducted a study focused on protein-bound miRNA in plasma free of cellular debris, microvesicles or exosomes. A total of 19 miRNAs emerged down-regulated, while three were up-regulated in serous OC compared to controls. In particular, six miRNAs (miR-106b, miR-126, miR-150, miR-17, miR-20a and miR-92a) resulted significantly decreased in OC patients [Shapira I et al. 2014]. Recently, Langhe et al, using the Exiqon discovery platform, identified a panel of four miRNAs (let-7i-5p, miR-122, miR-152-5p and miR-25-3p) significantly down-regulated in cancer patients, compared to patients with benign serous cystoadenomas [Langhe R et al. 2015]. Recently, Zuberi et al confirmed the members of the miR-200 family overexpressed and associated with tumor progression in OC samples [Zuberi M et al. 2015]. Moreover, the same group investigated the expression level of miR-199a by RT-qPCR. A significant down-regulation of miR-199a levels has emerged in the group of tumor patients compared with matched normal controls and its expression were significantly associated with more aggressive clinicopathological features [Zuberi M et al. 2016]. More recently, serum levels of exosomal miR-373, miR-200a, miR-200b and miR-200c were found significantly higher in OC patients than healthy donors, by TaqMan MicroRNA assay. In particular, members of miRNA-200 family were able to discriminate between malignant and benign

ovarian tumors. Moreover, miR-200b and miR-200c were observed significantly increased in advanced stage OC, suggesting a possible involvement in tumor progression [Meng X et al. 2016]. The above mentioned studies suggest that circulating miRNAs may be powerful diagnostic and prognostic tools in ovarian cancer patients. However, at present, the inconsistent results across studies do not support their application as biomarkers in daily clinical ovarian cancer management. Studies performed in large well-characterized cohorts and independently validated are urgently needed, before any clinical value of circulating miRNAs can be evaluated.

Table 1.1: Studies on circulating miRNAs as potential biomarkers of ovarian cancer

Authors	Years	Type of tissue	Histology	Control	Up-regulated miRNAs	Down-regulated miRNAs	Discovery platform
Taylor et al.	2008	Serum exosome	Serous	Benign ovarian tumor	miR-21,miR-141, miR-200a,b,c, miR-203, miR-205,miR-214	–	Custom microRNA arrays
Resnick et al.	2009	Serum	EOC	Healthy control	miR-21,miR-29a, miR-92, miR-93, miR-126	miR-127, miR-155 miR-99b	TaqMan array RT-qPCR
Hausler et al.	2010	Whole blood	EOC	Healthy control	miR-30c1	miR-342-3p miR-181a miR-450-p	Geniom Biochip
Kan et al.	2012	Serum	HGSC	HOSE/healthy control	miR-200a,b,c	–	TaqMan assays
Chung et al.	2013	Serum (tissue and ascites)	Serous	Healthy control	–	miR-132 miR-26a let-7b,miR-145	Microarray RT-qPCR
Zheng et al.	2013	Plasma	EOC	Healthy control	miR-205	let-7f	TaqMan Low-density array RT-qPCR
Xu et al.	2013	Serum	EOC	Healthy control	miR-21	–	RT-qPCR
Hong et al.	2013	Serum	EOC	Healthy control	miR-221	–	RT-qPCR
Ji et al.	2014	Serum	EOC	Healthy control/benign ovarian tumors	miR-22, miR-93	–	Solexa sequencing
Shapira et al.	2014	Plasma	serous	Healthy control/benign ovarian tumor	–	miR106a,126,146 a,150,16,17,19b, 20a,223,24,92a	TaqMan Open Array MicroRNA
Langhe et al.	2015	Serum	serous	Benign ovarian tumor	–	let-7i-5p,miR-122, miR-152-5p, miR-25-3p	Exiqon panel RT-qPCR
Gao et al.	2015	Serum	EOC/ borderline	Healthy control	miR-200c,miR-141	–	RT-qPCR
Zuberi et al.	2015	Serum	EOC	Healthy control	miR-200a,b,c	–	RT-qPCR
Zuberi et al.	2016	Serum	EOC	Healthy control	–	miR-199a	RT-qPCR
Meng et al.	2016	Serum exosomes	EOC	Healthy control	miR-373, miR-200a,b,c	–	TaqMan assay

1.2.8 miRNA involvement in hypoxic condition

Over the past few years, the “classic” protein coding hypoxia-regulated genes have been joined by specific miRNAs, thus adding a new paradigm of gene expression regulation in an already complex process and providing an additional link between tumor-specific stress factor and gene expression control. The first evidence of an hypoxic cancer-related miRNA signature was described by Kulshreshtha et al. They reported a group of miRNAs that included: miR-21,23a, 23b, 24, 26a, 26b, 27a, 30b, 93, 103, 106a, 107, 125b, 181a, 181b, 181c, 192, 195, 210 and 213, which were consistently expressed in response to low oxygen tension, in breast and colon cancer cell lines. [Kulshreshtha R et al. 2007 Mar]. These miRNAs, differently expressed in response to hypoxia, have been collectively termed “hypoxia-regulated miRNAs” (HRMs) or later, “hypoxamiRs”. During the last years, numerous studies have reported different hypoxic miRNA signatures, comprising more than 90 HRMs~~,~~ in a variety of cellular types and conditions. However, a significant number of HRM lists were not consistent across studies. This discrepancy was not surprising and could be attributable to a combination of technical variables, as the sensitivity of analysis methods, the duration and severity of oxygen deprivation, the cellular types and context. To date, miR-210 represents a unique HRM consistently reported up-regulated from multiple independent research groups, being robustly induced by HIF-1α, in a wide range of cell types in response to hypoxia [Chan SY and Loscalzo J 2010]. Furthermore, miR-210 has been identified over-expressed in a variety of cancer, including breast, glioblastoma, lung, melanoma, prostate and many others, with the exception of ovarian cancer, in which has been reported a frequent gene deletion, by Giannakakis et al and Vaksman et al [Giannakakis A et al. 2008; Vaksman O et al. 2011]. In a large genome-wide microarray profiling study, conducted by Volinia et al on a total of 540 tumor samples (including breast, lung, colon, stomach, prostate carcinomas and pancreatic endocrine tumors), a “common signature” of abnormally expressed miRNAs has emerged, compared to normal tissues [Volinia S et al. 2006]. In order to identify a possible correlation between the miRNA signature expression in solid tumors and in hypoxic condition, Kulshreshtha et al examined the pattern of miRNA changes during hypoxia within the same miRNA profile obtained by microarray. Notably, most of HRMs resulted overexpressed in at least some of analyzed tumors [Kulshreshtha et al. Mar 2007]. This result suggested that hypoxia may contribute to miRNA dysregulation in different types of cancer. In cellular adaptation to hypoxia, HRMs can play different roles, targeting important gene transcripts implicated in a wide range of processes, as metabolic reprogramming, DNA repair, apoptosis and angiogenesis, among many other cellular adaptations to low oxygen availability. Many HRMs can play an active role on HIF and promote its expression and/or activity. Some of these miRNAs are also direct transcriptional targets of HIF itself during hypoxia, resulting in a positive-feedback loops. For example, miR-210 is potently induced by HIF in response to hypoxia, and could repress glycerol-3-phosphate dehydrogenase 1-like (GPD1L), which, in turn, stabilize HIF1 by reducing hyperhydroxylation [Kelly TJ et al. 2011]. Moreover, the down-expression of miR-20b, miR-199a, and cluster miR-17-92 in hypoxia conditions, stabilize HIF1,

because these HRMs are able to repress the expression of HIF1 through direct targeting. In hypoxic endothelial cells, miR-424 is able to stabilize HIF1, suppressing cullin 2 (CUL2), a scaffolding protein critical to the assembly of the ubiquitin ligase [Ghosh G et al. 2010]. Many other HRMs, that contain hypoxia responsive elements (HREs) in their promoter regions, and thus being induced by HIF-dependent manner, also coordinate important adaptive response to hypoxia downstream of HIF. For instance, both miR-210 and miR-373, direct transcriptional targets of HIF, alter DNA repair responses by decreasing levels of DNA repair proteins, such as RAD52 and RAD23B, key members of homology-dependent repair (HDR) and nucleotide excision repair (NER) pathways [Crosby ME et al. 2009]. These results describe a role of HRMs in the regulation of DNA repair and genetic instability in response to hypoxia in cancer. In the last years, emerging evidences showed the activation of HIF-independent pathways in the adaptive cell response to low oxygen tension. Particularly, several other transcription factors (TFs), such as p53, NF-kB and PU.1 also regulate the transcription of specific miRNA involved in cell cycle arrest, inflammation response or reinforcement of HIF stabilization [Cummis EP and Taylor CT 2005]. As mentioned above, multiple miRNAs are known or suspected to be involved in various steps of angiogenesis response. One of the most important miRNA target of angiogenesis is VEGF. Experimentally, using HUVEC cell lines, miR-210 was demonstrated to be able to stimulate the formation of capillary-like structure, targeting the receptor tyrosine kinase ligand ephrin-A3 (EFNA3), as well as, to increase the VEGF-induced cell migration. Thus, miR-210, the master miRNA of hypoxia, is able to enhance VEGF and vascular endothelial growth factor receptor-2 (VEGFR2) expression and thereby to promote angiogenesis. The up-regulation of other two miRNAs, miR-20a and miR-20b, seems to have direct effect on VEGF levels, but these results need to be further confirmed [Hua Z et al. 2006; Lei Z et al. 2009]. Moreover, in breast cancer patients, high levels of miR-210 were found associated with VEGF expression, hypoxia and angiogenesis [Foekens JA et al. 2008]. Since angiogenesis plays an essential role in tumor development, it is critical to understand the role of miRNAs in governing this process during hypoxia. However, despite in recent years numerous studies have contributed to better elucidate the mechanisms of action of these HRMs, future studies will be essential to verify these functions *in vivo*. Moreover, since hypoxia has been reported to be correlated with chemoresistance, HRMs may potentially become interesting biomarkers and therapeutic targets for anticancer therapy.

1.2.9 Long non-coding RNAs

In the last five years, lncRNA received a widespread attention as a potentially new layer of biological regulation. Estimates of the lncRNA gene content in the human genome ranges from ~7,000 - 23,000 unique lncRNAs, exceeding that of protein-coding genes, ranging from 10,000 to 20,000 [Gibb EA et al. 2011]. Despite these large numbers, only few lncRNAs have been characterized. LncRNAs are poorly conserved and, typically, they are long > 200bp, up to 100kb [Cheetham SW et al. 2013]. One of the first evidence of lncRNAs was the discovery of H19 and

Xist, responsible for the inactivation of one of the two X chromosome in placental female, through DNA methylation. Most recently, the GENCODE annotation group has produced the most comprehensive, high quality human lncRNA annotation to date.

Recent transcriptomic studies in mammals have revealed an abundance of lncRNAs that lie interspersed with coding genes in complex ways. According to their genomic organization relative to protein-coding transcripts, they can be classified as overlapping transcripts (sense or antisense, promoter-/intronic-/3' UTR-associated), intergenic transcripts (lincRNAs, gene-desert regions), and divergent transcripts (sharing same promoter with coding gene, but antisense) [Ponting CP et al. 2009].

1.2.10 LncRNA biogenesis and function

LncRNA transcripts, typically, have mRNA-like characteristics. They are frequently transcribed by RNA polymerase II, often are capped and polyadenylated, and show complex alternative splicing, but they apparently lack of protein-coding capacity [Cheetham SW et al. 2013]. They do not contain open reading frame (ORF) and are able to code for small peptides (<100 amino acids), whose biological significance is not completely understood. LncRNAs are an heterogeneous group of RNA molecules and, therefore, they are now emerging as widespread regulators of numerous cell physiology processes. LncRNAs have been found involved in regulating imprinting, dosage compensation, chromatin state, cell cycle regulation, cell-cell signaling, pluripotency, retrotransposon silencing, meiotic entry, recombination, telomere length, and many other functions. They can act immediately after transcription, both in the nucleus and in the cytoplasm, and can regulate gene expression, positively or negatively, at numerous levels by a variety of mechanisms. In particular, they can be involved in transcriptional and post-transcriptional regulation, post-translational regulation of protein activity and organization of protein complexes. LncRNAs are biochemically versatile polymers. They are able to interact with sequence-specific nucleic acids, as RNA and DNA, and to fold into complex three-dimensional structures able to bind various ligands, including small molecules and peptides [Geisler S and Coller J 2013]. In particular, regarding interaction with proteins, lncRNAs can serve *i)* as decoys, precluding the access of regulatory proteins to DNA, *ii)* as scaffold, bringing two or more proteins into discrete complexes, and *iii)* guides, addressing specific protein complexes to proper localization. Moreover, lncRNA transcripts may act as *cis* and *trans*-acting modulators, influencing the expression of protein-coding genes in their immediate genomic neighborhood, or on distantly located genes. In addition, in the cytosol, they can act as "miRNA sponge" and sequester miRNAs to inactivate the negative regulation against their target genes. Regarding gene expression regulation, one of the most important mechanism is the chromatin modification. LncRNAs such as HOTAIR (HOX transcript antisense RNA) or Xist (X-inactive-specific transcripts) have been found associated with the proteins of the histone-modifying complex, as PRC2 (Polycomb repressive complex 2) and LSD1 (Ly-specific demethylase 1), inducing heterochromatin formation in specific genomic loci, and leading to reduce

target gene expression. In this way, HOTAIR and other lncRNAs function as scaffolds, coordinating the interaction and the localization of different proteins and forming cellular substructures and protein complexes [Gutschner T and Diederichs S 2012] .

1.2.11 LncRNAs in cancer

Several recent studies suggest that lncRNAs may have important roles in disease, most notably in oncogenesis. In Table 1.2 the majority of lncRNAs discovered so far and involved in different types of cancer are summarized [Gutschner T and Diederichs S 2012]. LncRNAs may, for example, confer to cancer cells the ability to evade growth suppression. For instance, the long intergenic ncRNA p21 (lincRNA-p21), located in the proximity of the cell cycle regulator gene *Cdkn1a*, was reported as a direct p53 target, in response to DNA damage. In normal cells, lincRNA-p21 mediates the binding of hnRNP-k (an RNA binding protein) to its genomic targets, which finally leads to gene silencing and induction of apoptosis. In cancer, lincRNA-p21 acts as an inhibitor of the p53-dependent transcriptional pathway, particularly as a transcriptional repressor on gene regulating apoptosis [Huarte M et al. 2010]. Ji et al identified Metastasis-associated Lung Adenocarcinoma Transcript 1 (MALAT-1), as a prognostic marker for metastasis and patient survival in non-small cell lung cancer (NSCLC). This lncRNA promotes the cell ability to invade and form distant metastases. MALAT-1 transcript regulates alternative splicing of pre-mRNAs by modulating the levels of active serine/arginine (SR) splicing factors. In particular, it was found to affect the transcriptional and post-transcriptional regulation of cytoskeletal and extracellular matrix genes [Ji P et al. 2003]. This transcript is highly conserved across species and it is widely expressed in many human tissues, and up-regulated in various cancer types, as breast, prostate, colon, liver and uterus. Particularly, its overexpression has been linked to an increase in cell proliferation and migration, in lung and colorectal cancer cells [Hauptman N and Glavac D 2013].
More interestingly, lncRNAs have been found implicated in angiogenic process. A natural antisense transcript (NAT), complementary to the 3' untranslated region of the hypoxia inducible factor-1α (HIF-1α), called αHIF, negatively regulates the expression of HIF-1α, an important regulator of angiogenesis. Overexpression of αHIF triggers HIF1α mRNA decay and HIF1α and αHIF constitute a negative feedback loop [Rossignol F et al. 2002]. LncRNA αHIF has been found in several cancers and, in particular, its overexpression has been associated with worst prognosis in breast cancer [Cayre A et al. 2003]. Regarding, the Cancer Hallmark "resisting cell death", PANDA (p21 associated ncRNA DNA damage activated) limits the expression of pro-apoptotic genes, such as FAS and BIK, by acting in trans as a decoy for the transcription factor NF-YA [Hung T et al. 2011]. These described lncRNAs are directly implicated in cancer initiation, progression and metastasis, and may become important diagnostic markers or therapeutic targets in the treatment of cancer. Moreover, many lncRNAs are expressed in a tissue- and cancer-type restricted manner and have already shown to be useful as prognostic markers (e.g HOTAIR in

breast cancer patients or MALAT-1 in early stage lung adenocarcinoma) [Gupta RA et al. 2010; Ji P et al. 2003].

Table 1.2: LncRNAs involved in cancer mechanisms

Cancer Hallmark	LncRNA	Mode of action
I. sustaining proliferative signaling	SRA	Transcriptional co-activator
	PCAT-1	Regulating gene expression
	RN7SK	Regulating transcription
	ncRNAs derived from cell cycle gene promoters	Unknown
	KRASP1	miRNA sponge
	PR antisense	Regulating gene expression
II. Evading growth suppressors	PSF-interacting RNA	Modulating protein activity
	ANRIL	Chromatin remodeling
	GAS5	Competitor
	lincRNA-p21	Transcriptional co-repressor
	E2F4 antisense	Regulating gene expression
III. Enabling replicative immortality	TERC	RNA primer
	TERRA	Enzymatic inhibitor
IV. Activating invasion and metastasis	MALAT1	Modulating protein activity; sensor; scaffold
	HOTAIR	Chromatin remodeling
	HULC	miRNA sponge
	BC200	Translational modulator
V. Inducing angiogenesis	αHIF	RNA decay
	sONE/NOS3AS	RNA decay
	tie-1AS	RNA decay
	ncR-uPAR	Regulating gene expression
VI. Resisting cell death	PCGEM1	Regulating gene expression
	CUDR	Regulating gene expression
	uc.73A(P)	Unknown
	SPRY4-IT1	Unknown
	PANDA	Modulating protein activity
	LUST	RNA-Splicing
	PINC	unknown

1.2.12 LncRNAs in HGSOC

Recently (2013) Akrami et al performed a large-scale genomic analysis of lncRNAs in HGSOC, based on TGCA molecular dataset generated on a total of 407 advance stage HGSOC tumor biopsies [Akrami R et al. 2013]. To investigate the global copy-number alterations and lncRNA expression across samples, they based the analyses on the comprehensive GENCODE lncRNA catalog. Analyzing data from deep coverage RNA sequencing and DNA copy-number arrays, they identified simultaneous copy-number profiles and expression data for 10,419 lncRNA genes. They described global association between DNA copy-number and lncRNA expression, and identified lncRNA signatures associated with the four robust subtypes of HGSOC (immunoreactive, differentiated, proliferative, and mesenchymal), based on their gene expression profiles. In particular, by examining region of focal copy number alteration, they discovered on a subset of tumors, an intergenic region, termed AXI region, between the ACBD6 and XPR1 genes, on chromosome 1. This region, characterized by focal somatic amplification, lacks of protein-coding genes, but contains a single annotated lncRNA gene, called OVAL (ovarian adenocarcinoma amplified lncRNA). Moreover, they screened other 16 TGCA cancer types, and, interestingly, they

reported OVAL locus focal amplification also in serous endometrial carcinoma, a disease sharing several clinical and molecular similarity with HGSOC.

Although focal amplification of the AXI region was found only in the 3.9% of HGSOC samples analyzed, the frequency is comparable to other somatic mutations, such as BRCA1 and BRCA2 (3.5% and 3.2%, respectively). It has been hypothesized that OVAL may exert its functions predominantly at cytoplasm level, and independently from the nearest protein-coding neighbors, but further experiments are needed to better understand its role in tumor development.

More recently, another group of research focused the attention on the analysis of HGSOC transcriptome [Barrett CL et al. 2015]. They developed and deeply evaluated a systematic process to identify mRNA isoforms with tumor-specific expression in HGSOC. Interestingly, as researchers premised in the paper, commonly the mRNA expression is defined tumor-associated, regarding the level of expression (up and down-regulated), compared to normal tissue. Notably, they focused the study on the selection of "tumor-specific" mRNA isoforms, arisen for example from fusion-transcripts, the existence of which is unknown. For the discovery of HGSOC-specific isoforms, they processed a large amounts of RNA-seq data of 296 HGSOC samples and 1839 normal tissues, obtained from TCGA and Genotype-Tissue Expression (GTEx) program, respectively. Applying their custom bioinformatic algorithms, they produced a list of 671 mRNA isoforms, rank-prioritized by likelihood of being tumor-specific. Initially, these selected isoforms were measured by RT-qPCR on pools of four different tumor samples and four different normal RNA samples, to filter out isoforms that were not expressed in tumors and/or were expressed in normal tissue. After this selection, only 86 isoforms were detected in the tumor pool. Then, the expression of selected 86 isoforms were measured in an expanded set of individuals, for a total of 12 tumor samples and 18 normal tissue samples, by RT-qPCR. Finally, a total of 33 tumor-specific or normal-restricted isoforms were identified and these isoforms represented 5% of the original 671 selected by RNA-seq analysis. These isoforms are variants of genes related to oncogenesis, known to maintain the malignant state, as the transcription factors FOXM1 and ETV4, and that have a direct role in driving aggressive tumor initiating cell behavior, or are necessary for maintaining a stem-cell phenotype. Moreover, 15 mRNA isoforms were not expressed in the ovary or fallopian tubes, and so they have the tumor specificity required for an early specific detection of ovarian cancers. Additionally, 5 mRNA isoforms contain a unique exon that confers upon the protein a unique primary structure, as parathyroid hormone receptor 2 gene (PTH2R) and CD9 isoforms, making them interesting candidate for specific antibody targeting.

The systematic processes, that Barrett et al developed for the discovery of tumor-specific mRNA isoforms, is readily and rapidly applicable to any of the 30 or more tumor types for which sufficient amounts or RNA-seq data already exist.

2. AIMS OF THE STUDY

High-grade serous ovarian carcinoma (HGSOC) is the most lethal gynecologic malignancy, mainly because the disease is frequently diagnosed at an advanced stage and it is characterized by the early onset of chemoresistant recurrences. The lack of reliable diagnostic and prognostic markers, together with the lack of effective therapies, are the major obstacles to the clinical management of patients with HGSOC. A new class of non-coding RNAs (ncRNAs), such as microRNA (miRNA) and long non-coding RNA (lncRNA), with a function of gene expression regulation, have been discovered to play an important role in human cancers. Increasing evidences suggest that ncRNAs are involved in cancer progression and development of chemoresistance, and support their role as potential diagnostic, predictive and prognostic biomarkers. The hypoxic condition within the tumor microenvironment, improving the tumor neovascularization, represents an essential event contributing to the development of a more aggressive HGSOC phenotype. Recently, a group of miRNAs, termed hypoxia regulated-miRNAs (HRMs), have been identified as key elements in response to hypoxia, regulating important mechanisms involved in tumor progression. The complexity of hypoxia molecular mechanisms has not been fully elucidated yet in HGSOC, therefore there is an urgent need to discover novel biomarkers clinically useful to select patients with hypoxic tumor, that may benefit of tailored treatments.

Starting from these premises, the study of my PhD project aims at elucidating the transcriptional and post-transcriptional signatures that characterize HGSOC, both at the serum and tissue levels.

In detail, the research effort includes:

i) The investigation of circulating miRNAs as novel potential biomarkers for HGSOC detection;

ii) The analysis of mRNA, miRNA and lncRNA expression profiles of HGSOC and normal tissues;

iii) The evaluation of hypoxia-regulated miRNA expression in HGSOC and normal tissues.

3. MATERIALS AND METHODS

3.1 Patient cohort

All patients enrolled in the study were diagnosed with high grade serous ovarian carcinoma (HGSOC), III-IV FIGO stage and underwent a radical surgical tumor debulking with a complete staging procedure, followed by platinum-based chemotherapy. No patients received chemotherapy before surgery. Healthy donors included in the study underwent hysterectomy and bilateral salpingo-oophorectomy for pelvic organ prolapse or benign pathologies. Patients with a past or concomitant history of malignancy were excluded from the study. Clinical and anatomo-pathologic patients' informations were registered and follow-up data were obtained from periodic gynecologic and oncological check-ups. All patients were followed from the date of surgery until death or for at least two years. Study approval was acquired from the institutional review board, and all patients signed an informed consent, according to institutional guidelines.

3.1.1 Serum sample collection

A retrospective cohort of 233 serum samples was gathered together from two independent Italian serum collections and divided into a training set and a validation set. The training set consists of serum samples from 110 patients with HGSOC III-IV FIGO stage and 52 age-matched donors, proven to be free of any gynecological disease, were collected at the Division of Obstetrics & Gynecology, ASST Spedali Civili, University of Brescia (Brescia, Italy), between 2003 and 2013.

The validation set consisted of an independent cohort of 58 serum specimens belonging to patients with HGSOC and 16 serum samples from healthy donors, collected at the Division of Gynecologic Oncology, Gemelli Hospital, Catholic University (Rome, Italy), between 2009 and 2013.

The two independent cohorts included in the study showed similar clinicopathologic characteristic distribution and are summarized in Table 3.1.

To obtain serum samples, 7.5 ml of blood were collected in S-Monovette with clot activator (Sarstedt AG & Co., Nümbrecht, Germany) and centrifuged after half an hour at 3000 rpm for 10 minutes at room temperature. The serum was then aliquoted and stored at -80°C within an hour. Free haemoglobin concentration was analyzed using miR-451a and miR-23a-3p expression ratio to exclude hemolysed samples from downstream analyses [Langhe R et al. 2015]. In the following Figure 3.1, the levels of the ratios across samples are represented. All samples showed a very homogeneous level of expression ratio, markedly below level 5, demonstrating the absence of hemolysis in our samples.

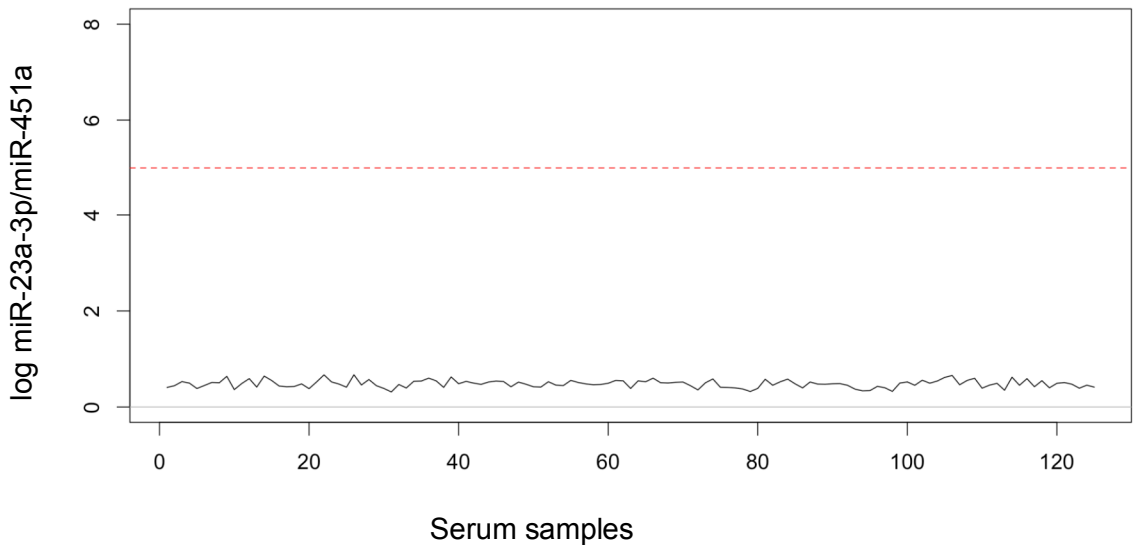

Figure 3.1. log ratio between miR-23a-3p and miR-451a expression across all samples using microarray technology. The dashed red line is referred to the level of 5.

Table 3.1. Clinicopathological features of HGSOC patients and healthy donors used in serum miRNA analysis

Clinicopathological characteristics		Training cohort		Validation cohort	
		HGSOC patients (n=110)	**Healthy donors** (n=52)	**HGSOC patients** (n=58)	**Healthy donors** (n=13)
Median age (range), years		61 (36-85)	61 (38-73)	57 (34-76)	52 (26-67)
Menopausal status	Pre	24 (22%)	-	16 (27%)	-
	Post	85 (77%)	-	41 (71%)	-
	Missing	1 (1%)	-	1 (2%)	-
FIGO Stage	III	78 (71%)	-	55 (95%)	-
	IV	32 (29%)	-	3 (5%)	-
Level of CA-125 (UI/mL)	> 943	52 (47.5%)	-	29 (50%)	-
	< 943	52 (47.5%)	-	28 (48%)	-
	Missing	6 (5%)	-	1 (2%)	-
Presence of ascites	Yes	90 (82%)	-	31 (54%)	-
	No	19 (17%)	-	3 (5%)	-
	Missing	1 (1%)	-	24 (41%)	-
Lymphnode metastasis	Yes	43 (39 %)	-	21 (36%)	-
	No	21 (19%)	-	36 (62%)	-
	Missing	46 (42%)	-	1 (2%)	-

3.1.2 Tissue sample collection

A total of 99 snap-frozen HGSOC biopsies were obtained from the Division of Obstetrics & Gynecology, ASST Spedali Civili, Univ. of Brescia, between 2003 and 2013. For a total of 76 out of 99 patients, matched serum and tumor tissue were collected.

On the basis of chemotherapy status, patients were classified in four groups:

- Platinum-sensitive patients, relapsing long after chemotherapy (>12 months), that could be re-challenged with platinum-chemotherapy, generally obtaining response.
- Platinum partially-sensitive patients, experiencing relapse within 6-12 months from the last round of chemotherapy. They were generally treated again with platinum-chemotherapy, although a less response rate is observed.
- Platinum-resistant patients, experiencing relapse within 6 months from the end of therapy, were not treatable again with platinum-chemotherapy. This last group also includes a small fraction of platinum-refractory patients, who did not respond to

platinum-therapy and experienced tumor progression during the course of chemotherapy.

Patients without information about platinum-status represented Missing/Too early group.

In particular, to define the response to chemotherapy, two endpoints were evaluated. Progression free survival (PFS) was considered as the time interval from diagnosis to the first appearance of disease progression after treatment and overall survival (OS) was represented as the time interval from diagnosis to the date of death due to cancer, or the last observation.

Neoplastic tissue specimens were sharp-dissected and frozen in liquid nitrogen within 30 minutes of debulking surgery. For each sample, a specular hematoxylin-eosin section was reviewed by a staff pathologist to check for epithelial purity and only samples containing at least 70% tumor epithelial cells were used for the following RNA extraction.

Normal ovarian and fallopian tube epithelial cells were obtained from a total of 30 age-matched patients at the Division of Obstetrics & Gynecology, ASST Spedali Civili, Univ. of Brescia, between 2011 to 2013.

Normal luminal fallopian tube epithelial cells and normal ovarian surface epithelial (HOSE) cells were collected by scraping in 1 ml of physiological saline solution immediately after surgery and centrifuged at 1000 rpm for 10 minutes. The cell pellet was then resuspended in 200 µl of TRIzol Reagent (Life Technologies, Carlsbad, CA, USA) and stored at -80°C. All the normal samples were verified to be free of any neoplastic pathology before using for total RNA extraction.

Patients clinical and pathologic characteristics are described in Table 3.2.

Table 3.2. Clinicopathological features of HGSOC patients and healthy donors used in tissue gene and miRNA analysis

Clinicopathological characteristics		**HGSOC patients** (n=99)	**Healthy donors** (n=30)	
			HOSEs (10 pools from 15 donors)	**Fallopian Tubes** (n=15)
Medianage (range), years		63 (36-85)	52 (43-65)	
Menopausal status	Pre	21 (21%)	-	
	Post	78 (79%)	-	
	Missing	0	-	
FIGO Stage	III	73 (74%)	-	
	IV	26 (26%)	-	
Tumor Residual	TR=0	21 (21%)	-	
	TR>0	78 (79%)	-	
Level of CA-125 (UI/mL)	≥ 923	46 (46.5%)	-	
	< 923	47 (47.5%)	-	
	Missing	6 (6%)	-	
Presence of ascites	Yes	85 (86%)	-	
	No	13 (13%)	-	
	Missing	1(1%)	-	
Positive neoplastic cytology	Yes	88 (89%)	-	
	No	7 (7%)	-	
	Missing	4 (4%)	-	
Lymph node metastasis	Yes	37 (37%)	-	
	No	16 (16%)	-	
	Missing	46 (47%)	-	
Response to platinum-based therapy	Resistant	40 (41%)	-	
	Sensitive	36 (36%)	-	
	Partially sensitive	21 (21%)	-	
	Missing	2 (2%)	-	

3.2 Total RNA extraction

Total RNA including miRNAs was extracted from 200 µl of serum using miRNeasy Mini kit (Qiagen, Milan Italy). In particular, serum samples were thawed in ice, then 1 ml of QIAzol Lysis Reagent (Qiagen) was added to the samples and they were kept at room temperature for 5 minutes. Ten synthetic spike-in RNA oligos, without sequence homology to known human miRNAs, were added to samples to control for variations during the preparation of total RNA and subsequent steps. RNA oligo sequences are displayed in Table 3.3. The spike-in RNA oligos were introduced in serum samples as a mixture of 12.5 fmol in a total volume of 2.5 µl. All the last steps of purification were performed following the manufacturer's instructions. RNA was eluted from spin columns in 35 µl of nuclease-free water and 15 µl were used for miRNA expression profiling.

Total RNA from tissue samples (included messenger RNA, microRNA and long non-coding RNA) was isolated using TRIZOL reagent (Life Technologies) and further purified using RNeasy MiniElute Cleanup kit (Qiagen), with a modified protocol for co-purification of small RNAs according to the manufacturer's instructions. RNA concentration and 260/280 absorbance ratio (A260/280) were measured with Infinite M200 spectrophotometer (TECAN). RNA integrity was assessed with RNA 6000 Nano LabChip kit using the Agilent 2100 Bioanalyzer (Agilent Technologies, Palo Alto, CA, USA). RNA integrity number (RIN), generated with Agilent 2100 Expert software, was superior to 8 for all RNA samples. Only samples with good RNA yield and no RNA degradation were retained for further experiments. RNA samples were diluted at 75 ng/µl and 50 ng/µl for gene expression and miRNA expression profiling, respectively.

Table 3.3. Ten synthetic spike-in RNA oligo sequences

Species	RNA Oligo	Sequence
Kaposi sarcoma associated herpesvirus	kshv-miR-K12-2	5'-rGrUrC rCrGrGrGrUrCrGrArU rCrUrG-3'
Human Citomegalovirus	hcmv-miR-UL112	5'-rCrGrG rUrGrArGrArUrCrCrArGrGrC rU-3'
Epstein-Barr virus	ebv-miR-BART8	5'-rCrGrG rUrUrUrCrCrUrArGrArUrUrGrUrArC rArG-3'
C.elegans	cel-miR-39-5p	5'-AGCUGAUUUCGUCUUGGUAAUA-3'
C.elegans	cel-miR-54-5p	5'-AGGAUAUGAGACGACGAGAACA-3'
C.elegans	cel-miR-238-3p	5'-UUUGUACUCCGAUGCCAUUCAGA-3'
Arabidopsis thaliana	ath-miR-160a	5'-UGCCUGGCUCCCUGUAUGCCA-3'
Arabidopsis thaliana	ath-miR-171b	5'-UUGAGCCGUGCCAAUAUCACG-3'
Arabidopsis thaliana	ath-miR-416	5'-GGUUCGUACGUACACUGUUCA-3'
arabidopsis thaliana	ath-miR771	5'-UGAGCCUCUGUGGUAGCCCUCA-3'

3.3 miRNA expression profiling by microarray

Two independent miRNA microarray profiling evaluations of serum and tissue samples were performed. In tissue miRNA arrays, 99 HGSOC tissues, 5 pools of HOSEs obtained from 17 women and 11 normal luminal fallopian tube epithelia were hybridized. In serum miRNA arrays, 110 sera from HGSOC patients and 19 sera from healthy controls were evaluated for miRNA expression profiling. Briefly, for tissue miRNA profiling, 100 ng of RNA, enriched in miRNA fraction, were Cyanine 3-pCp labeled and hybridized on the commercially available G4871A human miRNA Microarray, using a miRNA labeling and hybridization kit according to the manufacturer's instructions (Agilent Technologies). For the analysis of circulating miRNAs, we used the commercially available G4872A-046064 human miRNA Microarray (Agilent Technologies), customized with probes for the detection of specific RNA spike-in oligos. For circulating miRNA profile, we hybridized fixed volume of eluted total RNA, derived from fixed serum volumes, for all samples tested. The arrays were washed and scanned with a laser confocal scanner (G2565BA,

Agilent Technologies) according to the manufacturer's instructions. miRNA microarrays underwent standard post hybridization processing and the intensities of fluorescence were calculated by Feature Extraction software version 11 (Agilent Technologies).

Serum raw microarray data comprised 1361 miRNAs (included Agilent quality controls and spike-in oligos). After a filtering step based on Agilent quality controls (see Supplementary Material for details), 648 miRNAs (including the 10 spike-in) were retained for further analysis. The distributions of the raw expression values are reported in Supplementary Figure S1. Given the small amount of miRNAs in serum, normalization of circulating miRNA microarray data is a challenging task. Thus, different normalization strategies have been tested and compared. We chose the normalization resulting in the more invariant spike-in oligo expression distribution across samples (see Supplementary Materials for details). In our data the best normalization resulted to be the cyclic lowess [Bolstad BM et al. 2003], in which the 10 spike-in oligos and a set of 10 invariant low expressed miRNAs were used as references (Supplementary Figure S1 and S2). Empirical Bayes test (as implemented in limma Bioconductor package) has been used to identify differentially expressed miRNAs between patients and healthy controls with an FDR<0.05. Hierarchical clustering has been performed with Euclidean distance and complete linkage.

Tissue raw microarray data comprised 2017 microRNAs. A filter has been applied to select those miRNAs with reliable expression values across arrays. Specifically, we selected only miRNAs with at least 75% of good quality measures (as gIsPosAndSignificant Agilent flag) across samples. After these filtering steps, we remained with 363 miRNAs. The small amount of missing values still present after the filtering step was imputed with k-nearest neighbourhood method. Classic cyclic lowess normalization, as implemented in limmaBioC package, was applied. Empirical Bayes test (as implemented in limma R package) has been applied to identify differentially expressed miRNAs between HGSOC and normal tissues (data not shown). FDR was set to 0.05.

The present study was carried out following REMARK guidelines [McShane LM et al. 2005].

3.4 Gene expression profiling by microarray

One hundred and fifty nanograms of total RNA from 99 HGSOC, 6 pools of HOSEs obtained from 19 women and 10 luminal fallopian tube epithelia were Cyanine 3-CTP labeled and hybridized with a One-Color Microarray-Based gene expression analysis (Low input quick amp labeling) protocol, according to the manufacturer's instructions (Agilent Technologies). Commercially available G4851AB SurePrint G3 Human Gene Expression 8x60K v2 Microarray (Agilent Technologies) was used. It consists of 60K features printed in an 8-plex format (8×60 array), and can detect human known 27.958 genes/transcripts and 7.419 lncRNAs sourced from different public database. The arrays were washed and scanned with a laser confocal scanner (G2565BA, Agilent Technologies) according to the manufacturer's instructions. mRNA microarrays underwent standard post-hybridization processing and the intensities of fluorescence were calculated by Feature Extraction (FE) software version 11 (Agilent Technologies).

Expression matrix was obtained using gProcessedSignal. Matrix gene expression data were normalized with quantile [Bolstad BM et al. 2003] and the expression values of the same probes (ProbeUID) were averaged. Lines containing more than thirty unavailable (NA) values were discarderd. After normalization, identification of differentially expressed genes (DEG) was performed using Limma's Empirical Bayes test [Smyth GK 2004]. Raw p-values were adjusted for multiple testing with Benjamini and Hochberg False Discovery Rate [Reiner A et al. 2003]. After analysis, genes were deemed statistically significant if their corrected p-value was equal or lower than 0.01.

3.5 RNA sequencing

Among the cohort of 99 HGSOC samples, we selected a total of 28 RNA samples derived from 14 platinum-based chemotherapy resistant patients and 14 platinum-based chemotherapy sensitive patients. This group of 28 total RNA samples, together with 10 control tissues, derived from 3 HOSEs (pooled from 10 HOSEs of healthy donors) and 7 normal fallopian tubes were deep sequenced for the discovery of novel HGSOC specific transcripts.

The RNA sequencing was performed by Personal Genomics, a Spin-Off of the University of Verona operating within the Center of the Functional Genomics of University of Verona. The sequencing was carried out on the Illumina HiSeq1000 platform, using the standard sequencing kit TruSeq Stranded Total RNA LTwithRibo-Zero TM Gold, generating 2x100 bp paired end lane.

The high-throughput RNA-seq data alignment was performed using the Spliced Transcripts Alignment to a Reference (STAR) software [Dobin A et al. 2013]. STAR software was implemented with a strategy, called 2-pass STAR, known to be more reliable for discovery analysis [Engström PG et al 2013].

3.6 Serum samples: cDNA synthesis and RT-qPCR/ddPCR

RNA from 233 serum samples (training and validation cohorts) was reverse transcribed into cDNA, starting from 5 µl of RNA, according to the miScript Reverse Transcription protocol (Qiagen). A fixed volume of eluted RNA sample was used as input for RT-qPCR, rather than a fixed quantity of input RNA, as previously reported [Kroh EM et al. 2010]. Two microliter of cDNA were used for RT-qPCR experiments in triplicate using Rotor-Gene Thermal Cycler (Qiagen). Experiments were run in triplicate and plates were prepared by automatic liquid handling station on a final volume of 10 µl (QiaAgility). As there are no established endogenous miRNAs acting as normalizers for serum miRNA relative quantification, RT-qPCR analysis was performed on raw cycle thresholds (Cq).

The choice of using ddPCR, a recent technique optimized for the absolute quantification of circulating nucleic acids, combined with Exiqon chemistry, is based on their reported optimal precision, reproducibility and specificity [Mestdagh P et al. 2014]. Experimentally, 3 µl of RNA isolated from 168 serum samples (training cohort) were reverse-transcribed in a final reaction volume of 20 µl, with 5X reaction buffer and 1 µl of Enzyme Mix, as reagents (miRCURY locked-

nucleic-acid™ (LNA) Universal RT microRNA PCR system, Exiqon). According to the manufacturer's protocol, a poly-A tail was added to the RNA template and cDNA was synthesized using a poly-T primer with a 3' degenerate anchor and a 5' universal tag and incubating the reaction at 42°C for 60 min, heat-inactivating at 95°C for 5 minutes, then immediately cooling at 4°C. All cDNA samples were diluted 50-fold with nuclease-free water. Amplification mixture (20 µl) containing 10 µl 2X EvaGreensupermix (Bio-Rad), 8 µl diluted cDNA and 1 µl of miRCURY LNA PCR primer sets specific for hsa-miR-1246 (ID 205630,Exiqon). An absolute quantification of circulating miRNAs was performed with QX200 Droplet Digital PCR System (Bio-Rad). Briefly, each EvaGreen amplification mixture (20 µl) was mixed with 70 µl of droplet generator oil and loaded into the QX200 droplet generator, thus portioning each sample into 20,000 nanoliter-sized droplets. Emulsified samples were then transferred into a 96-well PCR plate to perform PCR to end point, using a conventional thermal cycle. The cycling steps were set as follow: 95°C for 5 min, (95°C for 30, 58°C for 1 min) x 40 cycles, 4°C for 5 min, 90°C for 5 min and infinite 4°C holding. The PCR plate was then loaded into the QX200 droplet reader for sample automated analysis. A no template control (no cDNA in PCR) and a negative control for each reverse transcription reaction (RT-neg) were included in every assay run for each miRNA.

3.7 Tissue samples: cDNA synthesis and RT-qPCR

Ten ng of total RNA, extracted from 99 HGSOC tissues and 25 normal tissues, were retrotranscribed in cDNA, according to miRCURY LNA™ Universal RT microRNA PCR system protocol (Exiqon), as described above. All cDNA templates were stored at -20°C and diluted 80-fold immediately before being amplified using CFX96 Touch™ Real-Time PCR Detection System (Biorad). The PCR reaction (10 µl) consisted of 5 µl PCR Master Mix (Exiqon), 1 µl sncRNA-specific forward and reverse primer Mix (Exiqon) and 4 µl of diluted template cDNA. PCR cycling steps were set as follow: 95°C for 10 min, (95°C for 10 sec and 60°C for 1 min, ramp-rate 1.6 °C/s) x 40 cycles and infinite 4°C holding. Each real-time qPCR amplifications were followed by melting curve analysis. Both PCR primers (forward and reverse) are optimized with LNA™, resulting in high sensitivity, as well as exceptional specificity, of the assays that allow discrimination between closely related microRNA sequences. Assays evaluated in our study meet the quality criteria set by Exiqon, with an amplification efficiency over than 85%. All reactions were run in triplicate and no template controls (no cDNA in PCR) were included in each assay run for each primer set. We included a minus-reverse transcriptase ("-RT") controls in real-time qPCR experiments for each sample and each sncRNA. An inter-run calibration sample was used in all plates to correct for the technical variance between the different runs and to compare results from different plates. Cq determination was performed with CFX Manager Software (Bio-Rad Laboratories) using the single threshold mode.

3.8 Statistical analysis

miRNA and gene microarray data analysis were described in paragraph 3.3 and 3.4, respectively. RNA sequencing analysis were reported in paragraph 3.5.

A supervised pathway analysis between different groups (platinum-resistant *vs* platinum-sensitive and partially sensitive patients) was performed. “Graphite web” is a novel tool recently developed by a group of statisticians of University of Padova (Padova, Italy) for topological-based pathway analysis, based on high-throughput gene expression data analyses [Sales G et al. 2013]. It was used for pathway analyses and network visualization for gene expression data. It combines topological and multivariate pathway analyses with an efficient and interactive system of network visualizations, using Clipper method. Clipper is a two-step empirical approach based on Gaussian graphical models, which identifies pathways with means or covariance matrices significantly different between experimental conditions. It also selects the portions of the pathway, called signal paths, which are associated the most with the given phenotype. AlphaMean represents an adjusted p-values of CliPPER test on the means of the pathways between groups.

For miRNA expression experiments, median values were compared using the non-parametric Mann-Whitney *t*-test. Differences were considered statistically significant with a two sided p-value less than 0.05. Survival curves were plotted using the Kaplan-Meier method, and differences were tested using the log-rank test. For survival analysis two end-points (cancer progression and death due to cancer) were used to calculate progression-free survival (PFS) and overall survival (OS), respectively. For all two end-points the last date of follow-up was used for censored subjects. Survival models were fitted using the Cox proportional hazard regression models. Linear discriminant analysis and the receiver-operating-characteristic (ROC) curves were used to estimate sensitivity and specificity for each biomarker in the training and validation sets. All statistical analyses were performed using the R language.

4. RESULTS

4.1 Circulating miRNA microarray analysis

4.1.1 Cohort description and study design

Sera collection was obtained from two independent cohorts of HGSOC patients (total cases, =168) and healthy donors (total cases, =65), with comparable distribution of clinic-pathologic characteristics as detailed in Table 3.1. The study was organized into two steps, namely "discovery" and "evaluation" phase. In the discovery phase, known miRNA species differentially expressed between the sera of HGSOC patients (n= 110) and healthy donors (19 out of 52) of the training set, were identified first by array technology and further validated by RT-qPCR. In the evaluation phase, the expression profile of the candidate circulating miRNAs was examined in an external and independent cohort of sera (from now onwards known as validation set) of HGSOC patients (n= 58) and healthy donors (n= 13). The median age at diagnosis was 61 and 57 years for the training and the validation set, respectively, with the vast majority of women in postmenopausal status (77% and 71% for the training and the validation set, respectively). Serum samples were withdrawn at diagnosis, before any treatment. All patients were staged according to FIGO (Federation International of Gynecology and Obstetrics) guidelines as stage III-IV [Prat J et al. 2015], with high-grade serous histological type. The median CA125 value at diagnosis was 943UI/ml. As shown in Table 3.1, the CA125 levels were higher than the above level in the 47% of patients of the training set and in the 50% of patients of the validation set. Some patients showed presence of ascites (82% training set and 54% validation set, respectively) and lymph node metastasis (39% for the training set and 36% for the validation set). miRNA landscape analysis was performed on the training set to discover differentially expressed known miRNAs between sera of healthy donors and sera of women with diagnosis of HGSOC. The validation set was used as a second and independent cohort of sera to support the robustness of our analysis and to validate miRNAs found differentially expressed in the training set.

4.1.2 Discovery of candidate diagnostic miRNAs in serum by microarrays

To identify the entire repertoire of currently known miRNAs expressed exclusively in patients with diagnosis of stage III-IV HGSOC, miRNA microarray experiments were performed on 110 sera of HGSOC patients and 19 healthy donors, enrolled in the training set. After a comparative analysis, we selected, as the best normalization strategy for our data, the cyclic lowess normalization with weights on spike-in RNA oligos and low invariant miRNAs (hereafter called CLWsim) (see Supplementary Materials for details). CLWsim normalization revealed a total of 97 miRNAs as differentially expressed between sera of HGSOC patients and healthy donors (from now on referred to as DEM, differentially expressed miRNA). The complete list of 97 DEM with relative log expression values in both healthy and ovarian cancer patients is reported in Supplementary Table S1. Of these, 92 miRNAs (95%) resulted up-regulated, and five (5%) resulted down-regulated in

the sera of patients compared to healthy donors. Similarity across samples was further investigated by unsupervised cluster analysis using DEM expression levels. The dendrogram depicted in Figure 4.1 shows a clear separation of three groups of patients (called C1, C2 and C3). With the exception of seven healthy patients, cluster C2 and C3 are mainly composed by HGSOC patients, while cluster C1 is mainly composed of healthy controls. No significant differences have been observed regarding the clinical characteristics of the C2 and C3 groups.

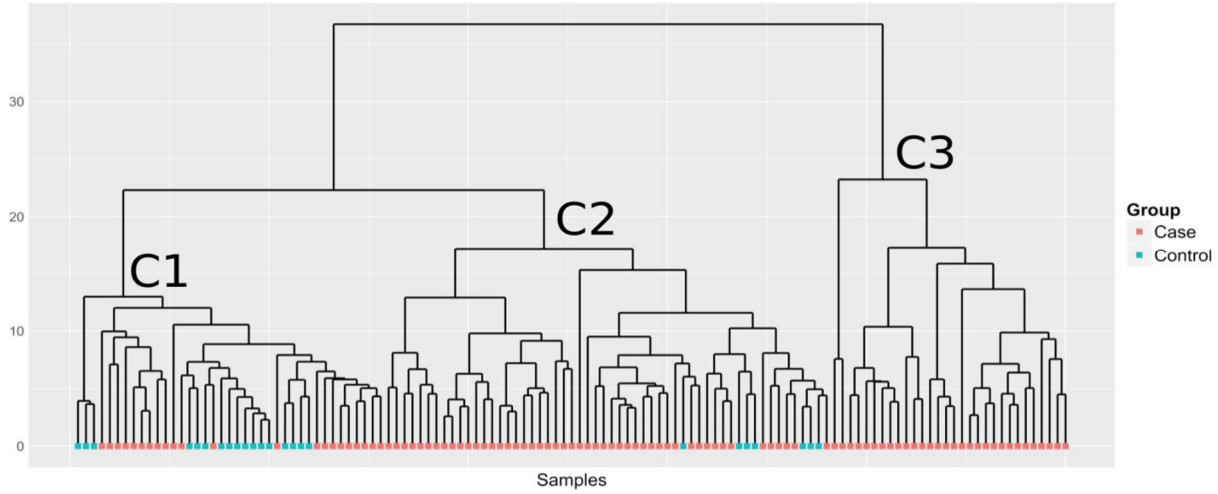

Figure 4.1: Heat map and cluster analysis, using all the differentially expressed miRNAs. Almost all healthy controls are grouped in Cluster C1.

4.1.3 Validation of candidate circulating miRNAs by RT-qPCR in the training set

Since above analyses are based on array measures, and therefore obtained within a complex mixture of transcripts, orthogonal validation miRNAs by independent techniques, like RT-qPCR, need to be performed before any assessment of their clinical relevance. Due to the limits of PCR-based approaches and the low abundance of miRNA species in the sera of HGSOC patients, validation experiments were performed on a selection of DEM according to the following criteria: *i)* highest average expression in both patients and healthy donors; *ii)* highest log fold change, measured in patients compared to healthy donors; *iii)* lower adjusted p-value. Then only miRNA expression with Ct <36 were considered reliable.

In Table 4.1 the complete panel of the nine DEM selected for independent validation is reported (i.e., *miR-1246, miR-595, miR-574-5p, miR-483-3p, miR-4290, miR-2278, miR-32, miR-4281, and miR-3148*). Of these, miR-1246 and miR-574-5p resulted as DEM in matched tissue samples. To note, except for miR-4281, all DEM selected for further RT-qPCR validation lies in the intersection of the three different normalization approaches (Figure 4.2).

RT-qPCR were performed on sera of 110 HGSOC patients and 52 healthy donors enrolled in the training set. Data reported in Table 4.2 show the median CT values for *miR-1246, miR-4290, miR-595, and miR-2278* (all p-values ≤0.0002, FC=9, FC=3.2, FC=8.4, FC=3, respectively) as the most

significantly up-regulated miRNAs in the serum of HGSOC patients compared to healthy donors in the training set. miR-574-5p and miR-483-3p were not confirmed. RT-qPCR Ct values for miR-32-3p, miR-4281 and miR-3148 resulted above the selected cut-off (i.e., Ct=36) and therefore were discarded from downstream validation.

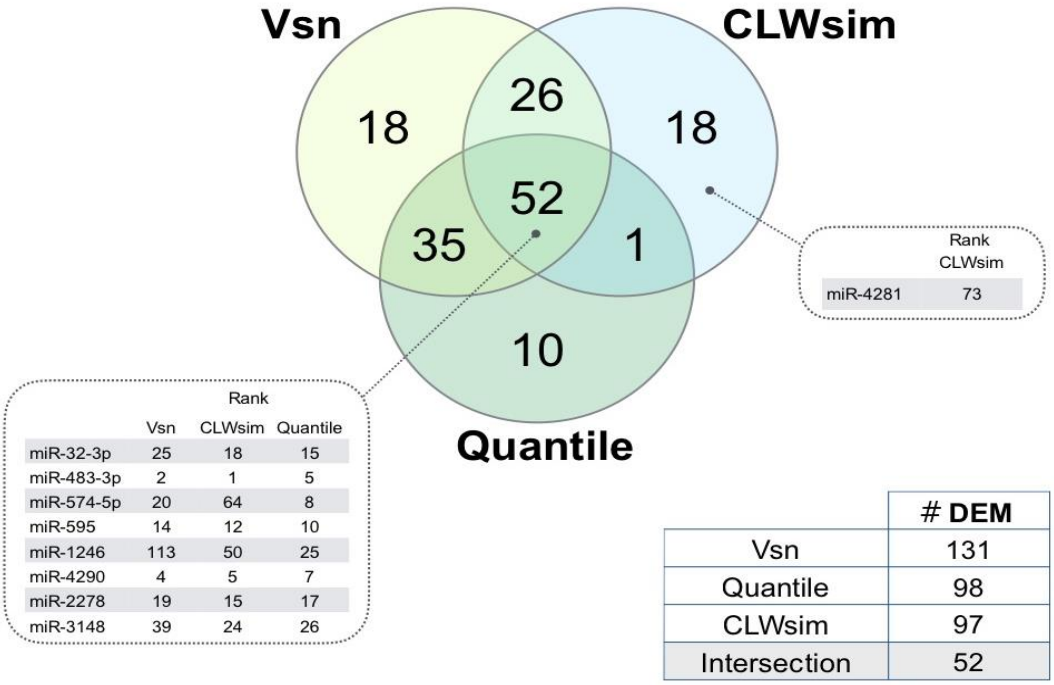

Figure 4.2: Venn diagram of the list of differentially expressed miRNAs between patients and controls according to different normalizations. In tables are reported the number of differentially expressed miRNAs identified by each normalizations and the rank of the selected miRNAs in each list of DEM.

Table 4.1: Nine circulating miRNAs selected for RT-qPCR validation, based on microarray results.

Rank from 1 to 97	miRNAs	Adjust μ -value	Mean log_2expression		log FC
			HGSOC	Control	
1	hsa-miR-483-3p	0.00001	4.45	3.42	1.03
5	hsa-miR-4290	0.00001	4.06	3.10	0.96
12	hsa-miR-595	0.0004	5.03	3.54	1.49
15	hsa-miR-2278	0.0005	4.41	3.19	1.22
18	hsa-miR-32-3p	0.0008	5.19	3.73	1.46
24	hsa-miR-3148	0.0008	4.57	3.23	1.34
50	hsa-miR-1246	0.0077	7.18	6.24	0.94
64	hsa-miR-574-5p	0.0154	7.27	5.83	1.44
73	hsa-miR-4281	0.0218	11.37	10.50	0.87

Table 4.2: Expression levels of nine selected miRNAs evaluated by RT-qPCR.

RT-qPCR		Training set		Validation set	
		Control	HGSOC	Control	HGSOC
miR-1246	**median (CT) [IQR]**	26.4 [2.13]	23.44 [2]	27.39 [0.49]	25.75 [1.3]
	mean (CT) [sd]	25.83 [1.33]	23.41 [1.6]	27.56 [0.62]	25.82 [1.15]
	p-value (2^{-CT})	**< 0.00001**		**<0.00001**	
miR-574-5p	**median (CT) [IQR]**	28.12 [1.59]	28.24 [2.23]	30.35 [1.31]	29.58 [1.85]
	mean (CT) [sd]	28.16 [1.38]	28.32 [1.66]	30.67 [0.97]	29.6 [1.24]
	p-value (2^{-CT})	0.6637		<0.00001	
miR-483-3p	**median (CT) [IQR]**	32.41 [1.17]	32.77 [1.57]	31.87 [0.8]	32.12 [1.17]
	mean (CT) [sd]	32.44 [0.91]	32.72 [1.24]	31.84 [0.62]	32.28 [1.16]
	p-value (2^{-CT})	0.9799		0.4145	
miR-4290	**median (CT) [IQR]**	33.25 [1.95]	32.27 [2.33]	30.11 [0.75]	31.09 [1.46]
	mean (CT) [sd]	33.4 [1.58]	32.62 [1.86]	30.21 [0.8]	31.08 [1.19]
	p-value (2^{-CT})	0.0002		0.0344	
miR-595	**median (CT) [IQR]**	34.29 [2.01]	33.23 [2.55]	34.44 [2.03]	32.87 [2]
	mean (CT) [sd]	34.37 [1.76]	33.17 [2.39]	34.13 [1.28]	32.85 [1.76]
	p-value (2^{-CT})	**0.0002**		**<0.0001**	
miR-2278	**median (CT) [IQR]**	36.71 [2.99]	33.90 [1.56]	33,59 [0,32]	33,45 [0,74]
	mean (CT) [sd]	36.44 [2.21]	34.06 [1.61]	33.58 [0.36]	33.39 [0.52]
	p-value (2^{-CT})	**0.0000**		**0.0373**	
miR-32-3p	**median (CT) [IQR]**	35.87 [1.8]	37.12 [1.67]	38.23 [1.53]	36.84 [2]
	mean (CT) [sd]	36.16 [1.48]	37.16 [1.7]	38.34 [2.42]	37.29 [1.68]
	p-value (2^{-CT})	-		-	
miR-4281	**median (CT) [IQR]**	38.79 [3.15]	36.68 [1.67]	37.43 [2.4]	37.57 [1.81]
	mean (CT) [sd]	38.75 [1.98]	36.81 [1.68]	37.8 [1.48]	37.61 [1.65]
	p-value (2^{-CT})	-		-	
miR-3148	**median (CT) [IQR]**	39.43 [3.29]	37.75 [2.45]	38.31 [1.64]	38.2 [1.38]
	mean (CT) [sd]	39.83 [2.46]	37.83 [2.42]	37.55 [2.08]	38.35 [1.53]
	p-value (2^{-CT})	-		-	

4.1.4 Independent evaluation of candidate circulating miRNAs in HGSOC patients

In order to evaluate the expression levels of candidate circulating miRNAs in the sera of HGSOC patients, we performed RT-qPCR analysis in a second independent cohort of 58 HGSOC and 13 healthy donors sera samples. Accordant with the results in the training set, the expression levels of miR-1246, miR-595 and miR-2278 displayed a significant over-expression (all p-value ≤0.03, FC=5, FC= 4.7, FC=0.42, respectively) in the serum of HGSOC patients compared to healthy donors (Table 4.2). Conversely, miR-4290 showed an opposite trend. The boxplots of RT-qPCR Ct values of the three candidate biomarkers in both training and validation sets are reported in Figure 4.3. Furthermore, miR-1246 and miR-595 remained significantly up-regulated in HGSOC patients of both training and validation sets, using miR-15b as normalizer (Supplementary Table S2). Indeed, miR-15b is one of the most invariant miRNAs in our cohort of serum samples by microarrays, in accordance with its previously reported role as a reliable reference for circulating miRNA analysis in lung cancer [Bianchi F et al. 2011].

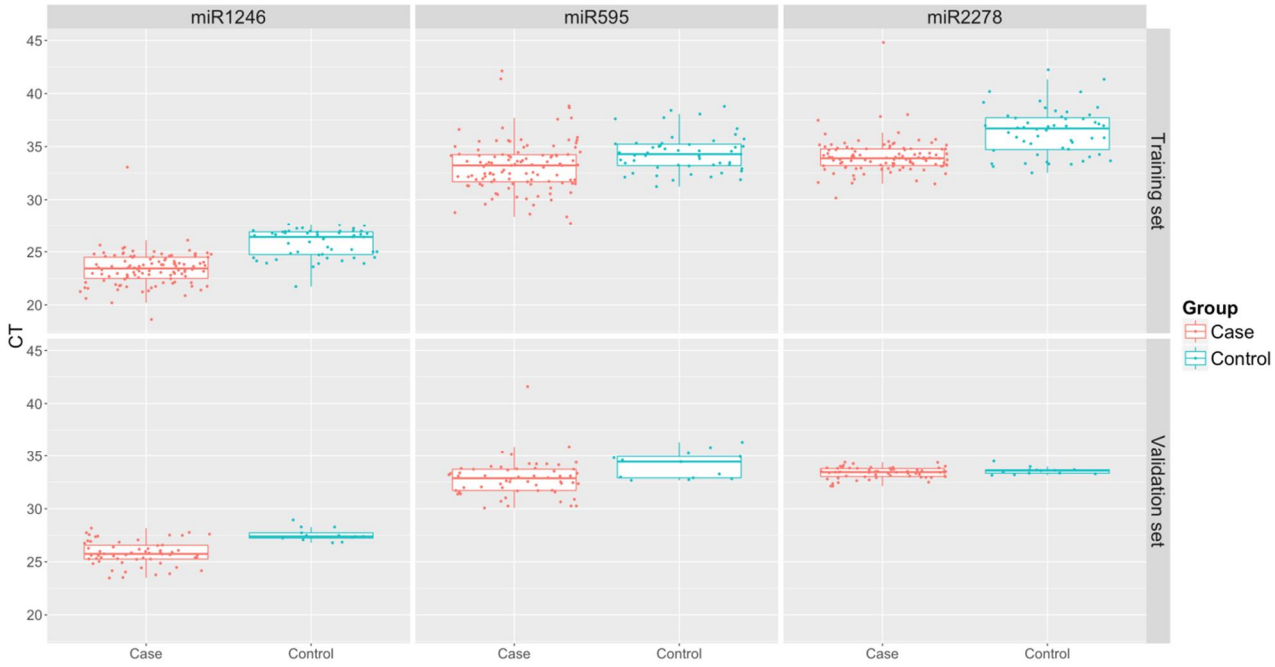

Figure 4.3: Boxplots of the RT-qPCR Ct values showing upregulation of the three candidate biomarkers in HGSOC patients compared to controls in both training and validation sets.

4.1.5 Evaluation of the diagnostic potential of miRNAs for HGSOC

To assess the efficiency of above three miRNAs as diagnostic markers for HGSOC detection, we performed ROC curve analysis on each miRNA to estimate sensitivity and specificity. Results, reported in Figure 4.4 and Table 4.3 on the entire cohort of 168 HGSOC and 65 healthy donors, revealed that the three candidate miRNAs were of value in distinguishing HGSOC patients from healthy donors. For miR-1246, the sensitivity was 87%, the specificity was 77% and the accuracy was 84%, with an AUC of 0.89. For miR-595, the sensitivity was 47%, the specificity was 84% and the accuracy was 57%, with an AUC of 0.69. For miR-2278, the sensitivity was 81%, the specificity was 66% and the accuracy was 77%, with an AUC of 0.76. These data indicated that miR-1246, which showed the greatest ability in differentiating HGSOC patients from controls, could act as a suitable biomarker for detecting HGSOC patients.

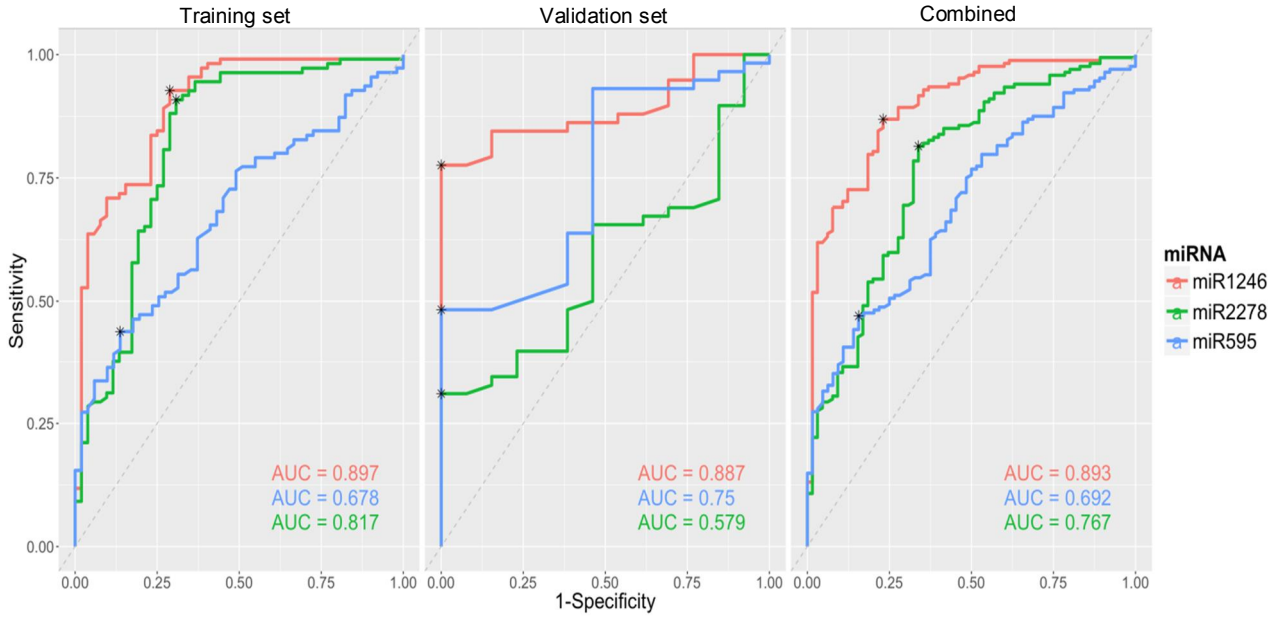

Figure 4.4: ROC curves showing the diagnostic performance of each single miRNA markers in the training set, in the validation set and the combination both patient's cohorts.

Table 4.3: Diagnostic performance of selected miRNA biomarkers in the training set, in the validation set and in the combination of both sets. (Sp for specificity, Se for sensitivity, Acc for accuracy and Th for threshold).

ROC	Index	Training set	Validation set	Combined
miR-1246	T_h	24.95	26.77	0.41
	S_p	0.71	1	0.77
	S_e	0.93	0.77	0.87
	A_{cc}	0.86	0.82	0.84
miR-595	T_h	32.47	32.65	-0.29
	S_p	0.86	1	0.84
	S_e	0.44	0.48	0.47
	A_{cc}	0.57	0.58	0.57
miR-2278	T_h	35.38	33.13	0.26
	S_p	0.69	1	0.66
	S_e	0.91	0.31	0.81
	A_{cc}	0.84	0.44	0.77

4.1.6 Absolute quantification of miR-1246 by droplet digital PCR (ddPCR)

According to the diagnostic accuracy, the statistical significance and the average expression difference between cases and controls (see Figure 4.3 and 4.4), miR-1246 was the most promising diagnostic serum biomarker. Thus, we decided to validate its expression levels with an additional technique, using EvaGreen-based ddPCR technology. The quantification by ddPCR, expressed as copies/µl, (Figure 4.5) further confirmed the diagnostic potential of miR-1246 ($p<0.0001$) in discriminating HGSOC patients and healthy donors.

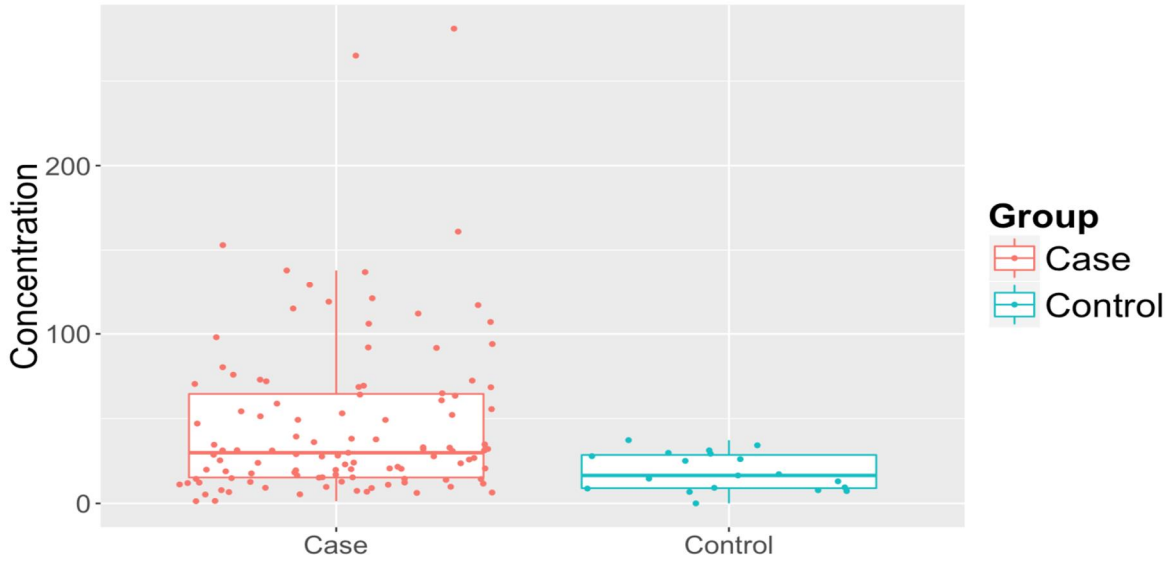

Figure 4.5: Boxplot of the absolute quantification of miR-1246 by ddPCR in HGSOC patients compared to controls. Results are presented as copies per microliter of the amplification reaction mixture.

4.2 Global gene and miRNA expression profiling in HGSOC tissue samples

4.2.1 Cohort description

Tissue samples enrolled in the study were obtained from 99 HGSOC patients and 30 age-matched healthy donors. As described in Table 3.2, the median age at diagnosis was 63 and 58 years, for HGSOC patients and healthy donors, respectively, with the 79% of patients in postmenopausal status. Tissue samples were collected at the time of surgery, before any treatment. All patients were staged according to FIGO guidelines (Federation International of Gynecology and Obstetrics) as stage III-IV, with high-grade serous histological type. Women with diagnosis of HGSOC showed a median CA125 value >943UI/ml in 46.5%, residual tumor >0 in 79%, presence of ascites in 86%, positive neoplastic cytology in 89% and lymph node metastasis in 37% of cases. According to response to standard treatment, patients were classified as platinum-resistant (n=40, 41%), platinum-sensitive (n=36, 36%) and platinum-partially sensitive (n=21, 21%).

4.2.2 Gene expression microarray analysis

Figure 4.6 showed the heatmap of the 18.626 mRNA values obtained after pre-processing and data normalization. On a global scale, a large part of the entire set of genes was similar across samples.

The unsupervised analysis, performed on the entire cohort of 99 HGSOC samples with their respective expression arrays, generated no evident clusters using all genes in the platform; this analysis did not help to separate patients on the basis of their response to chemotherapy.

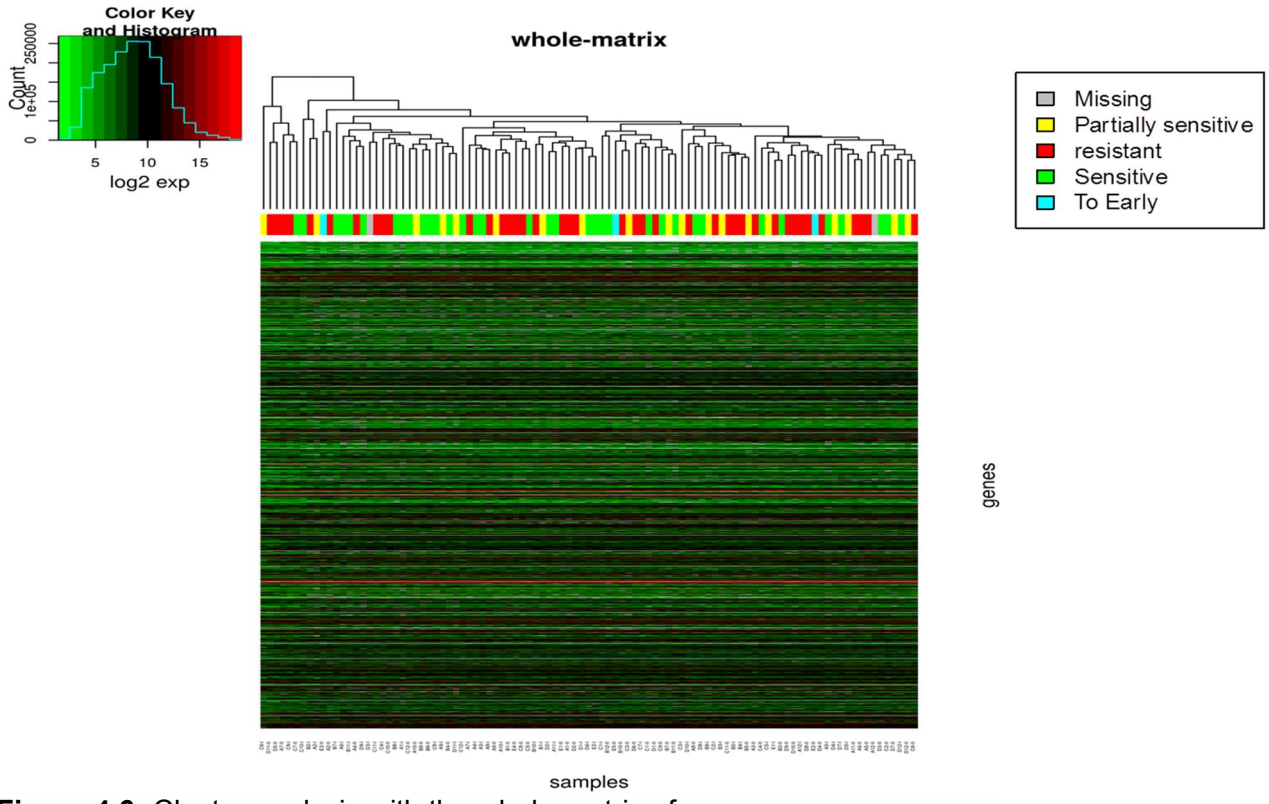

Figure 4.6: Cluster analysis with the whole-matrix of genes.

Secondly, we performed a statistical analysis to identify genes differentially expressed among patients grouped according to response to platinum-based therapy (see Table 3.2). Platinum-resistant patients (group 1) were compared with platinum-sensitive (group 2) and partially platinum-sensitive (group 3), but no differentially expressed genes (DEGs) were identified, with a FDR (false discovery rate) ≤ 0.05 (Table 4.4). On the other hand, limiting the comparison to 40 resistant patients versus 35 sensitive patients, HOMER2 was identified as the only significant DEG, with a FDR<0.05 (false discovery rate). HOMER2 was able to differentiate the two groups and demonstrated a downregulation in the group of resistant patients (Table 4.5).

Table 4.4: List of the first 10 DEGs resulted from the statistical comparison between 40 resistant patients and 54 sensitive plus partially sensitive ones. No gene is significantly differentially expressed between groups, considering the adjusted p-value.

entrez	GeneName	logFC	AveExpr	t	P.Value	adj.P.Val	B
55466	DNAJA4	-0.895337236	10.38942052	-4.220802332	5.52E-05	0.405259902	0.928152875
5589	PRKCSH	0.495856662	10.03358465	4.127848501	7.80E-05	0.405259902	0.68122894
221937	FOXK1	0.533224181	8.496412776	4.04324586	0.000106352	0.405259902	0.459472083
84445	LZTS2	0.363227373	11.16475223	3.996275837	0.000126126	0.405259902	0.337615452
23223	RRP12	0.457342782	9.249091824	3.993681322	0.000127315	0.405259902	0.330910975
10537	UBD	-1.729095542	11.59080448	-3.98849091	0.000130554	0.405259902	0.305022018
79184	BRCC3	-0.422545907	10.74263148	-3.923496285	0.000163869	0.407775943	0.150616867
389084	C2orf82	0.863088541	9.545985242	3.904849741	0.000175152	0.407775943	0.103067614
8269	TMEM187	-0.507172183	10.07578179	-3.858150571	0.000206757	0.42787196	-0.015360968
11043	MID2	-0.724619921	7.920394078	-3.809004962	0.00024586	0.432518378	-0.138969067

Table 4.5: List of the first 10 DEGs from the statistical comparison between 40 resistant patients and 35 sensitive ones. Only the first gene is statistically significant.

entrez	GeneName	logFC	AveExpr	t	P.Value	adj.P.Val	B
9455	HOMER2	-0.997887697	9.796511483	-5.068775589	2.68E-06	0.049823447	3.929026712
55466	DNAJA4	-1.045372196	10.36291821	-4.574533176	1.79E-05	0.166900106	2.384942151
55137	FIGN	1.136214465	6.840617391	4.297806403	4.98E-05	0.18964453	1.555013229
5064	PALM	1.042856055	12.75123986	4.279474612	5.33E-05	0.18964453	1.501021468
3018	HIST1H2BB	-0.688100213	10.82136958	-4.144025935	8.67E-05	0.18964453	1.106127357
9094	UNC119	0.512350528	9.107308338	4.113934531	9.65E-05	0.18964453	1.019386969
8348	HIST1H2BO	-0.716410004	12.54379751	-4.100677191	0.000101132	0.18964453	0.981288756
79184	BRCC3	-0.456859693	10.71309353	-4.08795967	0.000105791	0.18964453	0.944809542
64963	MRPS11	-0.494846302	12.10748044	-4.060255824	0.000116666	0.18964453	0.865574331
90139	TSPAN18	1.052818664	7.297700692	4.055384393	0.000118686	0.18964453	0.851674592

4.2.3 Pathway analysis

Applying Graphite and Clipper method, we performed a pathways analysis, comparing group 1 versus group 2 and 3. A total of 58 pathways differently expressed between groups has emerged. The topological pathway analysis compared 40 platinum-resistant patients with a total of 54 platinum-sensitive plus partially-sensitive patients. In Table 4.6 were reported the first ten pathways of the list.

Table 4.6: List of the first ten pathways significantly expressed among groups

Pathway	alphaMean	alphaVar
Amino sugar and nucleotide sugar metabolism	0.02	0
Dorso-ventral axis formation	0.04	0.01
Tryptophanmetabolism	0.01	0.06
Glioma	0.06	0.03
Metabolism of xenobiotics by cytochrome P450	0.01	0.08
Africantrypanosomiasis	0.07	0.03
ErbBsignalingpathway	0.05	0.06
RIG-I-like receptor signaling pathway	0.04	0.07
Prostate cancer	0.07	0.05
Hedgehogsignalingpathway	0	0.13

4.2.4 Discovery of specific HGSOC tissue miRNAs by microarray

Microarray analysis revealed 265 DEM (123 up-regulated and 142 down-regulated) in 99 HGSOC tissue samples compared to 16 tissues from HOSEs and fallopian tubes (data not shown). According to response to platinum-based chemotherapy and prognosis, we identified a total of 9 DEM (miR-199b-5p, miR-423-5p miR-455-3p, miR-22-3p, miR-199a-3p, miR-15b-5p, miR-140-5p, miR-1246 miR-320c) in the group of patients platinum-resistant and partially platinum-sensitive compared to platinum-sensitive patients, and significantly associated with survival variables (OS and PFS), as reported in Table 4.7.

Table 4.7: A total of 9 DEM associated with platinum-resistance and prognosis

Tissue miRNAs	Log Fold Change	*p*-value	OS *p*-value (median)	PFS *p*-value (median)
hsa-miR-199b-5p	0.847	0.002	0.002	**0.001**
hsa-miR-423-5p	0.362	0.001	0.009	**0.004**
hsa-miR-455-3p	0.769	0.002	0.005	**0.001**
hsa-miR-22-3p	0.616	0.004	0.009	**0.018**
hsa-miR-199a-3p	0.667	0.02	0.007	**0.003**
hsa-miR-15b-5p	-0.319	0.022	0.039	**0.0001**
hsa-miR-140-5p	0.297	0.039	0.032	**0.003**
hsa-miR-1246	0.482	0.042	0.008	**0.017**
hsa-miR-320c	0.32	0.017	0.04	**0.032**

4.2.5 Comparison of miRNA expression between matched serum and tissue samples

We next questioned whether or not DEM observed in the sera of HGSOC patients could reflect those present in the tumor masses. To that end, we compared miRNA expression in those patients for whom matched serum and tumor tissue were available. As described in Figure 4.7, ten miRNAs shared a differential expression in tissue and serum between cancer patients and normal donors. Of these, eight miRNAs showed the same trend of up/down regulation in cases and controls, while 2 miRNAs display an opposite trend.

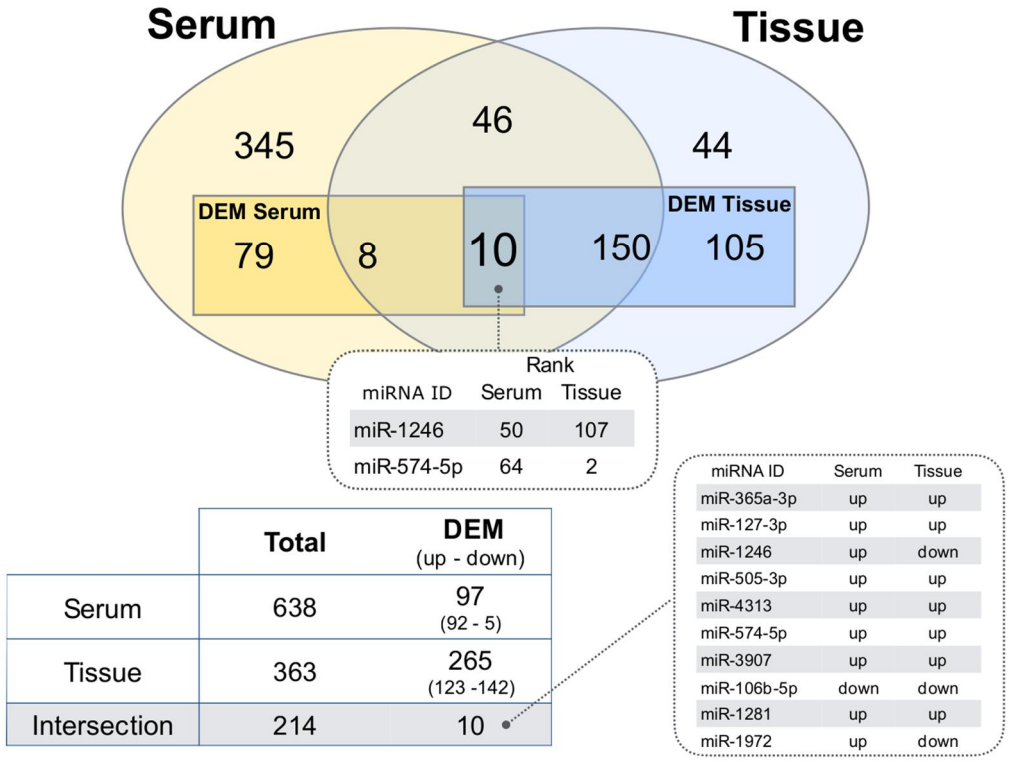

Figure 4.7: Venn diagram of the list of differentially expressed miRNAs between tissue and serum samples. After filtering steps, we detected 638 miRNAs in sera and 363 miRNAs in tissues. Of these, 214 were in common. Among these 214 miRNAs, we identified 10 miRNAs differentially expressed in both sera and tissues, of which 8 with the same trend.

4.2.6 Identification and validation of candidate reference for miRNA quantification by RT-qPCR in HGSOC tissue samples

Since there is a lack of consensus in the literature regarding the most suitable endogenous control, before starting with the experiments for the validation of miRNA expression data, we decided to identify and validate the most stable reference sncRNAs (small non-coding RNAs) for normalization of miRNA RT-qPCR expression data in HGSOC.

We selected a panel of seven potential endogenous controls derived from the literature (U6, SNORD48, miR-92a-3p, let-7a-5p, SNORD61, SNORD72, SNORD68), suggesting their use for normalization of qPCR studies in HGSOC tissue samples. Then, we added to the analysis four reference miRNAs, miR-103a-3p, miR-423-3p, miR-191-5p and miR-16-5p, selected and validated from Exiqon for normalization of miRNA expression levels in human tissue samples during real-time PCR. This panel of eleven miRNAs was integrated with additional two miRNAs, miR-26a-5p and miR-1249, emerged as the most invariant by microarray analysis, performed on 99 HGSOC and 16 normal tissue samples (see paragraph 3.3). Quantitative real-time PCR was performed on a portion of the entire cohort of HGSOC (n=75) and on 25 normal tissues (n=25, including ovarian and tubal epithelia), to assess the expression pattern of the 13 selected reference sncRNAs.

Stability of candidate endogenous controls was evaluated by geNorm [Vandesompele J et al. 2002] and NormFinder algorithms [Long JS et al. 2000] and validated with an equivalence test (Two-One-Sided Test approach, TOST) [Wellek S 2003].

Combining results from the three different statistical approaches, SNORD48 emerged as stably and equivalently expressed between malignant and normal tissues. Among malignant samples, considering groups based on residual tumor, miR-191-5p was identified as the most equivalent sncRNA (Table 4.8). Based on these results, for the following experiments of miRNA relative expression quantification, we decided to use SNORD48 and miR-191-5p, as best reference sncRNAs within our cohort of HGSOC compared to normal tissues and within HGSOC tissues, respectively.

Table 4.8: Log Fold changes in reference sncRNA expression between HGSOC and normal control samples, and among patients with no residual tumor versus patients with residual tumor (90% confidence intervals,; p-values for linear models; * null hypothesis of no equivalence rejected; [εL,εU]=[-0.36,0.36]).

	HGSOC *vs* Control			**RT=0 *vs* RT>0**		
sncRNAs	**Log FC**	**$CI_{90\%}$**	***p*-value**	**Log FC**	**$CI_{90\%}$**	***p*-value**
miR-16-5p	-1.87	-2.36;-1.38	<0.001	-0.16	-0.43;0.11	0.328
miR-191-5p	-0.10	-0.44;0.24	0.625	0.06	-0.23;0.36*	0.725
miR-423-3p	0.21	-0.18;0.59	0.375	0.60	0.04;1.15	0.087
let-7a-5p	-0.20	-0.59;0.19	0.401	0.48	-0.01;0.98	0.108
miR-103a-3p	-0.15	-0.60;0.31	0.601	0.28	-0.35;0.90	0.465
miR-92a-3p	-1.89	-2.23;-1.55	<0.001	0.40	0.005;0.80	0.096
SNORD68	-0.23	-0.55;0.09	0.229	0.28	-0.14;0.71	0.274
SNORD61	0.33	-0.08;0.74	0.190	-0.05	-0.42;0.32	0.828
SNORD72	1.21	0.80;1.63	<0.001	0.25	-0.25;0.74	0.408
SNORD48	0.02	-0.28;0.32*	0.924	0.25	-0.14;0.64	0.287
U6	-0.53	-0.84;-0.23	0.003	0.56	0.06;1.06	0.066
miR-26a-5p	0.57	0.34;0.80	0.013	-0.10	-0.35;0.14	0.102
miR-1249	1.33	1.13;1.54	0.000	-0.17	-0.38;0.04	0.154

4.2.7 miR-1246 expression validation by RT-qPCR and association with patient survival

Since the up-regulation of circulating miR-1246 levels in HGSOC patients has been confirmed by three different techniques and since miR-1246 up-regulation in HGSOC biopsies was correlated with platinum-resistance and worst prognosis by microarray analysis, we focused on the validation of its expression in our cohort of tumor and normal tissues (from HOSE and fallopian tubes) by RT-qPCR. Interestingly, by microarray analysis, miR-1246 expression emerged down-regulated in HGSOC tissues compared to normal controls. As represented in Figure 4.8 A, we confirmed the down-regulation of miR-1246 expression levels in HGSOC samples compared to HOSE, but we did not detect a significantly differential expression compared to fallopian tubes. This result mirrors the global miRNA expression trend emerged by microarray where, as revealed by principal component analysis (PCA) in Figure 4.9, luminal fallopian tube surface epithelium miRNA profile shares a higher similarity with HGSOC miRNA profile, compared to ovarian surface epithelium. Moreover, miR-1246 over-expression in HGSOC tissues was significantly associated with platinum-resistant compared to platinum-sensitive patients (p-value=0.047) (Figure 4.8), by RT-qPCR. Kaplan-Meier survival curves showed that OS and PFS decreased in patients with high miR-1246 expression compared to those with low miR-1246 expression (p-value<0.001, HR=2.57; p-value=0.024, HR=1.68; respectively). In addition, multivariate analysis, considering miR-1246 expression and residual tumor, revealed miR-1246 over-expression as an independent prognostic factor for poor OS and PFS (p-value=0.001, HR=2.42; p-value<0.05, HR=1.59; respectively).

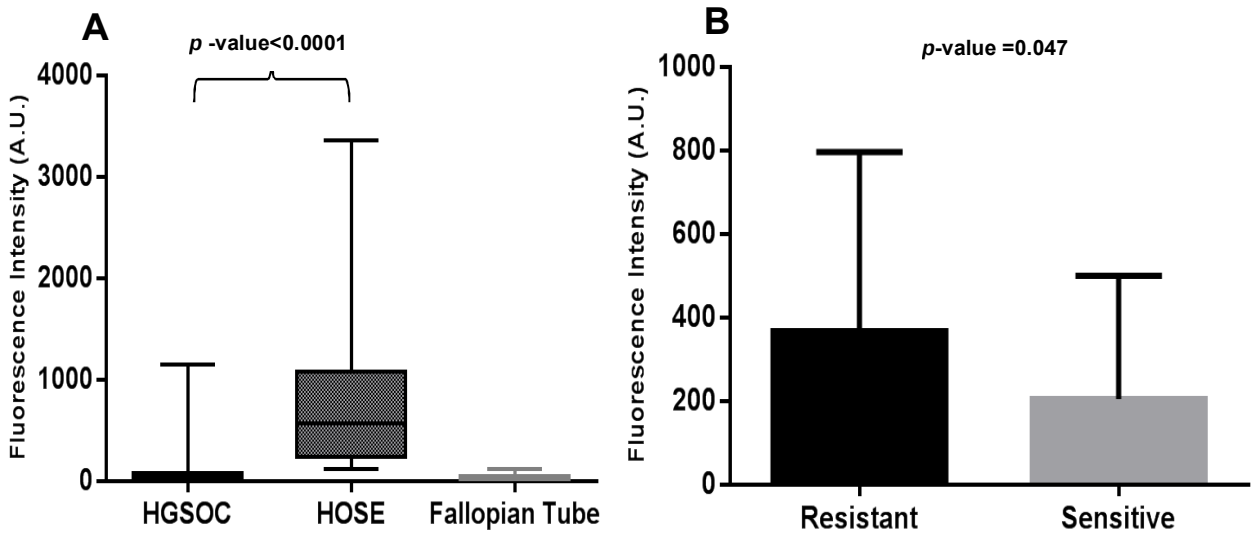

Figure 4.8: A miR-1246 expression levels in HGSOC samples compared to normal controls, composed by HOSE and fallopian tube by RT-qPCR. **B** miR-1246 expression levels among HGSOC samples: comparison between chemo-resistant *vs* chemo-sensitive patients.

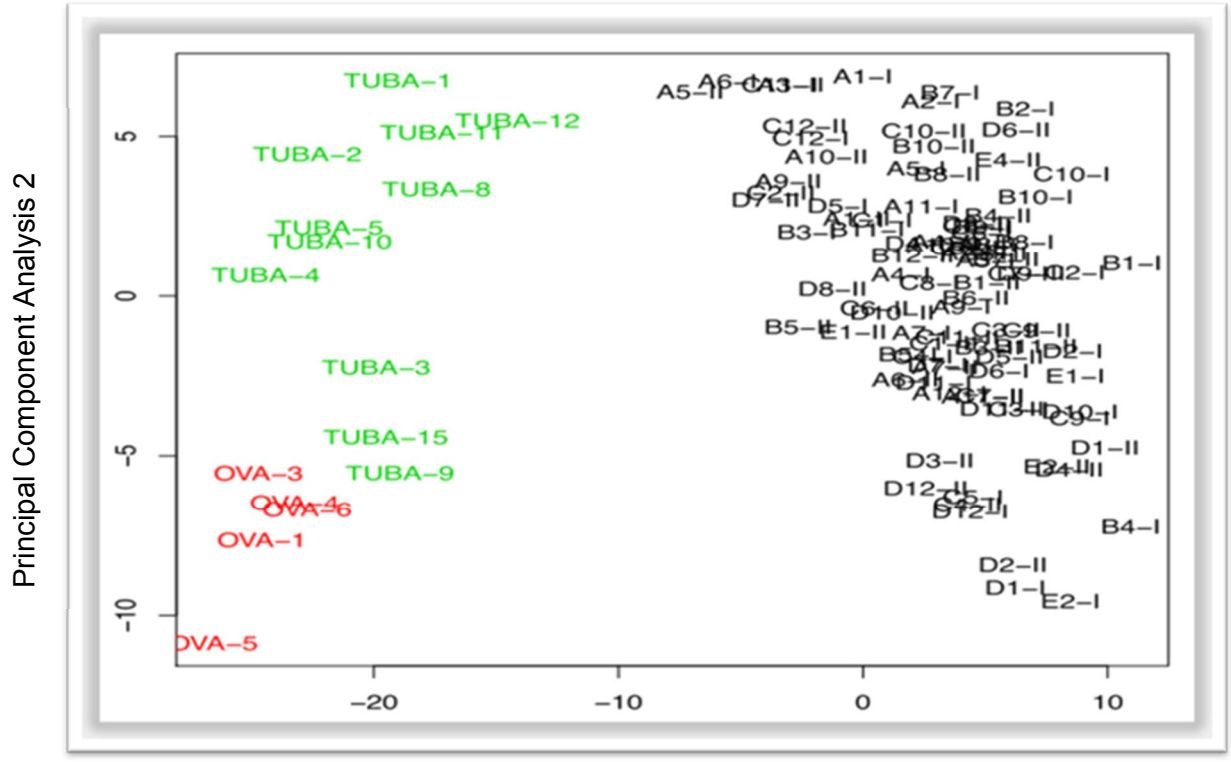

Figure 4.9: PCA based on the microarray expression levels of the 200 most variable miRNAs among 99 HGSOC, 11 fallopian tubes and 5 HOSEs (pooled from 17 healthy donors).

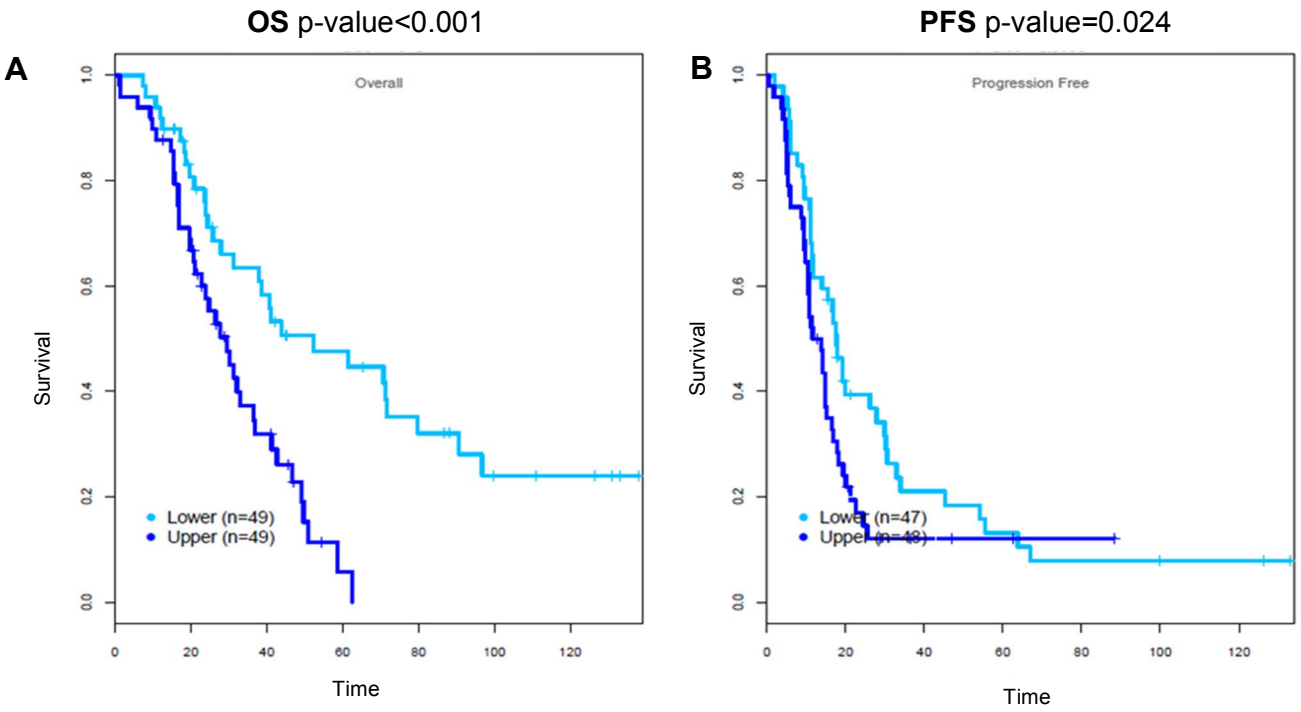

Figure 4.10: Kaplan-Meier survival curves for overall survival (OS) and progression-free survival (PFS) according to tissue miR-1246 expression from 99 HGSOC patients. **A** The OS rate of HGSOC patients with high or low miR-1246 expression; **B** The PFS rate of HGSOC patients with high or low miR-1246 expression.

4.2.8 Identification and validation of hypoxia-regulated miRNAs (HRMs) by RT-qPCR

We focused our analysis on a group of 16 miRNAs (miR-210/24-3p/23a-3p/27a-3p/21-5p/23b-3p/26b-5p/103a-3p/107/192-5p/93-5p/181b-5p/30b-5p/26a-5p/125b-5p/181a-5p) belonging to the group of hypoxia-regulated miRNAs (HRMs), selected from the literature and already emerged as relevant in other solid tumors. Most of the HRMs showed a significant differential expression in HGSOC compared to normal tissues, by microarray analysis (Table 4.9). Among them, miR-210, being the most widely studied miRNA associated with hypoxia and considered a master miRNA of the hypoxic response, was selected for further validations. Additionally, we validated miR-23a-3p and miR-27a-3p, showing a significant and a borderline significant association with poor overall survival, respectively (Table 4.9), and miR-24-3p located on the same miR-23a-3p/27a-3p gene cluster. RT-qPCR, using SNORD48 as reliable reference within HGSOC tissue samples and controls, confirmed the over-expression of all the four HRMs tested in HGSOC compared to normal tissues, as reported in Figure 4.11 (all p-values≤ 0.002). Moreover, we confirmed the significant over-expression of miR-23a-3p in the group of patients resistant compared to platinum-sensitive patients (p-value=0.03, Figure 4.12). In addition, in univariate survival analysis, miR-23a-3p over-expression resulted significantly associated with poor PFS (p-value<0.01, HR=1.8), whereas it did not show a significant correlation with OS. More interestingly, multivariate Cox regression analysis,

revealed miR-23a-3p up-regulation, along with tumor residual, significant correlated with shorter PFS (p-value=0.01, HR=1.78).

Table 4.9: HRMs emerged significantly differentially expressed in HGSOC *vs* normal tissues, by microarray analysis. miR-23a-3p and miR-27a-3p showed a borderline (p-value=0.056) and significant (p-value=0.036) association with platinum-resistant tumors.

Tissue HRMs	HGSOC *vs* Control				Resistant *vs* Sensitive			
	Log FC	Aver. Expr.	*p*-value	Adj. *p*-value	Log FC	Aver. Expr.	*p*-value	Adj. *p*-value
hsa-miR-210	1.377	7.868	0.0001	**0.0001**	0.037	8.009	0.85	0.907
hsa-miR-24-3p	1.451	10.244	0.0001	**0.0001**	-0.006	10.462	0.959	0.959
hsa-miR-23a-3p	2.076	10.017	0.0001	**0.0001**	0.361	10.311	0.007	**0.056**
hsa-miR-27a-3p	2.795	9.749	0.0001	**0.0001**	0.435	10.151	0.002	**0.036**
hsa-miR-21-5p	2.028	13.02	0.0001	**0.0001**	0.069	13.246	0.739	0.892
hsa-miR-23b-3p	1.303	9.344	0.0001	**0.0001**	-0.161	9.561	0.424	0.679
hsa-miR-26b-5p	-1.449	9.354	0.0001	**0.0001**	0.104	9.161	0.485	0.706
hsa-miR-103a-3p	-0.826	10.068	0.0001	**0.0001**	0.13	9.96	0.335	0.67
hsa-miR-107	-1.319	9.505	0.0001	**0.0001**	0.069	9.323	0.622	0.829
hsa-miR-192-5p	-1.413	4.851	0.0001	**0.0001**	-0.067	4.719	0.78	0.892
hsa-miR-93-5p	-1.319	8.625	0.0001	**0.0001**	-0.232	8.47	0.114	0.305
hsa-miR-181b-5p	1.249	5.604	0.0001	**0.0001**	0.146	5.762	0.389	0.679

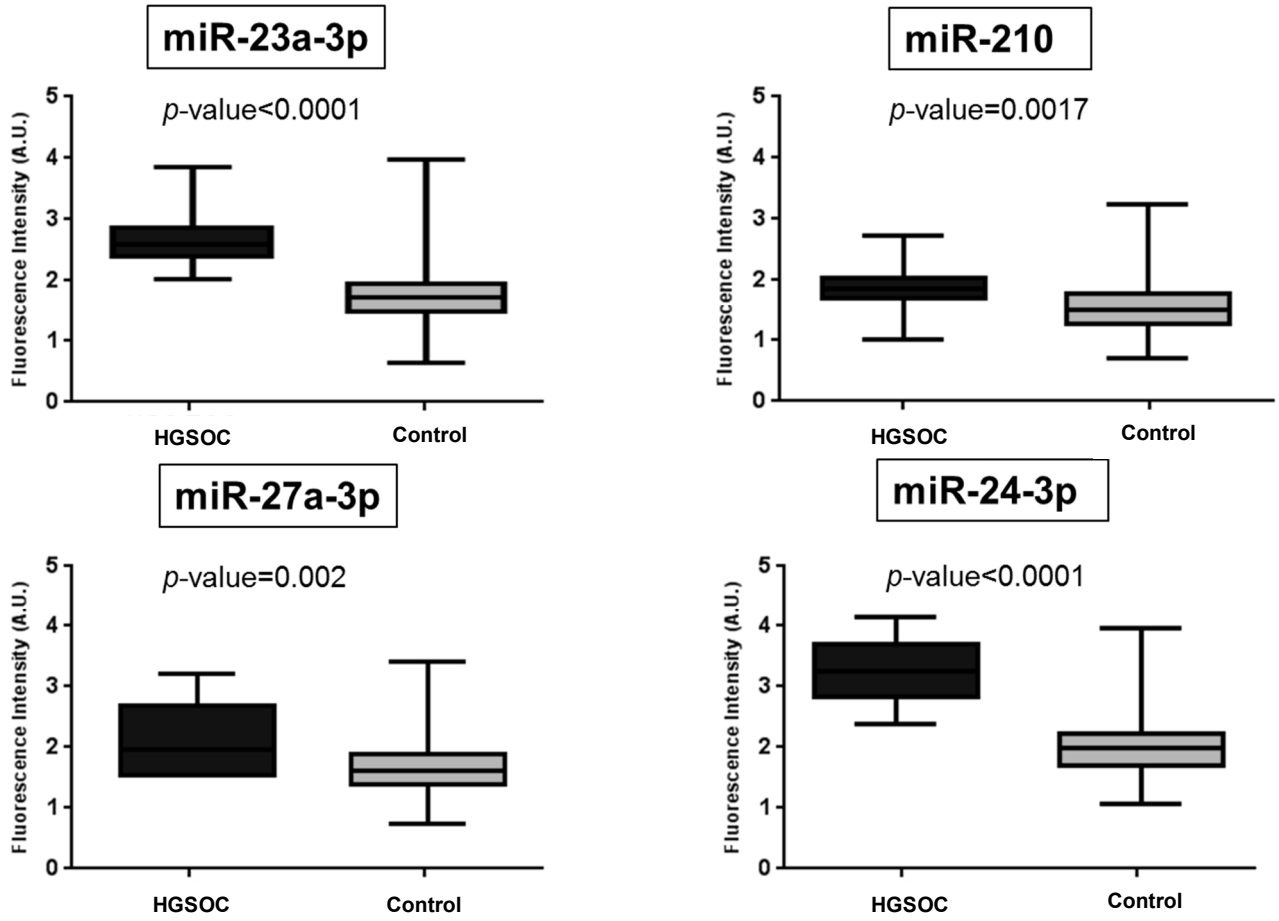

Figure 4.11: Significant over-expression of selected HRMs in 99 HGSOC compared to 25 normal tissues. Data are displayed as mean ± SD and are expressed normalized for SNORD48.

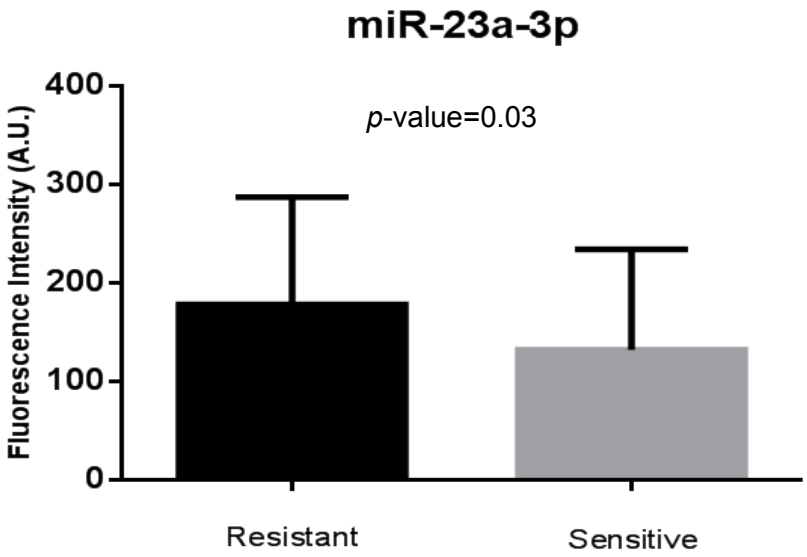

Figure 4.12: Significant over-expression of miR-23a-3p in 40 platinum-resistant compared to 36 platinum-sensitive patients. Data are displayed as mean ± SD and are expressed normalized for miR-191-5p.

4.2.9 Evaluation of HRMs in cancer stem cell-like (CSC) line

Starting from a primary ovarian cancer cell line OVA-BS4, established in our laboratory after sterile processing of a surgical metastatic high-grade serous tumor biopsy, under selective culture conditions, we isolated OVA-BS4 parent cell line formed non-adherent spheres, potentially enriched in cells with stem-like properties. This cell line has been extensively characterized in our laboratory by molecular and phenotypic characterization, that revealed a stem-like phenotype. More interestingly, OVA-BS4 spheres showed resistance to all the traditional anti-cancer agents tested (cisplatin, paclitaxel, etoposide, PS341, doxorubicin and trabectedin) compared to the parental OVA-BS4 adherent cell line. Starting from these evaluations, we decided to test miR-210, miR-23a-3p, miR-24-3p and miR-27a-3p in OVA-BS4 spheres with CSC-like properties, as a reliable *in-vitro* model of chemo-resistance. Three independent biological replicates were tested by RT-qPCR, using SNORD48 as miRNA expression normalizer, showing the lowest coefficient of variation among samples. In all three cases, mir-210 expression was consistently increased in OVA-BS4 spheres compared to OVA-BS4 adherent cell line (Figure 4.13). Although the scanty number of samples evaluated did not allow to reach a significant statistical difference between the two conditions, a noticeable trend of up-regulation of miR-210 emerged from the comparison ($p=0.07$). On the contrary, the other three HRMs analyzed did not show any evident differential expression between conditions.

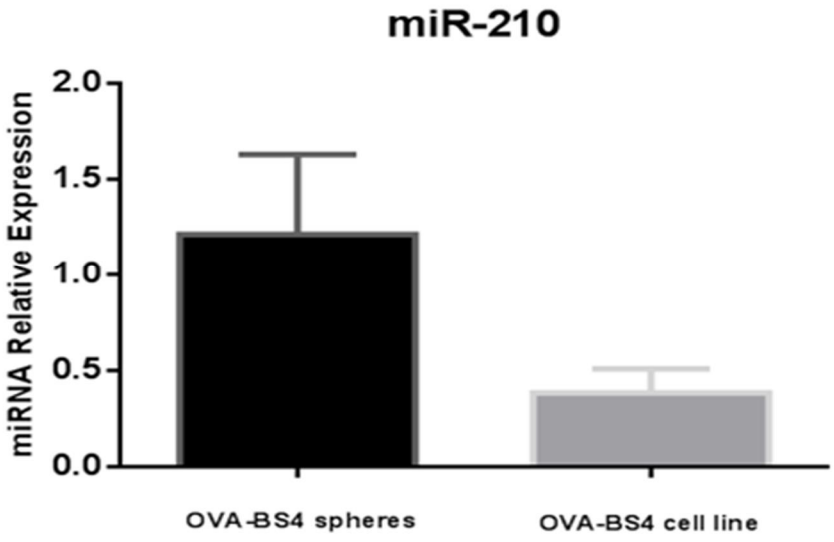

Figure 4.13 Expression of selected HRM miR-210 in OVA-BS4 spheres and in OVA-BS4 parental cell line. Data are displayed as mean ± SD of three independent experiments and are normalized using SNORD48.

4.2.10 Target prediction

Using TargetScan , we looked at identifying putative mRNA targets of miR-23a-3p, the hypoxia-related miRNA emerged significantly up-regulated in HGSOC patients and, more interestingly, in the group of patients resistant to platinum-based chemotherapy, compared to platinum-sensitive patients. An anti-correlation miRNA/mRNA pairs analyses was performed, based on gene and miRNA expression levels obtained by microarray. Thousands of genes emerged as potential targets of miR-23a-3p (data not shown). In particular, among the gene at the top of the list, showing the best value of anti-correlation, we identified APAF-1. This gene, coding for the apoptotic protease activating factor-1, plays a crucial role in the regulation of apoptosis, and it has been already demonstrated as potential target of miR-23a-3p in other types of solid tumors.

4.3 Discovery of HGSOC specific long non-coding RNAs

From RNA sequence data analysis, we identified a total of 1371 transcripts, differentially expressed between platinum-resistant (n=14) and platinum-sensitive patients (n=14) (data not shown). Only 125 out of 1371 transcripts (9%) were already known sequences, associated to coding or non-coding genes. Most of the transcripts detected (n=539, 39%) represented potentially novel isoforms of reference transcripts and almost 147 (11%) sequences showed a generic overlap with noted transcripts. Moreover, the data analysis identified 139 (10%) unknown, intergenic transcripts and 389 (28%) exonic transcripts overlapped with reference sequences on the opposite strand. Finally, almost 32 transcripts (3%) were due to read mapping errors. Interestingly, a very small part of the collected transcriptional alterations can be ascribed to coding-genes, suggesting a prominent non-coding role in HGSOC platinum resistance. Currently, we are validating a panel of ten selected transcripts to confirm our method of analysis.

5. DISCUSSION

Circulating miRNA as potential diagnostic markers in HGSOC

HGSOC represents the most lethal gynecologic malignancy, with survival rate virtually unchanged in the past 30 years. HGSOC high mortality reflects its asymptomatic nature, the lack of adequate screening test, the low predictive capacity of diagnosis in an early stage and the development of resistance to the standard therapies. The possibility to identify the early onset of HGSOC is thus of extreme importance for improving patients' clinical outcome. Studies performed so far have confirmed the limits of currently used diagnostic biomarkers, like CA-125, to identify early phases of tumor growth and disseminated disease [Jacobs IJ et al 2016; Terry KL et al 2016]. Considering the lack of ovarian cancer screening tests able to significantly reduce the mortality of patients, the development of novel strategies for early diagnosis, such as the identification of novel biomarkers, is one of the possible strategies to pursue.

Conceptually, there are different steps for a molecule to be selected as a biomarker, along the path from the bench to patient's bedside. Starting from these premises, in the first part of my PhD project, we aimed at identifying, in sera of patients, molecular features of tumor biology that could represent one step forward in the identification of novel biomarkers for early disease detection. In the last years, there has been a growing interest in the potential role of circulating miRNAs as diagnostic biomarkers in different types of carcinoma, including ovarian cancer. Indeed, a blood-based test can be easy accessible, minimally invasive and it could represent a promising screening test for early disease detection. In recent years, several circulating miRNAs have been identified as biomarkers with implications in ovarian cancer diagnosis. However, there is a lack of consensus in the normalization strategy of circulating miRNA levels exists in the literature, mainly due to the absence of reliable "reference miRNAs". Therefore, despite the relative abundance of published papers, the vast majority of them reveals a hastily data standardization and a normalization performed in a suboptimal way, using reference miRNAs arbitrarily chosen among those most commonly published. Moreover, most previously studies analyzed circulating miRNAs belonging to patients harbouring all ovarian carcinoma histotypes, while the few investigations focused on HGSOC specific miRNAs in serum/plasma are limited by a narrow sample size. Finally, RT-qPCR is the most reported technique for studying miRNA expression in biological fluids, while a high-throughput system is more desirable when reliable markers need to be discovered. In summary, many technical challenges in the analysis of circulating miRNAs (i.e., samples storage and processing, profiling methods and data normalization) have complicated the comparison of independent datasets and delayed their entering into clinical settings.

To overtake the several issues described above, my study focused into an experimental design that displays several improved features compared to other studies, including: *i)* serum samples belonging to patients harbouring HGSOC, the most frequent and aggressive ovarian cancer histological type, *ii)* two cohorts of patients, gathered from independent serum collections, that were used to obtain molecular data, reducing biases in statistical analysis, *iii)* serum from age-

matched healthy women as normal controls, *iv)* optimized protocol including collection, handling, storage and miRNAs extraction of serum samples, *v)* haemolysis monitoring of serum samples, *vi)* the use of an innovative and effective statistical approach of microarray data normalization, combining synthetic spike-in RNA oligos and the most invariant endogenous miRNAs, *vii)* the use of two RT-qPCR techniques for miRNA validation and, in particular, of Exiqon primer sets with LNA technology, which maximizes sensitivity and specificity in detecting miRNA amplicons. According to the aforementioned critical issues, we used microarray technology on a total of 110 serum from HGSOC patients and 19 healthy volunteers to achieve an efficient selection of the most promising miRNAs among the thousands of possible candidates sourced from the miRNome (miRBAse version 19). In addition, we developed a novel bioinformatic approach to identify specific circulating miRNAs characterizing HGSOC patients. In particular, we chose to apply an innovative approach of statistical analysis, using the expression levels of 10 different non-human spike-in oligos, combined with a set of most invariant low-expressed endogenous miRNAs, to normalize circulating miRNA levels.

The miRNA profile on the training set initially allowed us to identify 97 miRNAs with different expression levels between HGSOC patients and healthy controls. Among miRNAs selected for RT-qPCR validation, miR-1246, miR-595, miR-4290, miR-2278 confirmed to be significantly up-regulated in the HGSOC patients group compared to healthy donors. Importantly, the up-regulation of miR-1246, miR-595 and miR-2278 was furtherly validated by RT-qPCR in a completely independent dataset of serum samples, obtained from 58 HGSOC and 13 healthy donors. Moreover, since miR-1246 has emerged as the most reliable biomarker, we performed an absolute quantification of circulating miR-1246 copies using ddPCR, validating once more its significantly differential expression between the two groups of samples. Notably, we performed ROC curve analysis on miR-1246 to estimate its sensitivity and specificity, as diagnostic performance for HGSOC detection. Our findings confirmed miR-1246 as the most promising diagnostic biomarker, as it was able to accurately classify tumor patients compared to healthy donors, both in the training and in the validation cohorts. To the best of our knowledge, miR-1246 has not been associated to ovarian cancer previously, neither at the tissue nor at the serum levels. Nevertheless, its expression has been largely reported as upregulated in other cancer tissues, such as lung, oral, colorectal, esophageal, hepatic, pancreatic and cervical carcinoma [Kim G et al 2016; Liao L et al 2015; Wang S et al 2016; Fu HL et al 2013; Sun Z et al 2014; Hasegawa S et al 2014; Chen J et al 2014]. As circulating marker, miR-1246 has been proposed, alone or in combination with others, for the detection of multiple myeloma, oesophageal, colon, cervical carcinomas and early stage breast cancer [Jones CI et al 2012; Takeshita N et al 2013; Ogata-Kawata H et al 2014; Chen J et al 2013; Shimomura A et al 2016]. Furthermore, high levels of circulating miR-1246 and miR-595 have been reported associated to active forms of inflammatory bowel disease [Krissansen GW et al 2015].

Gene and miRNA expression in HGSOC compared to normal tissues

HGSOC is often an incurable gynecological malignancy. Although the majority of tumors initially respond to chemotherapy, most patients succumb to chemoresistant recurrent disease. Despite a variety of cytotoxic anti-cancer agents and targeted therapy such as bevacizumab have recently emerged, control over the progression of HGSOC remains inadequate. Chemoresistance is the principal factor limiting long-term survival in ovarian carcinoma patients. Currently available prognostic parameters are not able to adequately predict HGSOC relapse and clinical course. Therefore, the need to discover novel accurate outcome-informative markers would be critical to select those patients who could benefit from individualized therapies. The lack of reliable prognostic markers and the lack of effective therapies for patients with HGSOC in some way reflects the incomplete understanding of the molecular basis of its pathogenesis and progression. In this context, the recent identification of the regulatory role of non-coding RNAs (ncRNAs) extended the spectrum of possible key factors involved in essential biological processes of cancer development and progression. Starting from these premises, in the second part of my PhD project, we performed a global RNA expression profiling, including coding and ncRNAs, such as miRNAs and lncRNAs, in order to better understand the transcriptional and post-transcriptional mechanisms characterizing HGSOC. In particular, we have attempted to identify molecular markers to adequately predict HGSOC relapse and clinical course. Gene and miRNA expression profiles have been reported as associated with overall survival, primary surgical cytoreduction (debulking status), and response to platinum therapy in ovarian cancer [Crijns AP et al 2009; Bonome T et al. 2008; Jazaeri AA et al. 2005; Cancer Genome Atlas Research Network 2011]. Despite those encouraging developments, no biomarker for prediction of response to therapy has been clinically useful yet. The particular design of my study has been characterized by several features, including: *i)* a wide and well-characterized cohort of snap-frozen tumor tissue samples of high grade serous histological type, the most frequent and aggressive ovarian cancer, belonging to a single institution, *ii)* the inclusion of both ovarian surface and fallopian tube epithelia, as source of normal control tissues, to better understand the histogenesis of HGSOC, still debated, *iii)* a stringent quality control of isolated total RNA, *iv)* a genome wide RNA expression analysis, including mRNA/miRNA/lncRNA signature, by high-throughput microarray Agilent Technology®, *v)* the careful selection of putative reference sncRNAs, for an accurate quantification of miRNA levels by RT-qPCR, *vi)* the use of optimized Exiqon primer sets with LNA technology, maximizing sensitivity and specificity in amplicon detection, *vii)* the possibility to match tumor biopsies and serum samples from the majority of patients enrolled in the study.

In this study, we performed a comprehensive gene and miRNA expression profiling on a cohort of 99 advanced-stage HGSOC patients, partially matched with serum samples (n=76) and 16 healthy controls, obtained both from normal ovary and luminal fallopian tube surface epithelia. By microarray analysis, most of the genes and miRNAs have emerged aberrantly expressed in HGSOC tissue samples. After filtering steps, by microarray technology a total of 265 miRNAs (123

upregulated and 142 downregulated) have emerged significantly differentially expressed between HGSOC and normal tissues. To potentially clarify the HGSOC precursor, we performed a principal component analysis on miRNA expression profile, including all the HGSOC tissues of our cohort and the potential neoplasm precursors, obtained both from HOSEs and fallopian tube epithelium brushing. The analysis was based on the most variable miRNAs (n=200) among the three different types of tissues. Interestingly, this miRNA profile analysis was able to cluster our samples in three different and clearly separated groups. More importantly, luminal fallopian tube epithelium miRNA profile shared a higher similarity to HGSOC miRNA profile, compared to ovarian surface epithelium one. This preliminary result seems to unlock new insights on HGSOC biogenesis, supporting a recent novel theory on the origin of this aggressive tumor [Kurman RJ et al. 2010].

Gene, miRNA and lncRNA expression according to response to platinum-based chemotherapy in HGSOC

Within our large and uniform records, we examined the association of gene expression profile with chemotherapy status of patients. Using the whole platform of genes examined, unsupervised analysis did not generate any cluster able to differentiate patients according to chemotherapy status. However, the comparison between the group of platinum-resistant and platinum-sensitive patients identified Homer Protein Homolog 2 (HOMER2) as the only differentially expressed gene. This gene encodes a member of the homer family of dendritic proteins; members of this family regulate group 1 metabotrophic glutamate receptor function. In our cohort of samples, HOMER2 showed a down-regulation in the group of chemo-resistant patients. This gene is known in the literature to cooperate with a class myosin MYO18B and their co-expression enhances the ability of MYO18B to suppress the anchorage-independent growth of a human lung cancer cell line [Ajima R et al. 2007].

Based on high-throughput gene expression analysis, we performed a topological-based pathway analysis, using Graphite Web, a novel web tool developed by Sales et al [Sales G et al. 2013]. This method, combining topological and multivariate pathway analyses, allows identifying significant signal transduction paths within significantly altered pathways. Moreover, since a biological pathway is not a mere list of genes, but represents the biologic relations between genes, in this analysis, each gene can contribute to the statistical significance of the pathway with a final additive effect due to its interaction with the other genes within the network. Particularly, the gene set analysis on our cohort of HGSOC samples revealed a total of 58 pathways involved in the mechanism of platinum-resistance. Among them, we identified Tight junction, Erb signaling, Wnt signaling, Cell cycle, Jak/STAT signaling and cell adhesion molecules pathways. Some interesting pathways, among the differentially expressed, have been already reported contributing to the onset of resistance to therapy and warrant to be further investigated [Anastas JN et al. 2013, Ma J et al. 2014].

According to response to platinum-based chemotherapy and prognosis, we identified a total of 9 differently expressed miRNAs (miR-199b-5p, miR-423-5p miR-455-3p, miR-22-3p, miR-199a-3p, miR-15b-5p, miR-140-5p, miR-1246, miR-320c) in the group of patients platinum-resistant and partially platinum-sensitive compared to platinum-sensitive patients, and significantly associated with overall survival and progression free survival. Since the up-regulation of circulating miR-1246 levels in HGSOC patients has been confirmed by three different techniques (microarray, RT-qPCR and ddPCR) and since miR-1246 up-regulation in HGSOC biopsies was associated with platinum-resistance and worse prognosis by microarray analysis, we focused on the validation of its expression in our cohort of tumor and normal tissues by RT-qPCR.

Currently, there is no literature consensus on the most stably expressed endogenous controls that should be used in HGSOC miRNA RT-qPCR studies. Similarly to mRNA expression analysis, the choice of reference genes for miRNA RT-qPCR data normalization has a great impact on the study outcome, as different normalization strategies can lead to different interpretation of data resulting in ambiguous biological conclusions [Calin GA et al. 2006]. As already postulated, miRNA may act “in cascade” over several mRNA genes, regulating multiple target within the same pathway, thus small changes in miRNA expression could have important consequences for a given cellular function [Mestdagh P et al. 2014]. Accordingly, the validation of endogenous normalizers is even more critical for miRNA RT-qPCR experiments, considering that relatively small differences in miRNA expression may be biologically and clinically significant. Then, before proceeding with miRNA expression level validation by RT-qPCR, we identified the most suitable small non coding RNAs (sncRNAs) as endogenous controls for miRNA expression normalization in a subset of HGSOC samples and normal tissues. Eleven putative reference sncRNAs for normalization (U6, SNORD48, miR-92a-3p, let-7a-5p, SNORD61, SNORD72, SNORD68, miR-103a-3p, miR-423-3p, miR-191-5p, miR-16-5p) and miR-26a-5p and miR-1249, emerged as the most invariant miRNAs by our microarray analysis, were analyzed using a highly specific RT-qPCR. Combining results from three different statistical approaches, SNORD48 emerged as stably and equivalently expressed between malignant and normal tissues. Among malignant samples, considering groups based on residual tumor, miR-191-5p was identified as the most equivalents ncRNA. It was not surprising to find miR-26a-5p and miR-1249 not further confirmed as the most invariant miRNAs in our cohort of HGSOC and normal tissues, using RT-qPCR. It is well known that hybridization platform, such as microarray technology, has a lower sensitivity and specificity compared to quantitative PCR (qPCR), that represents the gold standard for single miRNA measurement. For all miRNA quantifications performed in this study by RT-qPCR on tissues, we decided to apply the Exiqon technology, that quantify miRNA expression in a two-step PCR process of modified RT-PCR, followed by a qPCR. In particular, starting from total RNA, a universal transcription system provided template for all mature miRNAs, overcoming the need for miRNA-specific RT whose efficiency can vary among different miRNAs. Both PCR amplification primers were miRNA-specific and chemically modified in the ribose mojety of nucleotides to stabilize the conformation of the

sugar groups, according to the Exiqon technology. The conformation of locked nucleic acid (LNA) oligos resulted in enhanced hybridization properties and increased sensitivity and specificity in detection of scnRNAs. Moreover, the RT mechanism allowed the amplification of mature miRNA only, without amplification of pre-miRNA whose interaction with oligos is prevented by the presence of the loop. The exceptional sensitivity, specificity and accuracy of the Exiqon RT-qPCR system have recently been confirmed by Mestdagh and colleagues in the widest peer-reviewed investigation of microRNA profiling platforms performed to date [Mestdagh P et al. 2014]. Then, based on our results, using SNORD48 as normalizer, we confirmed the downregulation of miR-1246 expression levels in HGSOC samples compared to HOSEs, by RT-qPCR. Interestingly, we did not detect a significantly differential expression between HGSOC compared to fallopian tubes. This result mirrors the previously reported global miRNA expression trend emerged by our microarray analysis, where luminal fallopian tube surface epithelium miRNA profile appears more similar to tumor miRNA profiles compared to ovarian surface epithelium one.

According to platinum response, miR-1246 showed a significantly increased expression in the group of chemoresistant compared to sensitive patients. Importantly, miR-1246 over-expression was significantly associated with poor OS and with shorter PFS in HGSOC patients by RT-qPCR. Moreover, we showed that miR-1246 over-expression represents an independent prognostic factor for OS and PFS in HGSOC patients. This result is in line with the aforementioned studies, where miR-1246 overexpression was correlated with poor patient survival in several type of cancers [Liao L et al 2015, Hong L et al 2013, Hasegawa S et al 2014]. Moreover, recently, several miR-1246 target mRNAs and related pathways have been identified and validated. In particular, miR-1246 has been associated with stemness in non-small cell lung cancer and reported to be involved in tumor metastasis by targeting CPEB4 mRNA [Kim G et al. 2016]. This association with cancer stem cells (CSCs) has been also described in pancreatic carcinoma, where miR-1246 negatively regulates CCNG2 mRNA and promotes resistance to chemotherapy [Hasegawa S et al. 2016]. The inhibition of CCNG2 induced by miR-1246 was described also in colorectal cancer, contributing to a more aggressive tumor phenotype [Wang S et al. 2016]. In hepatocarcinoma cell lines, miR-1246 enhanced migration and invasion by down-regulation of CADM1 gene and it is supposed to be regulated by p53, leading to suppression of cellular proliferation by targeting NFIB [Sun Z et al. 2014]. Finally, Chen et al reported that miR-1246 promotes proliferation, invasion and migration through the inhibition of its target gene THBS2 in cervical carcinoma [Chen J et al. 2014].

In the last part of the study with the aim to discover new coding and non-coding variants of known transcripts or totally novel transcripts, associated with the mechanism of resistance, we have sequenced the entire transcriptome of HGSOC tumor biopsies belonging to 14 platinum-sensitive and 14 platinum-resistant patients. The transcriptome reconstruction of the 28 sequencing experiments allowed us to identify 1371 transcripts differentially expressed between pt-resistant and pt-sensitive samples. Among them, 125 transcripts showed a complete match of intron chain with known transcripts, while 686 were potentially novel isoforms or showed a generic overlap with

known transcripts. The remaining, if validated, could be novel intergenic transcripts or transcripts with an exonic overlap with reference ones. Interestingly, a very small part of the collected transcriptional alterations can be ascribed to coding-genes, suggesting a prominent non-coding role in HGSOC platinum resistance. Further validation is necessary to better define the functional and predictive/prognostic role of the detected transcriptional alterations.

Comparison of miRNA expression profiles between matched serum and tissue samples

An important issue addressed in our study deals with the comparison between miRNA expression pattern observed in serum and in matched cancer tissues. Our results strengthen that, although both the HGSOC serum and tissue samples showed dysregulated global miRNA profile compared to normal counterpart, they did not show high correlation to each other. This discrepancy suggests the hypothesis that the circulating miRNA profiling is a contribute of tumor-specific and inflammation-specific miRNAs, or that miRNA could be released or captured in microvesicles and exosomes acting as a novel mechanism of genetic exchange between cells. Our findings are in line with previous reports on several solid cancers, where only 7% of the serum and tissue-derived signatures displayed excellent concordance in a discovery setting [Jarry J et al. 2014].

Hypoxia-regulated miRNAs in HGSOC

Tumor microenvironment, in particular the low O_2 tension that improves the tumor neovascularization, contributes to the onset of chemoresistance during HGSOC progression. Recently, a group of miRNAs, termed hypoxia regulated-miRNAs (HRMs), has been identified as key elements in response to hypoxia, regulating mechanisms that confer a more aggressive tumor phenotype. The complexity of hypoxia molecular mechanisms has not yet been fully elucidated in HGSOC, therefore there is an urgent need to discover novel biomarkers clinically useful to select patients with hypoxic tumors that may benefit of tailored treatments. In this context, we focused our analysis on a group of 16 miRNAs belonging to the group of HRMs emerged from literature as relevant in other solid tumors. Most of the HRMs showed a significant differential expression in HGSOC compared to normal tissues by microarray analysis. Among them, miR-210, being the most widely studied miRNA associated with hypoxia and considered a master miRNA of the hypoxic response, was selected for further validations. Additionally, we validated miR-23a-3p and miR-27a-3p, showing a significant and a borderline significant association with poor overall survival respectively by microarray analysis, and miR-24-3p located on the same miR-23a-3p/27a-3p gene cluster. RT-qPCR confirmed the over-expression of all the four HRMs tested in HGSOC compared to normal tissues, suggesting the presence of hypoxia areas within the HGSOC masses. miR-23a-3p over-expression was confirmed in platinum-resistant patients, highlighting the importance of hypoxia in HGSOC mechanism of drug resistance. More interestingly, we demonstrated miR-23a-3p over-expression as a novel prognostic factor for HGSOC patients, significantly correlated with worse PFS. Furthermore, we verified the expression of these four miRNAs in our cancer stem cell-

like (CSC) line, exhibiting resistance to all the traditional anti-cancer agents tested. Among them, miR-210 showed a borderline significant up-regulation in cancer stem cell-like line, compared to parental adherent cell line. Therefore, these preliminary results warrant further investigations to demonstrate the implication of HRMs and, in particular of miR-210, in chemoresistance mechanisms. Previous studies have already investigated the expression and involvement of these HRMs in several types of cancer. In particular, miR-27a-3p has been found to promote proliferation, migration and invasion in osteosarcoma cells by targeting MAP2K4 [Pan W et al. 2014]. Moreover, miR-27a-3p has been shown to induce esophageal cancer cell proliferation by FBXW7 suppression [Wu XZ et al. 2015]. Interestingly, in a study conducted on neuronal cell, miR-23a-3p and miR-27a-3p have been shown to alleviate hypoxia-induced neuronal apoptosis, suppressing Apaf-1 [Chen Q et al 2014]. Similarly, miR-23a-3p has been found to regulate Apaf-1 protein activity, in both pancreatic ductal adenocarcinogenesis and colorectal cancer [Liu N et al. 2015; Yong FL et al. 2014]. In line with these results, our target prediction analysis, using an anti-correlation microRNA/mRNA pairs, based on gene and miRNA expression profiles obtained by microarray analysis on the entire cohort of HGSOC and controls, revealed Apaf-1 at the top of mRNA anti-correlated to miR-23a-3p. Apaf-1 (Apoptotic protease activating factor 1) is a cytoplasmatic protein that plays a central role in the apoptosis regulatory network. If further validated, this result might explain a potential role of miR-23a-3p as oncogene, that contributes via Apaf-1 suppression to apoptosis inhibition and, consequently to confer chemoresistance to HGSOC cells.

Summary and future perspectives

In summary, during my PhD study, I mainly focused on the analysis of circulating miRNAs in HGSOC patients, as potential diagnostic biomarkers. Particularly, we optimized a reliable protocol to extract miRNAs from serum samples and to generate miRNA profiles with microarray technology. Our results indicate that there are specific miRNAs significantly differentially expressed in HGSOC patients compared to controls. The application of a robust method of statistical normalization, based on the use of nine different exogenous spike-in oligos and the most invariant endogenous miRNAs, allowed us to identify specific HGSOC circulating miRNAs with potential impact as diagnostic biomarkers. In particular, miR-1246 emerged as the most consistently up-regulated miRNA in the serum of HGSOC patients compared to healthy donors, as assessed by three independent technologies (microarray, RT-qPCR and ddPCR) and validated in two independent cohorts of patients. To the best of our knowledge, this is the first study demonstrating miR-1246 as a potential diagnostic serum biomarker in HGSOC. Prospective studies on larger cohort of serum samples are warranted to validate the performance of miR-1246 in HGSOC diagnosis. Future perspectives will include, firstly, the analysis of miR1246 in the serum of patients with benign serous cystoadenomas, in order to evaluate its diagnostic performance in discriminating malignant from benign disease. Secondly, we plan to assess miR-1246 as potential

biomarker in monitoring tumor response to treatment, taking advantage of longitudinal serum samples, collected during patient follow-up, already present in our biobank.

In the second part of the study, I focused on the generation of a miRNA/mRNA/lncRNA signature characterizing HGSOC tissues, on a wide and well-characterized group of patients, partially matched with the serum sample cohort (n=76). As normal counterpart, we have collected sixteen controls from normal ovary (HOSE) and luminal fallopian tube surface epithelia, both representing the hypothesized origin of HGSOC, whose histogenesis is still a matter of debate. Our preliminary results contribute to the recent theory that fallopian tube could represent the most likely HGSOC precursor, showing a higher similarity in miRNA profile between HGSOC and luminal fallopian tube epithelium, compared to HOSE.

High-throughput analysis on HGSOC tissues and normal controls generated a huge amount of data, still to be examined in detail. So far, by microarray analysis, most of the genes and miRNAs have emerged significantly differentially expressed between HGSOC and normal samples.

The miRNA profile analysis will be integrated with gene and lncRNA expression profiles in order to increase the comprehension of the mechanisms involved in HGSOC histogenesis and to potentially identify novel predictive and prognostic biomarkers.

In this regard, our preliminary analysis on miRNA expression profile in platinum-resistant vs platinum-sensitive patients revealed the involvement of miR1246 in the mechanism of drug response and prognosis. Indeed, its overexpression by microarray, further confirmed by RT-qPCR, emerged significantly associated with chemoresistance and worst prognosis in HGSOC patients.

As a corollary of our main study, since there is a lack in the literature regarding reliable reference for relative quantification in miRNA expression studies, we experimentally identified SNORD48 as the best reference sncRNA between HGSOC and normal controls. In addition, miR-191-5p has emerged as best reference sncRNA among HGSOC tissues.

Taken together, our results obtained both at the serum and tissue levels have highlighted the crucial role of miR-1246 in HGSOC development and chemoresistance. To further strengthen our hypothesis, we evaluated miR-1246 expression in an ovarian cancer stem cell-like (CSC) line, a model of *in-vitro* chemo-resistance, established in our laboratory under selective culture conditions. Interestingly, we have found a significantly miR-1246 overexpression in CSCs compared to parental adherent cell line by RT-qPCR (result not reported in the thesis). These preliminary results deserve further investigations, such as the evaluation of the functional role of miR-1246 in chemoresistance mechanisms, using *in-vitro* assays.

Among miRNAs resulted differentially expressed by microarray analysis, a group of hypoxia-regulated miRNAs (HRMs) emerged significantly over-expressed in HGSOC samples compared to normal counterpart, suggesting an important implication of miRNAs in response to hypoxic condition. Specifically, we have hypothesized the involvement of miR-23a-3p in chemoresistance mechanism, through APAF-1 inactivation. Further *in-vitro* studies are necessary to confirm these preliminary results and to explore the numerous mechanisms in which these miRNAs could be

involved in drug response. In this context, we planned to firstly evaluate HRM expression in our chemoresistance CSC model and in several primary HGSOC cell lines established in our laboratory. Secondly, we are going to treat these cell lines with cobalt chloride ($CoCl_2$) in order to mimic the hypoxic condition within the tumor, and then to investigate the functional role of HRMs.
Finally, data emerged from RNA sequencing preliminary analysis revealed a prominent role of non-coding transcripts in HGSOC platinum resistance mechanisms. Currently, we are validating a panel of ten transcripts, to confirm our method of analysis. These data will be integrated with gene and miRNA expression profiles previously obtained, with the aim to identify tumor circuits associated with response to treatment and prognosis, as well as to better elucidate the molecular mechanisms characterizing HGSOC progression and adaptation to hypoxic tumor microenvironment. Importantly, the identification of specific HGSOC pathways could lead to the individuation of novel molecular target for cancer therapy and for the personalization of treatment regimens. For instance, at present, the mutational status of genes involved in the homologous recombination (HR) DNA repair, as in particular BRCA1 and BRCA2, both at germline and somatic level, is a key determinant of platinum sensitivity in HGSOC patients, and provides a rational basis for the use of PARP inhibitors in first line treatment. In this context, we are currently performing targeted sequencing of a panel of selected genes involved in HR DNA repair on our cohort of HGSOC tissues, in order to better characterize their genomic profile and to correlate it to response to treatment and prognosis.

6. CONCLUSIONS

In conclusion, *miR-1246* emerged as the most consistently up-regulated miRNA in the serum of HGSOC patients compared to healthy donors, as assessed by three independent technologies (microarray, RT-qPCR and ddPCR) and validated in two independent cohorts of patients. To the best of our knowledge, this is the first report demonstrating *miR-1246* as a potential diagnostic serum biomarker in HGSOC.

At tissue level, most of the genes and miRNAs have emerged significantly differentially expressed between HGSOC and normal samples, by microarray analysis. Interestingly, luminal fallopian tube miRNA expression profile showed a higher similarity to HGSOC miRNA profile, compared to HOSE. This result strengthens the recent novel theory that fallopian tube could represent the most likely HGSOC precursor. Moreover, our results indicate, for the first time, that *miR-1246* over-expression correlates with a platinum-resistant HGSOC phenotype and may constitute a novel independent prognostic factor for HGSOC patients.

Regarding hypoxia-regulated miRNAs, our findings suggest an important role of miRNAs in response to hypoxic conditions within HGSOC masses. In particular, *miR-23a-3p* over-expression in chemoresistance patients may contribute to explain the importance of hypoxia in HGSOC mechanism of drug resistance and could represent a novel independent prognostic factor for this neoplasm.

Finally, preliminary analysis of RNA sequencing showed a prominent expression of non-coding transcripts in HGSOC platinum resistance mechanisms. These data will be integrated with gene and miRNA expression profiles previously obtained, with the aim to identify tumor circuits associated with response to treatment and prognosis, as well as to better elucidate the molecular mechanisms characterizing HGSOC progression and adaptation to hypoxic tumor microenvironment.

Taken together, these observations strongly support the crucial role that non-coding RNAs play in HGSOC development and drug response. In this context, the identification of specific HGSOC networks of gene regulation could lead to the individuation of novel molecular targets for cancer therapy and to the personalization of treatment regimens.

7. REFERENCES

Ajima R, Kajiya K, Inoue T et al. HOMER2 binds MYO18B and enhances its activity to suppress anchorage independent growth. Biochem Biophys Res Commun. 2007;356:851-6.

Akrami R, Jacobsen A, Hoell J et al. Comprehensive analysis of long non-coding RNAs in ovarian cancer reveals global patterns and targeted DNA amplification. PLoS One. 2013;8(11):e80306.

Anastas JN and Moon RT. WNT signalling pathways as therapeutic targets in cancer. Nat Rev Cancer. 2013;13(1):11-26.

Aqeilan RI, Calin GA, Croce CM. MiR-15a and miR-16-1 in cancer: discovery, function and future perspectives. Cell Death Differ. 2010;17:215–20.

Ashworth A. A synthetic lethal therapeutic approach: poly(ADP) ribose polymerase inhibitors for the treatment of cancers deficient in DNA double-strand break repair. J Clin Oncol. 2008;26:3785–90.

Audeh MW, Carmichael J, Penson RT, et al. Oral poly (ADP-ribose) polymerase inhibitor olaparib in patients with BRCA1 or BRCA2 mutations and recurrent ovarian cancer: a proof-of-concept trial. The Lancet. 2010;376:245–51.

Bandiera E, Romani C, Specchia C et al. Serum human epididymis protein 4 and risk for ovarian malignancy algorithm as new diagnostic and prognostic tools for epithelial ovarian cancer management. Cancer Epidemiol Biomarkers Prev. 2011;20(12):2496-506.

Barrett CL, DeBoever C, Jepsen K et al. Systematic transcriptome analysis reveals tumor-specific isoforms for ovarian cancer diagnosis and therapy. Proc Natl Acad Sci U S A. 2015;112(23):E3050-7.

Beltrame L, Di Marino M, Fruscio R et al. Profiling cancer gene mutations in longitudinal epithelial ovarian cancer biopsies by targeted next-generation sequencing: a retrospective study. Ann Oncol. 2015;26(7):1363-71.

Bianchi F, Nicassio F, Marzi M et al. A serum circulating miRNA diagnostic test to identify asymptomatic high-risk individuals with early stage lung cancer. EMBO Mol Med. 2011;3:495-503.

Bohnsack MT, Czaplinski K, Gorlich D. Exportin 5 is a RanGTP-dependent dsRNA-binding protein that mediates nuclear export of pre-miRNAs. RNA. 2004;10:185-91.

Bolstad BM, Irizarry RA, Astrand M et al. A comparison of normalization methods for high density oligonucleotide array data based on variance and bias. Bioinformatics. 2003;19:185-93.

Bonome T, Levine DA, Shih J et al. A gene signature predicting for survival in suboptimally debulked patients with ovarian cancer. Cancer Res. 2008;68(13):5478-86.

Bowtell DD. The genesis and evolution of high-grade serous ovarian cancer. Nat Rev Cancer. 2010;10(11):803-8.

Boyerinas B, Park SM, Murmann AE et al. Let-7 modulates acquired resistance of ovarian cancer to Taxanes via IMP-1-mediated stabilization of multidrug resistance 1. Int J Cancer. 2012;130(8):1787-97.

Bristow RE, Tomacruz RS, Armstrong DK et al. Survival effect of maximal cytoreductive surgery for advanced ovarian carcinoma during the platinum era: a meta-analysis. J Clin Oncol. 2002;20(5):1248-59.

Burger RA, Brady MF, Bookman MA, et al. Incorporation of bevacizumab in the primary treatment of ovarian cancer. N Engl J Med. 2011;365:2473–83.

Büssing I, Slack FJ, Grosshans H. let-7 microRNAs in development, stem cells and cancer. Trends Mol Med. 2008;14(9):400-9. Review.

Buys SS, Partridge E, Black A et al; PLCO Project Team. Effect of screening on ovarian cancer mortality: the Prostate, Lung, Colorectal and Ovarian (PLCO) Cancer Screening Randomized Controlled Trial. JAMA. 2011;305(22):2295-303.

Calin GA and Croce CM. MicroRNA signatures in human cancers. Nat Rev Cancer 2006;6:857-866.

Calin GA, Sevignani C, Dumitru CD et al. Human microRNA genes are frequently located at fragile sites and genomic regions involved in cancers. Proc Natl Acad Sci U S A. 2004;101(9):2999-3004.

Calura E, Fruscio R, Paracchini L et al. MiRNA landscape in stage I epithelial ovarian cancer defines the histotype specificities. Clin Cancer Res. 2013;19(15):4114-23

Cancer Genome Atlas Research Network. Integrated genomic analyses of ovarian carcinoma. Nature. 2011;474(7353):609-15.

Caramuta S, Egyházi S, Rodolfo M, et al. MicroRNA expression profiles associated with mutational status and survival in malignant melanoma. J. Invest. Dermatol. 2010;130:2062-70.

Cavazos DA, Brenner AJ. Hypoxia in astrocytic tumors and implications for therapy. Neurobiol Dis. 2015; pii: S0969-9961(15)00225-9.

Cayre A, Rossignol F, Clottes E et al. aHIF but not HIF-1alpha transcript is a poor prognostic marker in human breast cancer. Breast Cancer Res. 2003;5(6):R223-30.

Chan SY, Loscalzo J. MicroRNA-210: a unique and pleiotropic hypoxamir. Cell Cycle. 2010;9(6):1072-83. Review.

Cheetham SW, Gruhl F, Mattick JS et al. Long noncoding RNAs and the genetics of cancer. Br J Cancer. 2013;108(12):2419-25.

Chen J, Yao D, Li Y et al. Serum microRNA expression levels can predict lymph node metastasis in patients with early-stage cervical squamous cell carcinoma. Int J Mol Med 2013;32:557-67.

Chen J, Yao D, Zhao S et al. MiR-1246 promotes SiHa cervical cancer cell proliferation, invasion, and migration through suppression of its target gene thrombospondin 2. Arch Gynecol Obstet 2014;290:725-32.

Chen Q, Xu J, Li L et al. MicroRNA-23a/b and microRNA-27a/b suppress Apaf-1 protein and alleviate hypoxia-induced neuronal apoptosis. Cell Death Dis. 2014;5:e1132

Chen X, Ba Y, Ma L et al. Characterization of microRNAs in serum: a novel class of biomarkers for diagnosis of cancer and other diseases Cell Res. 2008;18(10):997-1006.

Cherry C, Ropka M, Lyle J et al. Understanding the needs of women considering risk-reducing salpingo-oophorectomy. Cancer Nurs. 2013;36(3):E33-8.

Chien J, Kuang R, Landen C et al. Platinum-sensitive recurrence in ovarian cancer: the role of tumor microenvironment. Front Oncol. 2013;3:251.

Cho KR, Shih IeM. Ovarian cancer. Annu Rev Pathol. 2009;4:287-313.

Choi HJ, Armaiz Pena GN, Pradeep S et al. Anti-vascular therapies in ovarian cancer: moving beyond anti-VEGF approaches. Cancer Metastasis Rev. 2015;34(1):19-40.

Chung YW, Bae HS, Song JY et al. Detection of microRNA as novel biomarkers of epithelial ovarian cancer from the serum of ovarian cancer patients. Int J Gynecol Cancer. 2013;23(4):673-9.

Cimmino A, Calin GA, Fabbri M et al. miR-15 and miR-16 induce apoptosis by targeting BCL2. Proc Natl Acad Sci U S A. 2005;102(39):13944-9.

Ciriello G, Miller ML, Aksoy BA et al. Emerging landscape of oncogenic signatures across human cancers. Nat Genet. 2013;45(10):1127-33.

Cittelly DM, Dimitrova I, Howe EN, et al. Restoration of miR-200c to ovarian cancer reduces tumor burden and increases sensitivity to paclitaxel. Mol Cancer Ther, 2012; 11:2556–65.

Cooke SL, Ng CK, Melnyk N et al. Genomic analysis of genetic heterogeneity and evolution in high-grade serous ovarian carcinoma. Oncogene. 2010;29(35):4905-13.

Creighton CJ, Hernandez-Herrera A, Jacobsen A et al. Cancer Genome Atlas Research Network. Integrated analyses of microRNAs demonstrate their widespread influence on gene expression in high-grade serous ovarian carcinoma. PLoS One. 2012;7(3):e34546.

Creighton CJ, Reid JG, Gunaratne PH. Expression profiling of microRNAs by deep sequencing. Brief Bioinform. 2009;10(5):490-7. Review.

Crijns AP, Fehrmann RS, de Jong S et al. Survival-related profile, pathways, and transcription factors in ovarian cancer. PLoS Med. 2009;6(2):e24. doi: 10.1371/journal.pmed.1000024.

Croce CM. Causes and consequences of microRNA dysregulation in cancer. Nat Rev Genet. 2009;10(10):704-14. Review.

Crosby ME, Devlin CM, Glazer PM et al. Emerging roles of microRNAs in the molecular responses to hypoxia. Curr Pharm Des. 2009;15(33):3861-6.

Crosby ME, Kulshreshtha R, Ivan M et al. MicroRNA regulation of DNA repair gene expression in hypoxic stress. Cancer Res. 2009;69(3):1221-9.

Crum CP, Drapkin R, Miron A et al. The distal fallopian tube: a new model for pelvic serous carcinogenesis. Curr Opin Obstet Gynecol. 2007;19(1):3-9.

Cummins EP, Taylor CT. Hypoxia-responsive transcription factors. Pflugers Arch. 2005;450(6):363-71. Review.

Dahiya N, Sherman-Baust CA, Wang TL et al. MicroRNA expression and identification of putative miRNA targets in ovarian cancer. PLoS One. 2008;3(6):e2436.

Dai F, Zhang Y, Zhu X, at al. Anticancer role of MUC1 aptamer-miR-29b chimera in epithelial ovarian carcinoma cells through regulation of PTEN methylation. Target Oncol. 2012;7:217–25.

Dalmay T, Edwards DR. MicroRNAs and the hallmarks of cancer. Oncogene. 2006;25(46):6170-5.

de Koning AP, Gu W, Castoe TA et al. Repetitive elements may comprise over two-thirds of the human genome. PLoS Genet. 2011;7(12):e1002384.

Do K, Cehn AP. Molecular pathways: targeting PARP in cancer treatment. Clin Cancer Res. 2012;19:977–84.

Dobin A, Davis CA, Schlesinger F et al. STAR: ultrafast universal RNA-seq aligner. Bioinformatics. 2013;29(1):15-21.

Domchek SM, Friebel TM, Singer CF et al. Association of risk-reducing surgery in BRCA1 or BRCA2 mutation carriers with cancer risk and mortality. JAMA. 2010;304(9):967-75.

Drapkin R, von Horsten HH, Lin Y et al. Human Epididymis Protein 4 (HE4) is a secreted glycoprotein that is overexpressed by serous and endometrioid ovarian carcinomas. Cancer Res 2005;65:2162-2169.

Eiring AM, Harb JG, Neviani P, et al. miR-328 functions as an RNA decoy to modulate hnRNP E2 regulation of mRNA translation in leukemic blasts. Cell. 2010;140:652–65.

Eisenkop SM, Spirtos NM, Lin WC. “Optimal” cytoreduction for advanced epithelial ovarian cancer: a commentary. Gynecol Oncol. 2006;103:329-35.

Ellis LM and Hicklin DJ. VEGF-targeted therapy: mechanisms of anti-tumour activity. Nat Rev Cancer. 2008;8:579–91.

Eltabbakh GH, Mount SL, Beatty B et al. Factors associated with cytoreducibility among women with ovarian carcinoma. Gynecol Oncol. 2004;95(2):377-83.

ENCODE Project Consortium Identification and analysis of functional elements in 1% of the human genome by the ENCODE pilot project. Nature. 2007;447(7146):799-816.

Engström PG, Steijger T, Sipos B et al. Systematic evaluation of spliced alignment programs for RNA-seq data. Nat Methods. 2013;10(12):1185-91.

Etheridge A, Lee I, Hood L et al. Extracellular microRNA: a new source of biomarkers. Mutat Res. 2011;717(1-2):85-90.

Farazi TA, Horlings HM, Ten Hoeve JJ et al. MicroRNA sequence and expression analysis in breast tumors by deep sequencing. Cancer Res. 2011;71(13):4443-53.

Flesken-Nikitin A, Hwang CI, Cheng CY et al. Ovarian surface epithelium at the junction area contains a cancer-prone stem cell niche. Nature. 2013;495(7440):241-5.

Foekens JA, Sieuwerts AM, Smid M et al. Four miRNAs associated with aggressiveness of lymph node-negative, estrogen receptor-positive human breast cancer. Proc Natl Acad Sci U S A. 2008;105(35):13021-6.

Fong PC, Boss DS, Yap TA et al. Inhibition of poly (ADP-ribose) polymerase in tumors from BRCA mutation carriers. N Engl J Med. 2009;361:123–34.

Fu HL, Wu de P, Wang XF et al. Altered miRNA expression is associated with differentiation, invasion, and metastasis of esophageal squamous cell carcinoma (ESCC) in patients from Huaian, China. Cell Biochem Biophys 2013;67:657-68.

Gao YC, Wu J. MicroRNA-200c and microRNA-141 as potential diagnostic and prognostic biomarkers for ovarian cancer. Tumour Biol. 2015;36(6):4843-50.

Garofalo M, Quintavalle C, Romano G et al. miR221/222 in cancer: their role in tumor progression and response to therapy. Curr Mol Med. 2012;12(1):27-33. Review.

Garzon R, Marcucci G, Croce CM. Targeting microRNAs in cancer: rationale, strategies and challenges. Nat Rev Drug Discov. 2010;9:775–89.

Geisler S, Coller J. RNA in unexpected places: long non-coding RNA functions in diverse cellular contexts. Nat Rev Mol Cell Biol. 2013;14(11):699-712. Review.

Geller SC, Gregg JP, Hagerman P et al. Transformation and normalization of oligonucleotide microarray data. Bioinformatics. 2003;19:1817-23.

George J, Alsop K, Etemadmoghadam D et al. Nonequivalent gene expression and copy number alterations in high-grade serous ovarian cancers with BRCA1 and BRCA2 mutations. Clin Cancer Res. 2013;19(13):3474-84.

Ghosh G, Subramanian IV, Adhikari N et al. Hypoxia-induced microRNA-424 expression in human endothelial cells regulates HIF-α isoforms and promotes angiogenesis. J Clin Invest. 2010;120(11):4141-54.

Giannakakis A, Sandaltzopoulos R, Greshock J et al. miR-210 links hypoxia with cell cycle regulation and is deleted in human epithelial ovarian cancer. Cancer Biol Ther. 2008;7(2):255-64.

Gibb EA, Brown CJ, Lam WL. The functional role of long non-coding RNA in human carcinomas. Mol Cancer. 2011;10:38.

Giovannetti E, Funel N, Peters GJ, et al. MicroRNA-21 in pancreatic cancer: correlation with clinical outcome and pharmacologic aspects underlying its role in the modulation of gemcitabine activity. Cancer Res. 2010;70:4528–38.

Gómez-Raposo C, Mendiola M, Barriuso J et al. Angiogenesis and ovarian cancer. Clin Transl Oncol. 2009;11(9):564-71.

Gonzalez S, Pisano DG, Serrano M. Mechanistic principles of chromatin remodeling guided by siRNAs and miRNAs. Cell Cycle. 2008;7:2601–8.

Gultekin M, Diribas K, Buru E et al. Interval debulking in epithelial ovarian carcinomas: the past, present and the future. Eur J Gynaecol Oncol. 2008;29(3):242-5.

Gupta RA, Shah N, Wang KC et al. Long non-coding RNA HOTAIR reprograms chromatin state to promote cancer metastasis. Nature. 2010;464(7291):1071-6.

Gutschner T, Diederichs S. The hallmarks of cancer: a long non-coding RNA point of view. RNA Biol. 2012;9:703-19.

Hasegawa S, Eguchi H, Nagano H et al. MicroRNA-1246 expression associated with CCNG2-mediated chemoresistance and stemness in pancreatic cancer. Br J Cancer. 2014;111(8):1572-80.

Hashimoto T, Shibasaki F. Hypoxia-inducible factor as an angiogenic master switch. Front Pediatr. 2015;3:33. Review.

Hauptman N, Glavac D. MicroRNAs and long non-coding RNAs: prospects in diagnostics and therapy of cancer. Radiol Oncol. 2013;47(4):311-8. Review.

Häusler SF, Keller A, Chandran PA et al. Whole blood-derived miRNA profiles as potential new tools for ovarian cancer screening. Br J Cancer. 2010;103(5):693-700.

Hong F, Li Y, Xu Y et al. Prognostic significance of serum microRNA-221 expression in human epithelial ovarian cancer. J Int Med Res. 2013;41(1):64-71.

Hong L, Han Y, Zhang H et al. Prognostic markers in esophageal cancer: from basic research to clinical use. Expert Rev Gastroenterol Hepatol. 2015;9(7):887-9. Review.

Hong L, Yang Z, Ma J, et al. Function of miRNA in controlling drug resistance of human cancers. Curr Drug Targets. 2013;14:1118–27.

Hoskins WJ, McGuire WP, Brady MF et al. The effect of diameter of largest residual disease on survival after primary cytoreductive surgery in patients with suboptimal residual epithelial ovarian carcinoma. Am J Obstet Gynecol. 1994;170:974-9.

Hu X, Macdonald DM, Huettner PC et al. A miR-200 microRNA cluster as prognostic marker in advanced ovarian cancer. Gynecol Oncol. 2009;114:457–64.

Hua Z, Lv Q, Ye W et al. MiRNA-directed regulation of VEGF and other angiogenic factors under hypoxia. PLoS One. 2006;1:e116.

Huarte M, Guttman M, Feldser D et al. A large intergenic noncoding RNA induced by p53 mediates global gene repression in the p53 response. Cell. 2010;142(3):409-19.

Hung T, Wang Y, Lin MF et al. Extensive and coordinated transcription of noncoding RNAs within cell-cycle promoters. Nat Genet. 2011;43(7):621-9.

Hutvanger G and Zamore PD. A microRNA in a multiple-turnover RNAi enzyme complex. Science 2002;297:2056-60.

Hwang HW, Mendell JT. MicroRNAs in cell proliferation, cell death, and tumorigenesis. Br J Cancer. 2006;94(6):776-80.

Iorio MV, Ferracin M, Liu CG, et al. MicroRNA gene expression deregulation in human breast cancer. Cancer Res 2005;65:7065–70.

Iorio MV, Visone R, Di Leva G et al. MicroRNA signatures in human ovarian cancer. Cancer Res. 2007;67(18):8699-707.

Jacobs IJ, Menon U, Ryan A et al. Ovarian cancer screening and mortality in the UK Collaborative Trial of Ovarian Cancer Screening (UKCTOCS): a randomised controlled trial. Lancet. 2016;387(10022):945-56.

Jarry J, Schadendorf D, Greenwood C et al. The validity of circulating microRNAs in oncology: five years of challenges and contradictions. Mol Oncol. 2014;8(4):819-29.

Jazaeri AA, Awtrey CS, Chandramouli GV et al. Gene expression profiles associated with response to chemotherapy in epithelial ovarian cancers. Clin Cancer Res. 2005;11(17):6300-10.

Ji P, Diederichs S, Wang W et al. MALAT-1, a novel noncoding RNA, and thymosin beta4 predict metastasis and survival in early-stage non-small cell lung cancer. Oncogene. 2003;22(39):8031-41.

Ji T, Zheng ZG, Wang FM et al. Differential microRNA expression by Solexa sequencing in the sera of ovarian cancer patients. Asian Pac J Cancer Prev. 2014;15(4):1739-43.

Johnson SM, Grosshans H, Shingara et al. RAS is regulated by the let-7 microRNA family. Cell. 2005;120(5):635-47.

Jones CI, Zabolotskaya MV, King AJ et al. Identification of circulating microRNAs as diagnostic biomarkers for use in multiple myeloma. Br J Cancer 2012;107:1987-96.

Kaelin WG Jr. The concept of synthetic lethality in the context of anticancer therapy. Nat Rev Cancer. 2005;5:689–98.

Kalir T, Firpo-Betancourt A, Nezhat FR. Update on ovarian cancer pathogenesis: history, controversies, emerging issues and future impact. Exp Rev Obstet Gynecol. 2013;8:1–9

Kan CW, Hahn MA, Gard GB et al. Elevated levels of circulating microRNA-200 family members correlate with serous epithelial ovarian cancer. BMC Cancer. 2012;12:627.

Katz B, Tropé CG, Reich R et al. MicroRNAs in Ovarian Cancer. Hum Pathol. 2015;46(9):1245-56.

Kelly TJ, Souza AL, Clish CB et al. A hypoxia-induced positive feedback loop promotes hypoxia-inducible factor 1alpha stability through miR-210 suppression of glycerol-3-phosphate dehydrogenase 1-like. Mol Cell Biol. 2011;31(13):2696-706.

Kim DH, Saetrom P, Snøve O, et al. MicroRNA directed transcriptional gene silencing in mammalian cells. Proc Natl Acad Sci USA. 2008;105:16230–5.

Kim G, An HJ, Lee MJ et al. Hsa-miR-1246 and hsa-miR-1290 are associated with stemness and invasiveness of non-small cell lung cancer. Lung Cancer 2016;91:15-22.

Kim J, Coffey DM, Ma L et al. The ovary is an alternative site of origin for high-grade serous ovarian cancer in mice. Endocrinology. 2015;156(6):1975-81.

Kim VN, Han J, Siomi MC. Biogenesis of small RNAs in animals. Nat. Rev. Mol. Cell Biol. 2009;10:126-39.

Kindelberger DW, Lee Y, Miron A et al. Intraepithelial carcinoma of the fimbria and pelvic serous carcinoma: Evidence for a causal relationship. Am J Surg Pathol. 2007;31(2):161-9.

Konecny GE, Wang C, Hamidi H et al. Prognostic and therapeutic relevance of molecular subtypes in high-grade serous ovarian cancer. J Natl Cancer Inst. 2014;106(10) pii:dju249.

Kozomara A, Griffiths-Jones S. miRBase: annotating high confidence microRNAs using deep sequencing data. Nucleic Acids Res. 2014;42(Database issue):D68-73.

Krissansen GW, Yang Y, McQueen FM et al. Overexpression of miR-595 and miR-1246 in the sera of patients with active forms of inflammatory bowel disease. Inflamm Bowel Dis. 2015;21(3):520-30.

Kroh EM, Parkin RK, Mitchell PS et al. Analysis of circulating microRNA biomarkers in plasma and serum using quantitative reverse transcription-PCR (qRT-PCR). Methods. 2010;50:298-301.

Kuhn E, Kurman RJ, Vang R et al. TP53 mutations in serous tubal intraepithelial carcinoma and concurrent pelvic high-grade serous carcinoma--evidence supporting the clonal relationship of the two lesions. J Pathol. 2012;226(3):421-6.

Kulshreshtha R, Davuluri RV, Calin GA et al. A microRNA component of the hypoxic response. Cell Death Differ. 2008;15(4):667-71.

Kulshreshtha R, Ferracin M, Negrini M et al. Regulation of microRNA expression: the hypoxic component. Cell Cycle. 2007 Jun;6(12):1426-31

Kulshreshtha R, Ferracin M, Wojcik SE et al. A microRNA signature of hypoxia. Mol Cell Biol. 2007 Mar;27(5):1859-67.

Kung JT, Colognori D, Lee JT. Long noncoding RNAs: past, present, and future. Genetics. 2013;193(3):651-69.

Kuo KT, Guan B, Feng Y et al. Analysis of copy number alterations in ovarian serous tumors identifies new molecular genetic changes in low-grade and high-grade carcinomas. Cancer Res. 2009;69:4036-42.

Kurman RJ, Shih IeM. The origin and pathogenesis of epithelial ovarian cancer: a proposed unifying theory. Am J Surg Pathol. 2010;34(3):433-43.

Kurman RJ, Shih IeM. The Dualistic Model of Ovarian Carcinogenesis: Revisited, Revised, and Expanded. Am J Pathol. 2016;186(4):733-47.Review.

Kwon JS, Tinker A, Pansegrau G et al. Prophylactic salpingectomy and delayed oophorectomy as an alternative for BRCA mutation carriers. Obstet Gynecol. 2013;121(1):14-24.

Langhe R, Norris L, Saadeh FA et al. A novel serum microRNA panel to discriminate benign from malignant ovarian disease. Cancer Lett. 2015;356(2 Pt B):628-36.

Lawrie CH, Gal S, Dunlop HM et al. Detection of elevated levels of tumour-associated microRNAs in serum of patients with diffuse large B-cell lymphoma. Br J Haematol. 2008;141(5):672-5.

Lee RC, Ambros V. An extensive class of small RNAs in Caenorhabditis elegans. Science. 2001;294(5543):862-4.

Lee RC, Feinbaum RL, Ambros V. The C. elegans heterochronic gene lin-4 encodes small RNAs with antisense complementarity to lin-14. Cell. 1993;75:843-54

Lee Y, Kim M, Han J, et al. MicroRNA genes are transcribed by RNA polymerase II. EMBO J. 2004; 23:4051-60.

Lei Z, Li B, Yang Z et al. Regulation of HIF-1alpha and VEGF by miR-20b tunes tumor cells to adapt to the alteration of oxygen concentration. PLoS One. 2009;4(10):e7629.

Leskelä S, Leandro-García LJ, Mendiola M, et al. The miR-200 family controls β-tubulin III expression and is associated with paclitaxel-based treatment response and progression-free survival in ovarian cancer patients. Endocr Relat Cancer. 2011;18:85–95.

Li X, Zhang Y, Zhang Y, et al. Survival prediction of gastric cancer by a seven-micro-RNA signature. Gut. 2010; 59:579–85.

Liao L, Wang J, Ouyang S et al. Expression and clinical significance of microRNA-1246 in human oral squamous cell carcinoma. Med Sci Monit. 2015;21:776-81.

Liu N, Sun YY, Zhang XW et al. Oncogenic miR-23a in Pancreatic Ductal Adenocarcinogenesis Via Inhibiting APAF1. Dig Dis Sci. 2015;60(7):2000-8.

Lloyd KL, Cree IA, Savage RS. Prediction of resistance to chemotherapy in ovarian cancer: a systematic review. BMC Cancer. 2015;15:117.

Long JS and Ervin LH. Using heteroscedasity consistent standard errors in the linear regression model. The American Statistician. 2000;54:217–22

Lytle JR, Yario TA, Steitz JA. Target mRNAs are repressed as efficiently by microRNA-binding sites in the 5’ UTR as in the 3’ UTR. Proc Natl Acad Sci USA. 2007;104:9667–72.

Ma J, Lyu H, Huang J et al. Targeting of erbB3 receptor to overcome resistance in cancer treatment. Mol Cancer. 2014;13:105.

Malpica A, Deavers MT, Lu K et al. Grading ovarian serous carcinoma using a two-tier system. Am J Surg Pathol. 2004;28(4):496-504.

Marchini S, Cavalieri D, Fruscio R et al. Association between miR-200c and the survival of patients with stage I epithelial ovarian cancer: a retrospective study of two independent tumour tissue collections. Lancet Oncol. 2011;12:273–85.

McGuire WP, Hoskins WJ, Brady MF et al. Cyclophosphamide and cisplatin compared with paclitaxel and cisplatin in patients with stage III and stage IV ovarian cancer. N Engl J Med. 1996;334(1):1-6.

McShane LM, Altman DG, Sauerbrei W et al. Statistics Subcommittee of the NCI-EORTC Working Group on Cancer Diagnostics. REporting recommendations for tumour MARKer prognostic studies (REMARK). Br J Cancer. 2005;93:387-91.

Medeiros F, Muto MG, Lee Y et al. The tubal fimbria is a preferred site for early adenocarcinoma in women with familial ovarian cancer syndrome. Am J Surg Pathol. 2006;30(2):230-6.

Meng X, Müller V, Milde-Langosch K et al. Diagnostic and prognostic relevance of circulating exosomal miR-373, miR-200a, miR-200b and miR-200c in patients with epithelial ovarian cancer. Oncotarget. 2016.

Menon U, Gentry-Maharaj A, Hallett R et al. Sensitivity and specificity of multimodal and ultrasound screening for ovarian cancer, and stage distribution of detected cancers: results of the prevalence screen of the UK Collaborative Trial of Ovarian Cancer Screening (UKCTOCS). Lancet Oncol. 2009;10(4):327-40.

Mestdagh P, Hartman N, Baeriswyl L et al. Evaluation of quantitative miRNA expression platforms in the microRNA quality control (miRQC) study. Nature Methods 2014;11(8):809-15.

Montani F, Marzi MJ, Dezi F et al. miR-Test: a blood test for lung cancer early detection. J Natl Cancer Inst. 2015;107(6):djv063.

Moore RG, McMeekin DS, Brown AK et al. A novel multiple marker bioassay utilizing HE4 and CA125 for the prediction of ovarian cancer in patients with a pelvic mass. Gynecol Oncol 2009;112:40-46.

Nakayama K, Nakayama N, Jinawath N et al. Amplicon profiles in ovarian serous carcinomas. Int J Cancer. 2007;120(12):2613-7.

Nam EJ, Yoon H, Kim SW, et al. MicroRNA expression profiles in serous ovarian carcinoma. Clin Cancer Res. 2008;14:2690– 5.

Nowak M, Janas Ł, Stachowiak G et al. Current clinical application of serum biomarkers to detect ovarian cancer. Prz Menopauzalny. 2015;14(4):254-9.

Ogata-Kawata H, Izumiya M, Kurioka D et al. Circulating exosomal microRNAs as biomarkers of colon cancer. PLoS One 2014;9:e92921.

Ohman AW, Hasan N, Dinulescu DM. Advances in tumor screening, imaging, and avatar technologies for high-grade serous ovarian cancer. Front Oncol. 2014;4:322.

Oncotype DX®: Development. http://prostate-cancer.oncotypedx.com/ en-US/Professional/IntroducingGPS/Development.aspx.

O'Neill CJ, Deavers MT, Malpica A et al. An immunohistochemical comparison between low-grade and high-grade ovarian serous carcinomas: significantly higher expression of p53, MIB1, BCL2, HER-2/neu, and C-KIT in high-grade neoplasms. Am J Surg Pathol. 2005;29(8):1034-41.

Pan W, Wang H, Jianwei R et al. MicroRNA-27a promotes proliferation, migration and invasion by targeting MAP2K4 in human osteosarcoma cells. Cell Physiol Biochem. 2014;33(2):402-12.

Paolicchi E, Gemignani F, Krstic-Demonacos M et al. Targeting hypoxic response for cancer therapy. Oncotarget. 2016

Park SM, Gaur AB, Lengyel E et al. The miR-200 family determines the epithelial phenotype of cancer cells by targeting the E-cadherin repressors ZEB1 and ZEB2. Genes Dev. 2008;22:894–907

Patch AM, Christie EL, Etemadmoghadam D et al. Whole-genome characterization of chemoresistant ovarian cancer. Nature. 2015;527(7578):398.

Perren TJ, Swart AM, Pfisterer J, et al. A phase 3 trial of bevacizumab in ovarian cancer. N Engl J Med. 2011;365:2484–96.

Peters L, Meister G. Argonaute proteins: mediators of RNA silencing. Mol Cell. 2007;26(5):611-23. Review.

Piccart MJ, Bertelsen K, James K et al. Randomized intergroup trial of cisplatin-paclitaxel versus cisplatin-cyclophosphamide in women with advanced epithelial ovarian cancer: three-year results. J Natl Cancer Inst. 2000;92(9):699-708.

Piek J.M, van Diest P.J, Zweemer RP et al. Dysplastic changes in prophylactically removed Fallopian tubes of women predisposed to developing ovarian cancer. J Pathol, 2001;195:451–456

Ponting CP, Oliver PL, Reik W. Evolution and functions of long noncoding RNAs. Cell. 2009;136(4):629-41. Review.

Prat J. New insights into ovarian cancer pathology. Ann Oncol. 2012;23(10):x111-7.

Prat J. Ovarian carcinomas: five distinct diseases with different origins, genetic alterations, and clinicopathological features. Virchows Arch. 2012;460(3):237-49.

Prat J, Belhadj H, Berek J et al. FIGO Committee on Gynecologic Oncology. Abridged republication of FIGO's staging classification for cancer of the ovary, fallopian tube, and peritoneum. Eur J Gynaecol Oncol. 2015;36:367-9.

Przybycin CG, Kurman RJ, Ronnett BM et al. Are all pelvic (nonuterine) serous carcinomas of tubal origin? Am J Surg Pathol. 2010;34(10):1407-16.

Ramalingam P. Morphologic, Immunophenotypic, and Molecular Features of Epithelial Ovarian Cancer. Oncology (Williston Park). 2016;30(2):166-76.

Raspollini MR, Castiglione F, Garbini F, et al. Correlation of epidermal growth factor receptor expression with tumor microdensity vessels and with vascular endothelial growth factor expression in ovarian carcinoma. Int J Surg Pathol. 2005;13:135–42

Rebbeck TR, Kauff ND, Domchek SM. Meta-analysis of risk reduction estimates associated with risk-reducing salpingo-oophorectomy in BRCA1 or BRCA2 mutation carriers. J Natl Cancer Inst. 2009;101(2):80-7.

Reiner A, Yekutieli D, Benjamini Y. Indentifying differentially expressed genes using false discovery rate controlling procedures. Bioinformatics 2003;19:368-75.

Resnick KE, Alder H, Hagan JP et al. The detection of differentially expressed microRNAs from the serum of ovarian cancer patients using a novel real-time PCR platform. Gynecol Oncol. 2009;112(1):55-9.

Rigakos G, Razis E. BRCAness: finding the Achilles heel in ovarian cancer. Oncologist. 2012;17(7):956-62.

Rossignol F, Vaché C, Clottes E. Natural antisense transcripts of hypoxia-inducible factor 1alpha are detected in different normal and tumour human tissues. Gene. 2002;299(1-2):135-40.

Rouleau M, Patel A, Hendzel M J. et al. PARP inhibition: PARP1 and beyond. Nat Rev Cancer. 2010;10:293–301.

Sales G, Calura E, Martini P et al. Graphite Web: Web tool for gene set analysis exploiting pathway topology. Nucleic Acids Res. 2013 ;41(Web Server issue):W89-97. doi: 10.1093/nar/gkt386.

Schetter AJ, Leung SY, Sohn JJ, et al. MicroRNA expression profiles associated with prognosis and therapeutic outcome in colon adenocarcinoma. JAMA. 2008;299:425–36.

Sempere LF, Christensen M, Silahtaroglu A, et al. Altered MicroRNA expression confined to specific epithelial cell subpopulations in breast cancer. Cancer Res. 2007;67:11612–20.

Sennino B, McDonald DM. Controlling escape from angiogenesis inhibitors. Nat Rev Cancer. 2012; 12(10): 699-709.

Shapira I, Oswald M, Lovecchio J et al. Circulating biomarkers for detection of ovarian cancer and predicting cancer outcomes. Br J Cancer. 2014;110(4):976-83.

Shimomura A, Shiino S, Kawauchi J et al. Novel combination of serum microRNA for detecting breast cancer in the early stage. Cancer Sci. 2016;107(3):326-34.

Siegel RL, Miller KD, Jemal A. Cancer statistics, 2016. CA Cancer J Clin. 2016;66(1):7-30.

Slodkowska EA, Ross JS. Mammaprint™ 70-gene signature: another milestone in personalized medical care for breast cancer patients. Expert Rev Mol Diagn. 2009;9(5):417–22.

Smyth GK. Linear models and empirical bayes methods for assessing differential expression in microarray experiments. Stat Appl Genet Mol Biol 2004;3:3.

Stronach EA, Alfraidi A, Rama N et al. HDAC4-regulated STAT1 activation mediates platinum resistance in ovarian cancer. Cancer Res. 2011;71(13):4412-22.

Sun Z, Meng C, Wang S et al. MicroRNA-1246 enhances migration and invasion through CADM1 in hepatocellular carcinoma. BMC Cancer 2014;14:616.

Takeshita N, Hoshino I, Mori M et al. Serum microRNA expression profile: miR-1246 as a novel diagnostic and prognostic biomarker for esophageal squamous cell carcinoma. Br J Cancer 2013;108:644-52.

Taylor DD, Gercel-Taylor C. MicroRNA signatures of tumor-derived exosomes as diagnostic biomarkers of ovarian cancer. Gynecol Oncol. 2008;110(1):13-21.

Terraneo L, Bianciardi P, Caretti A et al. Chronic systemic hypoxia promotes LNCaP prostate cancer growth in vivo. Prostate. 2010;70(11):1243-54.

Terry KL, Schock H, Fortner RT et al. A prospective evaluation of early detection biomarkers for ovarian cancer in the European EPIC cohort. Clin Cancer Res 2016; pii: clincanres.0316.2016.

Tothill RW, Tinker AV, George J et al. Novel molecular subtypes of serous and endometrioid ovarian cancer linked to clinical outcome. Clin Cancer Res. 2008;14(16):5198-208.

Vaksman O, Stavnes HT, Kaern J et al. miRNA profiling along tumour progression in ovarian carcinoma. J Cell Mol Med. 2011;15(7):1593-602.

Vandesompele J, De Preter K, Pattyn F et al. Accurate normalization of real-time quantitative RT-PCR data by geometric averaging of multiple internal control genes. Genome Biol 2002;18:3(7).

Vang R, Shih IeM, Kurman RJ. Ovarian low-grade and high-grade serous carcinoma: pathogenesis, clinicopathologic and molecular biologic features, and diagnostic problems. Adv Anat Pathol. 2009;16(5):267-82.

Vecchione A, Belletti B, Lovat F et al. A microRNA signature defines chemoresistance in ovarian cancer through modulation of angiogenesis. Proc Natl Acad Sci U S A. 2013;110(24):9845-50.

Venkitaraman AR. Cancer susceptibility and the functions of BRCA1 and BRCA2. Cell. 2002;108(2):171-82.

Vilming Elgaaen B, Olstad OK, Haug KB et al. Global miRNA expression analysis of serous and clear cell ovarian carcinomas identifies differentially expressed miRNAs including miR-200c-3p as a prognostic marker. BMC Cancer. 2014;14:80.

Volinia S, Calin GA, Liu CG et al. A microRNA expression signature of human solid tumors defines cancer gene targets. Proc Natl Acad Sci U S A. 2006;103(7):2257-61.

Walsh T, Lee MK, Casadei S et al. Detection of inherited mutations for breast and ovarian cancer using genomic capture and massively parallel sequencing. Proc Natl Acad Sci U S A. 2010;107(28):12629-33.

Wang S, Zeng Y, Zhou JM et al. MicroRNA-1246 promotes growth and metastasis of colorectal cancer cells involving CCNG2 reduction. Mol Med Rep 2016;13:273-80.

Weber B, Stresemann C, Brueckner B et al. Methylation of human microRNA genes in normal and neoplastic cells. Cell Cycle. 2007;6(9):1001-5.

Wellek S. Testing statistical hypotheses of equivalence. 2003 Chapman and Hall/CRC.

Wu XZ, Wang KP, Song HJ et al. MiR-27a-3p promotes esophageal cancer cell proliferation via F-box and WD repeat domain-containing 7 (FBXW7) suppression. Int J Clin Exp Med. 2015;8(9):15556-62

Xu YZ, Xi QH, Ge WL et al. Identification of serum microRNA-21 as a biomarker for early detection and prognosis in human epithelial ovarian cancer. Asian Pac J Cancer Prev. 2013;14(2):1057-60.

Yanaihara N, Caplen N, Bowman E, et al. Unique microRNA molecular profiles in lung cancer diagnosis and prognosis. Cancer Cell. 2006;9:189–98.

Yang D, Khan S, Sun Y et al. Association of BRCA1 and BRCA2 mutations with survival, chemotherapy sensitivity, and gene mutator phenotype in patients with ovarian cancer. JAMA 2011;306:1557–65.

Yang D, Sun Y, Hu L et al. Integrated analyses identify a master microRNA regulatory network for the mesenchymal subtype in serous ovarian cancer. Cancer Cell. 2013 Feb 11;23(2):186-99.

Yang N, Kaur S, Volinia S et al. MicroRNA microarray identifies Let-7i as a novel biomarker and therapeutic target in human epithelial ovarian cancer. Cancer Res. 2008;68(24):10307-14.

Yemelyanova A, Vang R, Kshirsagar M et al. Immunohistochemical staining patterns of p53 can serve as a surrogate marker for TP53 mutations in ovarian carcinoma: an immunohistochemical and nucleotide sequencing analysis. Mod Pathol. 2011;24(9):1248-53.

Yong FL, Wang CW, Roslani AC et al. The involvement of miR-23a/APAF1 regulation axis in colorectal cancer. Int J Mol Sci. 2014;15(7):11713-29.

Zhang L, Volinia S, Bonome T et al. Genomic and epigenetic alterations deregulate microRNA expression in human epithelial ovarian cancer. Proc Natl Acad Sci U S A. 2008;105(19):7004-9.

Zheng H, Zhang L, Zhao Y et al. Plasma miRNAs as diagnostic and prognostic biomarkers for ovarian cancer. PLoS One. 2013;8(11):e77853.

Zhu C, Ren C, Han J et al. A five-microRNA panel in plasma was identified as potential biomarker for early detection of gastric cancer. Br J Cancer. 2014;110(9):2291-9.

Zuberi M, Khan I, Gandhi G et al. The conglomeration of diagnostic, prognostic and therapeutic potential of serum miR-199a and its association with clinicopathological features in epithelial ovarian cancer. Tumour Biol. 2016.

Zuberi M, Mir R, Das J et al. Expression of serum miR-200a, miR-200b, and miR-200c as candidate biomarkers in epithelial ovarian cancer and their association with clinicopathological features. Clin Transl Oncol. 2015;17(10):779-87.

8. SUPPLEMENTARY MATERIALS

8.1 Serum Microarray Data Analysis: filtering and normalizations

Serum raw microarray data comprised 1361 miRNAs (included controls and spikes) repeated 40 times. The expression of these 40 replicates *per* miRNA have been used as technical replicates and quality control. A first filter has been applied to select those miRNAs with reliable expression values within arrays. Specifically, within each experiment we selected only miRNAs with at least of 20% good quality measures among the 40 replicates (using gisPosandSig Agilent flag), otherwise they were considered NA (not available). Then, a second filter was applied among arrays. Specifically, we selected only miRNAs with at least 75% of good quality measures (not NA) across samples. After these filtering steps, we remain with 648 miRNAs (including the 10 spikes). Then the miRNA replicates within samples were summarised using the median. The small amount of missing values still present after the filtering step was imputed with k-nearest neighbourhood method. The distributions of the raw expression values are reported in the first panel of Supplementary Figure S1.

As expected, spikes raw measurements are characterised by high expression and large variability. In principle, after normalization we would expect *i)* that spikes distribution were stable on high expression levels across samples and with low variability and *ii)* that the boxplot of expression values of the experiments should be centered in mean. To identify the best normalization technique we performed a comparative evaluation using different algorithms: quantile [Bolstad BM et al. 2003], variance stabilising normalization (vsn) [Geller SC et al. 2003] and classic cyclic loess [Bolstad BM et al. 2003] and custom cyclic lowess in which spike-in controls are used as stabilising factors. Specifically, we applied two types of modified loess: *i)* the first in which the local regression parameters are estimated using only spikes genes (CLWs); *ii)* the second in which the local regression parameters are estimated using both spikes and a set of 20 selected invariant low expressed genes (CLWsin). Invariant low expressed miRNAs have been selected as miRNAs with expression values less than 3 (in log scale) and with the smallest difference in mean between cases and controls. Normalised expression distributions with different normalization methods are reported in Supplementary Figure S1.

miRNA serum expression distributions are characterised by a very skew distribution towards small values (that is, a distribution with a large number of very small expression values and few number of highly expressed values). Thus, the use of only spikes (characterised by large expression values) as normalizing factors leads to a bias transformation of the data towards large expression values. This bias is evidenced in Supplementary Figure S1 were the lowess normalization using only spikes leads to highly heterogeneous boxplots. However, in this context, an appropriate set of normalising factors should contain both high and low expressed invariant features. For this reason, as well as spikes, we included, in the set of normalizing factors, 20 invariant low expressed miRNAs (different number of invariant miRNAs have been used from 10 to 30 but with small

differences in performance, data not shown). As shown in Supplementary Figure S1, the application of this last strategy leads to the best compromise between stable distribution of spikes expression values across samples and centered arrays boxplot.

Another basic plot to verify the goodness of a normalization is the Relative Log Expression (RLE) plot. The RLE plot shows the distribution of the ratio between the expression of a miRNA and the median expression of this miRNA across all arrays of the experiment. It is assumed that most miRNAs are not changed across the arrays, so it is expected that these ratios are around 0 on a log scale. The boxplots presenting the distributions should then be centered near 0 and have similar spread. Other behaviour would be a sign of low quality. The RLE plots obtained after each normalization were reported in Supplementary Figure S2. As expected by construction classic loess, quantile and vsn have more homogeneous RLEs, but a wrong distribution of spikes. However, lowess with weight on spikes and low invariant genes has the best compromise between a stable distribution of spike expression and homogeneous distribution of RLE plots. Then we decide to use this approach as the best in our case.

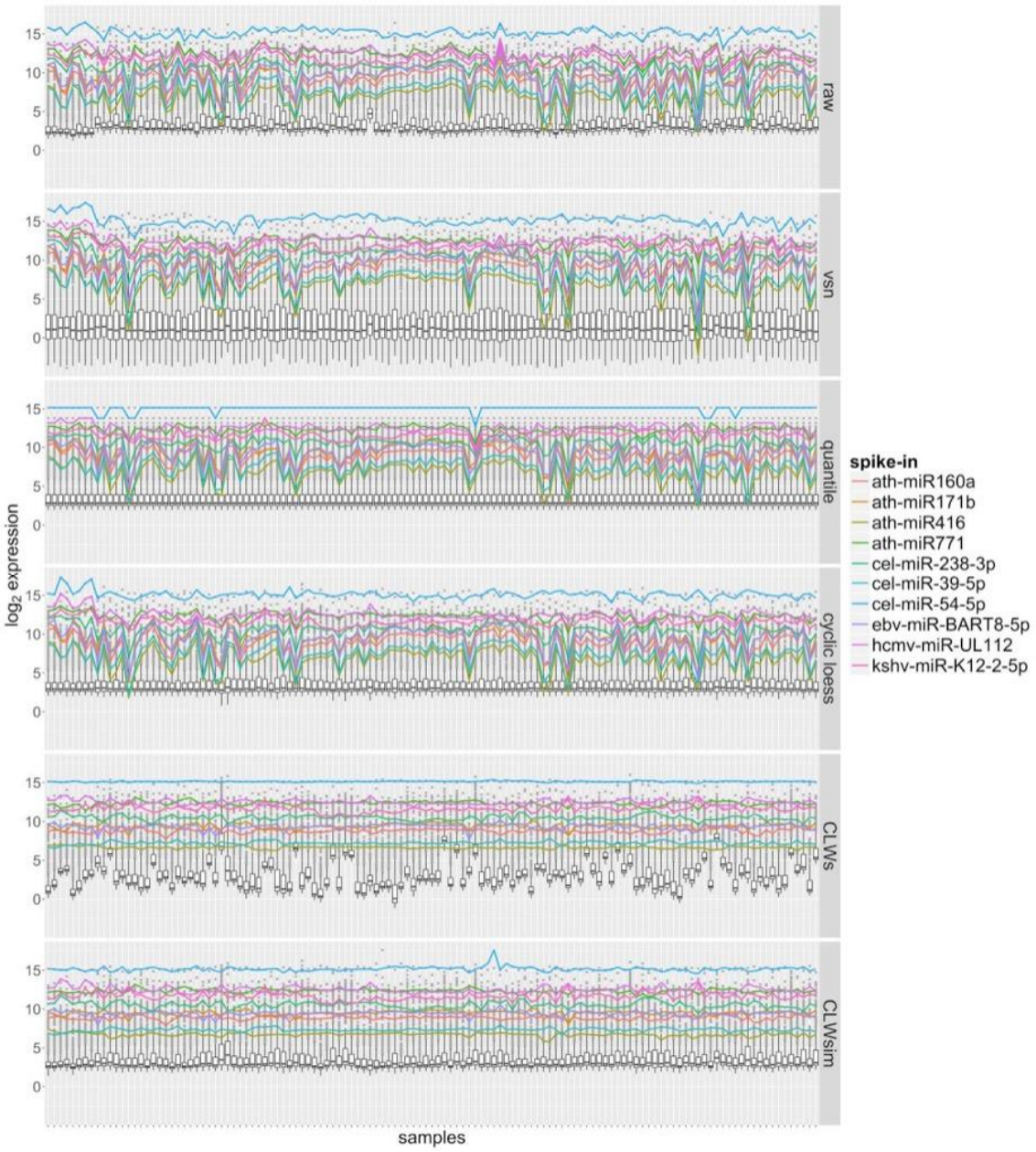

Supplementary Figure S1: Distribution of the raw and normalised expression values with highlighted spike-in data. The type of normalization is reported on the right gray bar of each panel.

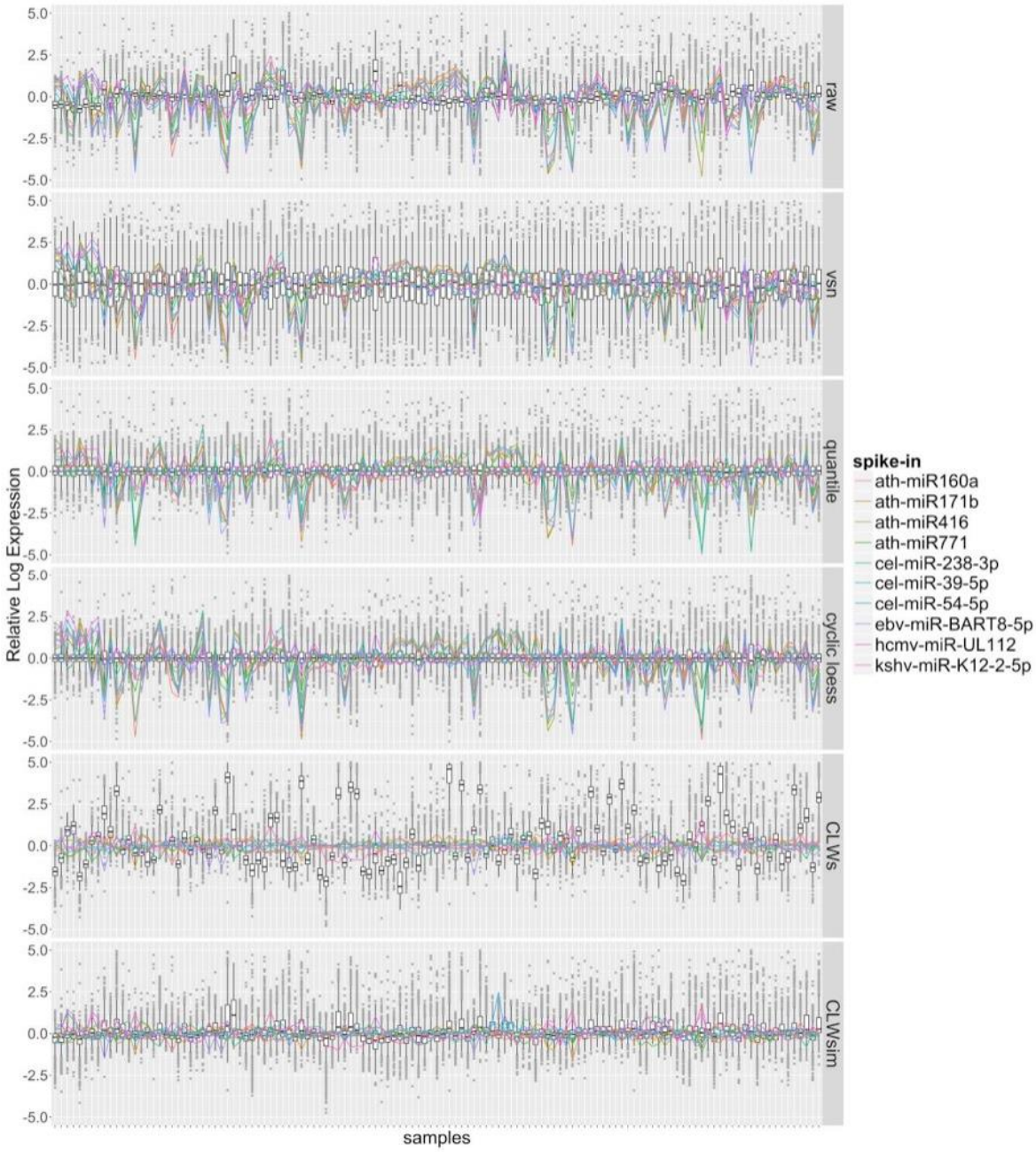

Supplementary Figure S2: RLE plots of expression data after normalization. The type of normalization is reported on the right gray bar.

Supplementary Table S1: List of 97 circulating miRNAs emerged significantly differentially expressed between HGSOC patients vs healthy donors by microarray technology (those in bold were selected for validation).

rank	microRNA	adjust ɻ -value	Mean log_2 expression		log Fold Change
			Control	Case	
1	**hsa-miR-483-3p**	**0,0000**	**3,42**	**4,45**	**1,04**
2	hsv2-miR-H6-3p	0,0000	2,50	3,02	0,52
3	hsa-miR-1290	0,0000	3,60	4,60	1,01
4	hsa-miR-1224-3p	0,0000	2,61	3,15	0,54
5	**hsa-miR-4290**	**0,0000**	**3,10**	**4,06**	**0,96**
6	hsa-miR-328	0,0002	3,15	3,76	0,60
7	hsv1-miR-H1-3p	0,0002	2,71	3,27	0,57
8	hsa-miR-129-2-3p	0,0002	2,66	3,13	0,47
9	hsv1-miR-H6-3p	0,0002	3,03	3,92	0,89
10	hsa-miR-485-3p	0,0003	2,69	3,24	0,55
11	hsa-miR-4284	0,0004	3,37	4,05	0,67
12	**hsa-miR-595**	**0,0004**	**3,54**	**5,03**	**1,49**
13	hsa-miR-664a-3p	0,0004	2,57	2,92	0,35
14	ebv-miR-BART16	0,0004	3,43	4,97	1,54
15	**hsa-miR-2278**	**0,0005**	**3,19**	**4,41**	**1,22**
16	hcmv-miR-US4	0,0007	3,64	3,11	-0,54
17	hsa-let-7b-3p	0,0007	2,95	3,69	0,74
18	**hsa-miR-32-3p**	**0,0008**	**3,73**	**5,19**	**1,46**
19	hsa-miR-3147	0,0008	3,90	3,17	-0,72
20	hsa-miR-365a-3p	0,0008	3,10	3,69	0,59
21	hsa-miR-129-1-3p	0,0008	2,65	3,06	0,41
22	hsv2-miR-H9-3p	0,0008	2,76	3,31	0,55
23	hsa-miR-4323	0,0008	2,73	3,28	0,55
24	**hsa-miR-3148**	**0,0008**	**3,23**	**4,57**	**1,34**
25	hsa-miR-615-3p	0,0008	2,50	2,84	0,35
26	hsa-miR-766-3p	0,0008	3,49	4,07	0,57
27	hsa-miR-3675-3p	0,0008	2,60	3,10	0,49
28	hsa-miR-3149	0,0011	3,69	5,14	1,45
29	hsa-let-7f-1-3p	0,0011	3,18	3,87	0,69
30	hsa-miR-92b-3p	0,0016	2,49	2,93	0,44
31	hsa-miR-1825	0,0016	4,18	5,02	0,84

32	hsa-miR-211-5p	0,0021	2,67	2,94	0,28
33	hsa-miR-3613-3p	0,0026	2,59	3,11	0,52
34	hsa-miR-1180	0,0026	2,75	3,80	1,05
35	ebv-miR-BART12	0,0026	3,67	4,94	1,27
36	hsa-miR-1228-5p	0,0032	2,84	3,89	1,05
37	hsa-miR-4312	0,0039	2,74	3,20	0,46
38	hsa-miR-634	0,0046	2,68	3,03	0,35
39	hsa-miR-127-3p	0,0046	2,75	3,38	0,63
40	hsa-miR-877-3p	0,0046	3,46	4,21	0,75
41	hsa-miR-3647-3p_v17.0	0,0057	2,75	3,42	0,67
42	hsa-miR-2277-3p	0,0059	3,11	3,52	0,41
43	hsa-miR-576-5p	0,0061	2,68	2,90	0,21
44	hsa-let-7f-2-3p	0,0063	2,57	2,74	0,18
45	hsa-miR-539-5p	0,0064	2,75	3,44	0,69
46	hsa-miR-670	0,0065	3,00	4,06	1,06
47	hsa-miR-609	0,0067	2,58	2,83	0,26
48	hsa-miR-3676-3p	0,0073	2,82	3,47	0,65
49	hsa-miR-449c-3p	0,0073	2,53	2,93	0,40
50	**hsa-miR-1246**	**0,0077**	**6,24**	**7,18**	**0,94**
51	hsa-miR-3180-5p	0,0087	2,59	3,03	0,44
52	hsa-miR-3679-3p	0,0087	2,90	3,22	0,32
53	hsa-miR-1539	0,0109	2,82	3,48	0,66
54	ebv-miR-BART4-5p	0,0111	2,75	3,40	0,66
55	hsa-miR-2116-3p	0,0117	2,79	3,41	0,62
56	hsa-miR-613	0,0125	2,41	2,69	0,27
57	hsa-miR-299-5p	0,0132	2,51	2,77	0,27
58	hsa-miR-505-3p	0,0135	2,54	2,73	0,19
59	hsa-miR-337-3p	0,0146	2,71	2,97	0,26
60	hsa-miR-656	0,0146	2,48	2,71	0,22
61	hsa-miR-933	0,0146	3,01	3,47	0,47
62	hsa-miR-18b-3p	0,0150	2,60	2,97	0,38
63	hsa-miR-4313	0,0151	3,32	4,07	0,75
64	**hsa-miR-574-5p**	**0,0154**	**5,83**	**7,27**	**1,44**
65	hsa-miR-1237-3p	0,0156	2,75	3,22	0,47
66	hsa-miR-4310	0,0164	2,85	3,52	0,66

67	hsa-miR-23c	0,0164	2,90	3,48	0,59
68	ebv-miR-BART10-3p	0,0169	2,60	3,27	0,67
69	hsa-miR-1306-3p	0,0172	2,81	3,60	0,79
70	hsa-miR-329	0,0176	2,52	2,76	0,24
71	hsa-miR-425-3p	0,0191	2,96	3,58	0,62
72	hsv1-miR-H7-3p	0,0191	3,45	3,97	0,51
73	**hsa-miR-4281**	**0,0218**	**10,50**	**11,37**	**0,87**
74	hsa-miR-181a-5p	0,0218	3,58	3,14	-0,44
75	hsa-miR-133a	0,0218	2,50	2,76	0,26
76	kshv-miR-K12-12-5p	0,0218	2,59	2,97	0,39
77	ebv-miR-BART3-5p	0,0218	2,68	3,23	0,55
78	ebv-miR-BART10-5p	0,0218	2,57	2,77	0,19
79	hsa-miR-3907	0,0223	2,76	3,35	0,59
80	hsa-miR-631	0,0240	2,48	2,72	0,23
81	hsa-miR-937-3p	0,0247	2,50	2,80	0,30
82	hsa-miR-320a	0,0247	5,19	4,46	-0,73
83	hsa-miR-133b	0,0247	2,56	2,77	0,21
84	hsa-miR-885-5p	0,0271	2,73	3,08	0,35
85	hsa-miR-106b-5p	0,0271	5,45	4,79	-0,66
86	kshv-miR-K12-8-5p	0,0299	2,62	2,94	0,32
87	hsa-miR-1281	0,0323	4,99	5,69	0,70
88	hsa-miR-297	0,0365	2,56	3,03	0,47
89	hsa-miR-195-3p	0,0407	2,75	3,50	0,75
90	hsa-miR-602	0,0414	2,71	3,15	0,44
91	hsa-miR-454-5p	0,0429	2,66	2,96	0,30
92	ebv-miR-BART17-3p	0,0469	2,44	2,71	0,26
93	dmr_31a	0,0476	10,04	10,53	0,49
94	hsa-miR-191-3p	0,0476	3,36	3,93	0,57
95	hsa-miR-1972	0,0476	2,67	3,06	0,39
96	hsa-miR-3650	0,0476	2,52	2,98	0,47
97	hsa-miR-206	0,0476	2,71	3,55	0,84

8.2 miR-15b normalization strategy

To further validate our data, we identified miR-15b as a putative reference miRNA, resulting to be the most invariant in our cohort of samples (Supplementary Figure S3), as well as in others reported in the literature [Bianchi F et al. 2011]. Using delta-Ct method and miR-15b as reference, we normalized the expression levels of candidate miRNAs across all HGSOC samples and healthy controls. As shown in Supplementary Table S2, miR-1246 and miR-595 were also successfully validated by this further normalization approach, either in training set or in validation cohort of samples. miR-4294 maintained its opposite trend. On the contrary, miR-2278 confirmed its differential expression level between HGSOC and controls in the training set ($p<0.0001$), while not in the validation set ($p=0.461$). Therefore, it was excluded from further validations.

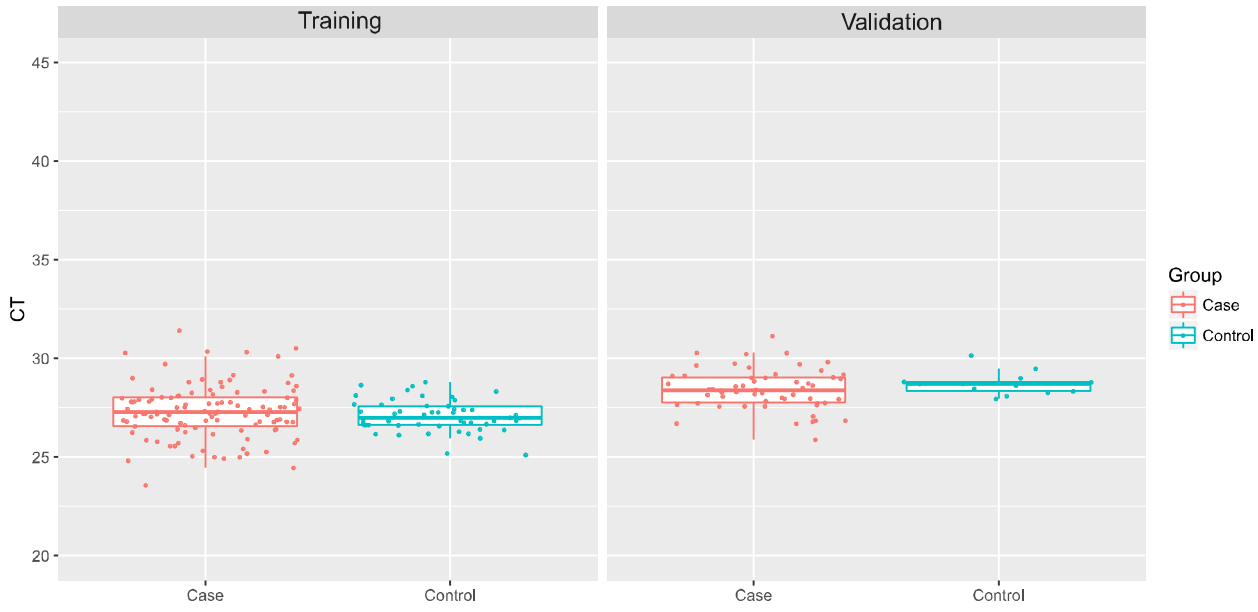

Supplementary Figure S3: Boxplot of the miR-15b Ct values for both training and validation sets.

Supplementary Table S2: Expression levels of nine selected miRNA, normalized according to miR-15b, evaluated by RT-qPCR in the sera of two independent cohorts of HGSOC and healthy donors

RT-qPCR		Training set		Validation set	
		Control	Case	Control	Case
miR-1246	**median (qCT) [IQR]**	0.963 [0.089]	0.859 [0.075]	0.959 [0.031]	0.907 [0.058]
	mean (qCT) [sd]	0.957 [0.057]	0.868 [0.066]	0.953 [0.042]	0.910 [0.047]
	p-value (2^{-qCT})	0.0000		0.0041	
miR-574-5p	**median (qCT) [IQR]**	1.014 [0.092]	1.038 [0.101]	1.072 [0.045]	1.039 [0.061]
	mean (qCT) [sd]	1.022 [0.064]	1.038 [0.074]	1.081 [0.045]	1.039 [0.054]
	p-value (2^{-qCT})	0.1768		0.0068	
miR-483-3p	**median (qCT) [IQR]**	1.207 [0.094]	1.222 [0.112]	1.128 [0.049]	1.129 [0.062]
	mean (qCT) [sd]	1.200 [0.074]	1.214 [0.083]	1.124 [0.051]	1.133 [0.052]
	p-value (2^{-qCT})	0.3256		0.5754	
miR-4290	**median (qCT) [IQR]**	1.208 [0.094]	1.186 [0.108]	1.059 [0.027]	1.083 [0.072]
	mean (qCT) [sd]	1.221 [0.080]	1.191 [0.081]	1.055 [0.042]	1.093 [0.058]
	p-value (2^{-qCT})	0.0270		0.0132	
miR-595	**median (qCT) [IQR]**	1.267 [0.118]	1.220 [0.135]	1.193 [0.057]	1.148 [0.094]
	mean (qCT) [sd]	1.265 [0.084]	1.227 [0.107]	1.197 [0.057]	1.155 [0.073]
	p-value (2^{-qCT})	0.0098		0.0268	

miR-2278	**median (qCT) [IQR]**	1.342 [0.146]	1 257 [0.100]	1.170 [0.043]	1.180 [0.059]
	mean (qCT) [sd]	1.354 [0.114]	1.260 [0.091]	1.167 [0.034]	1.176 [0.047]
	p-value (2^{-qCT})	0.0000		0.4605	
miR-32-3p	**median (qCT) [IQR]**	1.333 [0.100]	1.357 [0.100]	1.337 [0.076]	1.293 [0.112]
	mean (qCT) [sd]	1.336 [0.082]	1.370 [0.086]	1.360 [0.112]	1.307 [0.079]
	p-value (2^{-qCT})	-		-	
miR-4281	**median (qCT) [IQR]**	1.436 [0.116]	1.362 [0.099]	1.328 [0.102]	1.307 [0.088]
	mean (qCT) [sd]	1.433 [0.094]	1.368 [0.085]	1.336 [0.066]	1.319 [0.072]
	p-value (2^{-qCT})	-		-	
miR-3148	**median (qCT) [IQR]**	1.443 [0.174]	1.391 [0.149]	1.335 [0.104]	1.343 [0.081]
	mean (qCT) [sd]	1.460 [0.109]	1.382 [0.117]	1.318 [0.082]	1.348 [0.074]
	p-value (2^{-qCT})	-		-	

9. TRACK RECORD OF PUBLICATIONS

I am the last co-author of the paper entitled “Identification of stably expressed reference small non coding RNAs for microRNA quantification in high-grade serous ovarian carcinoma tissuesò, in press in the *Journal of Cellular and Molecular Medicine*. Additionally, I am the first co-author of the paper entitled “Circulating miRNA landscape identifies miR-1246 as promising diagnostic biomarker in high-grade serous ovarian carcinoma: a validation across two independent cohorts”, submitted to *Oncotarget.*

Grant Support

The first study was supported by CARIPLO Foundation (Grant Number 2013-0815 to S.M, C.R. and E.S.), by Italian Association for Cancer Research (Grant Number IG15177 to S.M, IG17185 to CR and MFAG11676 to MF) and by the Italian Ministry of Instruction, University and Research FIRB 2011 to MN (Project RBAPIIBYNP).

The second study was supported by CARIPLO Foundation (Grant Number 2013-0815 to E. Sartori).

10. ACKNOWLEDGMENTS

I would like to express my deepest and sincere gratitude to my PhD supervisor, Professor Michele Samaja, for his essential scientific support to the study and constant encouragement.
I would like to thank my co-supervisor Dr Antonella Ravaggi for her important scientific help and critical revision of the manuscript.
I would like to express my honest gratitude to Dr Eliana Bignotti for her great experimental support, fruitful discussion, encouragement, guidance and unconditional help during all these years of PhD period.
My gratitude is extend to my colleagues Dr Chiara Romani, Dr Laura Zanotti and Dr Germana Tognon for their careful revising of the manuscript and sincere comments.
I also would like to acknowledge Prof. Chiara Romualdi and, especially Dr Elisa Salviato, from University of Padova, Dr Emanuela Ferracin, from University of Ferrara, and Dr Sergio Marchini from Mario Negri Institute of Milano, for their fundamental collaboration to the study
I am grateful to Dr Laura Ardighieri for giving assistance in the collection of fallopian tube and ovarian surface epithelia.
A special gratitude goes to Maria Flora Mangano, for never-ending enthusiasm, warm heart, interesting conversations, invaluable moral support and guidance.
I would like to deeply thank my family for their unfailing support and encouragement.
I am indebted to all of the patients and their families who contributed to this study. I thank all the nurses working in the OR and in the Division of Obstetrics and Gynecology, Spedali Civili of Brescia, Italy, for the essential contribution in the collection of tumor tissue samples.

This work was supported by CARIPLO Foundation (Grant Number 2013-0815 to S.M, C.R. and E.S.), by Italian Association for Cancer Research (Grant Number IG15177 to S.M, IG17185 to CR and MFAG11676 to MF) and by the Italian Ministry of Instruction, University and Research FIRB 2011 to MN (Project RBAPIIBYNP).